WOOD SMOKE CONTRIBUTION TO AMBIENT AEROSOL IN FRESNO DURING WINTER 2003-2004

By

Courtney A. Gorin[1], Pierre Herckes[2], and Jeffrey L. Collett, Jr.[1]

[1]Department of Atmospheric Science
Colorado State University
Fort Collins, CO

[2] Department of Chemistry
University of Arizona
Tempe, AZ

Funding agency:
San Joaquin Valley-wide Air Pollution Study Agency
Contract # NSF ATM-0222607

Colorado State University

Department of Atmospheric Science

Paper No. 763

WOOD SMOKE CONTRIBUTION TO AMBIENT AEROSOL IN FRESNO DURING WINTER 2003-2004

By

Courtney A. Gorin[1], Pierre Herckes[2], and Jeffrey L. Collett, Jr.[1]

[1]Department of Atmospheric Science
Colorado State University
Fort Collins, CO

[2] Department of Chemistry
University of Arizona
Tempe, AZ

Funding agency:
San Joaquin Valley-wide Air Pollution Study Agency
Contract # NSF ATM-0222607

WOOD SMOKE CONTRIBUTION TO AMBIENT AEROSOL IN FRESNO DURING WINTER 2003-2004

by

Courtney A. Gorin

Department of Atmospheric Science

Colorado State University

Fort Collins, CO

San Joaquin Valley-wide Air Pollution Study Agency
Under grant ATM 0222607

November 2005

Atmospheric Science Paper No. 763

ABSTRACT

WOOD SMOKE CONTRIBUTION TO AMBIENT AEROSOL IN FRESNO DURING WINTER 2003-2004

The city of Fresno is located in the San Joaquin Valley in central California. This region experiences anomalously high levels of air pollution and, in particular, elevated levels of particulate matter (PM) during the winter season. In an effort to better quantify winter time PM and the contribution of wood smoke to pollution events in Fresno, a field campaign was conducted between December 24th, 2003 and January 15th, 2004. Over this three week period both coarse and fine daily PM samples were collected at five locations in Fresno including residential, urban, and industrial sites. Subsequent analyses of the collected samples were performed to examine the spatial and temporal variability of wood smoke concentrations in the city of Fresno, CA and to estimate the contribution of residential wood combustion to $PM_{2.5}$ concentrations.

The estimation of residential wood combustion contribution to ambient PM is based on the quantification of levoglucosan, a compound emitted exclusively from biomass burning. Levoglucosan was measured for all collected samples by high performance anion exchange chromatography (HPAEC) coupled with pulsed amperometric detection (PAD). The use of this approach has many advantages and results compare well with concentrations estimated from other, more traditional methods, namely Gas Chromatograph/Mass Spectrometry (GC/MS).

To determine the percent of $PM_{2.5}$ that is from a specific source, like residential wood burning, a source apportionment technique is performed. The source apportionment method adopted here involves several steps. First, laboratory measurements are required to ascertain

concentrations of $PM_{2.5}$, organic and elemental carbon (OC and EC), and several important organic molecular markers. Molecular markers emitted from motor vehicles, meat cooking, and residential wood burning are quantified in this study by GC/MS for only a subset of samples; although the wood smoke tracer concentration is known for each sample with the aid of the HPAEC-PAD instrument. Then, estimations of the percent contribution from each major urban source to organic aerosol and total $PM_{2.5}$ are calculated by combining tracer concentrations with a ratio of each tracer to total emissions for each source type.

Laboratory measurements revealed low spatial variability and similar temporal patterns of $PM_{2.5}$, total carbon (TC), and levoglucosan. The daily mass concentrations of $PM_{2.5}$, TC, and levoglucosan seem to vary with meteorological conditions such as precipitation, wind, and fog events. Daily $PM_{2.5}$ concentrations measured during this study did not exceed the federal 24-hour standard and the study average of 30 $\mu g/m^3$ is two-thirds lower than a previous Fresno winter average. Lower concentrations appear to be due in part to frequent precipitation during the study period. In this study the carbonaceous fraction is similar to previous findings where the composition of $PM_{2.5}$ is approximately half organic; here the remaining half is assumed to be inorganic. On a daily basis, however, the carbon fraction of $PM_{2.5}$ mass can fluctuate dramatically and minimum values occurred during fog events. During the first portion of the study, levoglucosan has a strong relationship to the concentration of $PM_{2.5}$. In the later portion of the study there is a significant reduction in levoglucosan relative to $PM_{2.5}$ suggesting a difference in the removal processes (e.g., due to fog events). Combined, the emissions from wood smoke, meat cooking, and motor vehicles appear to contribute approximately 70-80% of OC, with wood smoke, on average, accounting for approximately 45% of OC and 20% of $PM_{2.5}$. Two sites, CSUF and Clovis, have significantly higher contributions of wood smoke to OC than the other three sites, as expected based on the residential nature of the sites and location within older neighborhoods.

Although the efforts of this study focus on the impact of residential wood burning on winter-time levels of $PM_{2.5}$, it is apparent that other sources, both known and unknown, contribute to exceedance of federal $PM_{2.5}$ 24-hour and annual standards. If residential wood burning were to be completely banned, the average $PM_{2.5}$ concentration over the study duration is estimated to decline from 30 to 26 $\mu g/m^3$, a 15% reduction, which is still significantly greater than the annual standard of 15 $\mu g/m^3$. In the future, it will be important to further quantify contributions of other sources to organic and total $PM_{2.5}$ levels in efforts to achieve attainment status in urban Fresno as well as in outlying areas including the agricultural basin of the San Joaquin Valley.

ACKNOWLEDGMENTS

Within the atmospheric chemistry group and associated staff at Colorado State University there were many who contributed to this work either directly or indirectly. We would like to thank those present during the Fresno field study for diligently collecting the samples analyzed here: Taehyoung Lee, Sarah Youngster, and Andy Simpson. Also, we would like to thank Guenter Engling, who optimized the HPAEC-PAD instrument for anhydrous sugar analysis, for all his assistance. Additionally, we appreciate the comments from the reviewers of this report: Dr. Sonia Kreidenweis and Dr. John Volckens.

This study was funded by the San Joaquin Valley-wide Air Pollution Study Agency.

TABLE OF CONTENTS

LIST OF FIGURES vii

LIST OF TABLES ix

LIST OF ACROYNMS XI

CHAPTER 1 INTRODUCTION 1

1.1 AIR POLLUTION LEVELS IN CALIFORNIA'S CENTRAL VALLEY 1
1.2 STUDY MOTIVATION AND OBJECTIVES 3
1.3 OVERVIEW OF STUDY DESIGN 5
1.3.1 PHASE I 6
1.3.2 PHASE II 8

CHAPTER 2 METHODOLOGY 12

2.1 PHASE I: SAMPLE COLLECTION AND FILTER HANDLING 12
2.2 MASS DETERMINATION OF $PM_{2.5}$ 13
2.3 CARBONACEOUS COMPOSITION 16
2.3.1 MEASUREMENT METHOD 16
2.3.2 KNOWN INTERFERENCES 20
2.3.3 QUALITY CONTROL/QUALITY ASSURANCE 23
2.3.4 WATER SOLUBLE ORGANIC CARBON 26
2.4 WOOD SMOKE TRACER QUANTIFICATION VIA HPAEC-PAD 27
2.4.1 INSTRUMENT DESIGN AND APPLICATION 27
2.4.2 AQUEOUS EXTRACTION METHOD 29
2.4.3 DISCOVERED INTERFERENCES 31
2.4.4 QUALITY CONTROL/QUALITY ASSURANCE 32
2.5 GC/MS 34
2.5.1 SAMPLE PREPARATION PROCEDURES 38
2.5.2 SAMPLE ANALYSIS 42

CHAPTER 3 RESULTS 43

3.1 METEOROLOGICAL CONDITIONS AND INFLUENCE ON RESULTS 43
3.2 $PM_{2.5}$ MASS CONCENTRATION 45
3.3 CARBONACEOUS COMPONENT 48
3.3.1 TOTAL CARBON, ORGANIC CARBON, AND ELEMENTAL CARBON 48

3.3.2 Estimation of Organic Adsorption Artifact via Filter Slicing 53
3.3.3 Water Soluble Organic Carbon Content 56
3.4 Wood smoke Tracer: Levoglucosan 58
3.5 Other Compound Measurements 63
3.6 Source Apportionment 68
3.6.1 Meat Cooking: source profiles and apportionment results 79
3.6.2 Motor Vehicles: source profiles and apportionment results 81
3.6.3 Residential Wood Combustion: source profiles and apportionment results 85

CHAPTER 4 CONCLUSIONS 92

CHAPTER 5 FUTURE WORK 99

REFERENCES 103

APPENDIX A A-1

LIST OF FIGURES

Figure 1. Map of the city of Fresno and the location/classification of the five sampling sites. 7
Figure 2. Hi-Vol instruments with a PM_{10} inlet (left side) and without a PM_{10} inlet (right side). 13
Figure 3. Comparison of CSU lab's 20-hour average $PM_{2.5}$ mass concentration to averaging of CARB's hourly $PM_{2.5}$ mass concentration. The bold line is the 1-to-1 ratio, while the light line is a linear regression between the two measurements. A five percent error is shown for both instruments. 15
Figure 4. Sunset Laboratory Semi-Continuous Carbon Analyzer [photo from Sunset Laboratory's website, 2004] 17
Figure 5. One cycle of the voltage applied across the electrode to charge analyte and clean electrode surface. 28
Figure 6. Sample chromatogram produced by HPAEC-PAD showing levoglucosan and other carbohydrates in a sample collected over Christmas Eve. 28
Figure 7. Structures of chemical compounds used as source tracers for the three most significant sources of organic aerosol in Fresno, CA. Cholesterol is a meat cooking tracer, the hopane is a motor vehicle tracer, and levoglucosan is a biomass combustion tracer. 35
Figure 8. Hourly temperature (left axis) and relative humidity (right axis) over the study period. 44
Figure 9. Hourly precipitation (left axis) and wind speed (right axis) over the study period. 44
Figure 10. $PM_{2.5}$ concentration ($\mu g/m^3$) at each site with invalid data removed. There is a five percent uncertainty in concentration values. 46
Figure 11. Daily average $PM_{2.5}$ concentration (right axis) shown with continuous precipitation measurements (in dark blue on left axis) and liquid water content (in light grey on left axis: actual values are 100x). 47
Figure 12. Hourly ARB $PM_{2.5}$ concentration ($\mu g/m^3$) over study period. 48
Figure 13. Daily average $PM_{2.5}$, total carbon mass (TC'), and inorganic or unknown (Inorganic) concentrations as averaged over available sites for the study period. Error bars represent the 99% confidence level. 50
Figure 14. Hourly OC/EC data collected at CSUF. 51
Figure 15. Timeline of fine total carbon mass (TC') concentrations for available sites over the study period. TC' is estimated as the sum of OC*1.6 and EC concentrations. TC' concentrations have a 13% uncertainty based on OC and EC measurement precision at the 99% confidence level. Additional uncertainty in the OC multiplier is not quantified. 52
Figure 16. Fraction of total particulate carbon collected by coarse filters. Clovis and Drummond coarse fractions are PM_{10}-$PM_{2.5}$, while other sites' coarse fractions are TSP- $PM_{2.5}$. The cumulative error in coarse and fine samples results in a 20% uncertainty at the 99% confidence level. 53
Figure 17. Estimated fraction of OC attributed to gaseous adsorption based on the method of slicing quartz filters plotted against total filter OC concentration. Included is a non-linear regression line for the absorption as a function of OC concentration for fine filters only. Both coarse and fine filter test results are included in the figure. 55
Figure 18. A timeline of the water soluble organic carbon as a percent of OC for $PM_{2.5}$ filters from each site. 57

Figure 19. Fraction of total levoglucosan collected by coarse filters. Clovis and Drummond coarse fractions are PM_{10}-$PM_{2.5}$, while other sites' coarse fractions are TSP- $PM_{2.5}$. The cumulative error in coarse and fine samples results in a 20% uncertainty at the 99% confidence level.....60
Figure 20. Values of levoglucosan (left axis) at each site and average $PM_{2.5}$ (right axis) concentrations in $\mu g/m^3$ over the study period. Uncertainty is estimated to be 10% at the 99% confidence level.....60
Figure 21. Carbon mass of levoglucosan as a percent of OC over the study period at each site. The cumulative error in levoglucosan and OC measurements results in a 20% uncertainty at the 99% confidence level.....62
Figure 22. Scatter plot of levoglucosan concentrations ($\mu g/m^3$) estimated from GC/MS and HPAEC-PAD with two different regression forms superimposed. An exponential fit to the data produces a better correlation than a linear fit. Uncertainty is 10% for HPAEC-PAD at the 99% confidence level and GC/MS is assumed to 20%.....62
Figure 23. The relative variation of wood smoke markers guaiacol, acetovanillone, vanillin, and retene as identified and quantified by GC/MS, are fairly consistent for each sample.....66
Figure 24. The variation of wood smoke markers guaiacol, acetovanillone, vanillin, and retene as a percent of OM.....66
Figure 25. The tracers for meat cooking, cholesterol, and motor vehicles, 17α, 21β-hopane, are shown as a percent of OM based on quantification by GC/MS.....67
Figure 26. Percent of total OC that is attributable to meat cooking for samples analyzed by GC/MS. Two cases are shown: one with 1991 values, and a second representing a perceived change in meat cooking practice since 1991.....81
Figure 27. Percent of total OC that is attributable to motor vehicles for samples analyzed by GC/MS. Error bars indicate apportionment changes corresponding to a 50% decrease in diesel fuel or a doubling of gasoline consumed by non-catalyst equipped engines. 84
Figure 28. Percent of total PM2.5 that is attributable to motor vehicle primary fine particle emissions for samples analyzed by GC/MS. Error bars indicate apportionment changes corresponding to a 50% decrease in diesel fuel or a doubling of gasoline consumed by non-catalyst equipped engines.....84
Figure 29. The contribution of wood smoke to total OC and total $PM_{2.5}$ as a daily average of all sites.....89
Figure 30. Site average contribution of residential wood burning to OM for the study duration. The percent of OM attributable to wood smoke on average is indicated above each site.....89
Figure 31. OM concentration from wood smoke ($\mu g/m^3$) estimated using different wood smoke markers. 91
Figure 32. Cumulative contribution to OC as estimated for the three major sources: residential wood burning, motor vehicles, and meat cooking.....91

LIST OF TABLES

Table 1. Comparison of filter weight differences (g) between CSU and CDPHE. 16
Table 2. Sunset OCEC Analyzer environmental controls and routine for sample analysis. 18
Table 3. Independent estimate of method detection limit (MDL), reliable detection limit (RDL), and limit of quantitation (LOQ) for OC, EC and TC based on the standard deviation of 19 method blanks..... 24
Table 4. Estimate of method detection limit (MDL), reliable detection limit (RDL), and limit of quantitation (LOQ) for levoglucosan analyzed by HPAEC-PAD based on the standard deviation of 22 method blanks..... 33
Table 5. Compounds quantified by GC/MS and outline of quantification/ calibration method.... 36
Table 6. Sample selection for GC/MS analysis..... 39
Table 7. The volume and concentration of deuterated internal standards added to samples prior to extraction. 39
Table 8. Sample preparation details for chemicals quantified by GCMS for all species quantified in Table 5, except silylated species. 39
Table 9. Sample preparation details for GC/MS quantification of silylated species..... 41
Table 10. $PM_{2.5}$ gravimetric mass measurements data completeness..... 45
Table 11. Site average $PM_{2.5}$ concentration for study duration. 46
Table 12. Carbon Analysis data completeness for coarse and $PM_{2.5}$ filters. 49
Table 13. Data completeness results for levoglucosan quantification via HPAEC-PAD. 58
Table 14. Site average levoglucosan percent of $PM_{2.5}$ for the first period (12/25/2003-1/9/2004) compared with the second period (1/10/2004-1/15/2004)..... 61
Table 15. Concentration of chemical compounds identified and quantified by GC/MS for individual samples. 69
Table 16. Concentration of chemical compounds identified and quantified by GC/MS for site composites. 73
Table 17. Meat cooking source profiles and ratio of tracer to OC as used for this study. Mass values are in g/kg of meat cooked. 79
Table 18. Percentage of tracer attributable to frying and charbroiling based on the tracer emitted per mass of meat. Two cases are shown: one case with ratios published in 1991, and a second case with a hypothesized increase in charbroiling to an equal ratio of charbroiling and frying..... 80
Table 19. Motor vehicle source profiles and ratio of tracer to OC and $PM_{2.5}$ as used for this study. Mass values are in g/gallon of fuel consumed..... 82
Table 20. Percentage of tracer attributable to catalyst equipped gasoline engines, non-catalyst equipped gasoline engines and diesel engines based on source profiles normalized by fuel consumed. Three different estimates are shown: a base case, one half diesel fuel, and double the gasoline consumed in non-catalyst equipped engines..... 82
Table 21. Fireplace source profiles and ratio of tracer to OC and $PM_{2.5}$ as used for this study. Mass values are in g/kg of wood burned. 86
Table 22. Wood stove source profiles and ratio of tracer to OC and $PM_{2.5}$ as used for this study. Actual source profile is shown as well as the calculated percent of emissions of the same wood type combusted in a fireplace. 87

Table 23. Percentage of tracer attributable to wood stoves versus fireplaces based on source profiles calculated as outlined in the text. 88

LIST OF ACRONYMS

BAM	Beta Attenuation Monitors
BET	Brunauer, Emmett, and Teller
CARB	California Air Resources Board
CC	Carbonate Carbon
CDPHE	Colorado Department of Public Health and Environment
CIG	Carbon impregnated glass filter
CMB	Chemical Mass Balance apportionment technique
CPI	Carbon preference index
CRPAQS	California Regional Particulate Air Quality Study
CSU	Colorado State University
DCM	Methylene chloride
EC	Elemental Carbon
EPA	Environmental Protection Agency
FTIR	Fourier Transform Infrared Spectroscopy
GC/MS	Gas Chromatograph/Mass Spectroscopy
HPAEC-PAD	High Performance Anion Exchange Chromatograph with Pulsed Amperometric Detection
IMS95	Integrated Monitoring Study 1995
IPCC	Intergovernmental Panel on Climate Change
IS	Internal standard
LOD	Limit of detection
LOL	Limit of Linearity
LOQ	Limit of Quantification
MDL	Method Detection Limit (or minimum detection limit)
NAAQS	National Ambient Air Quality Standards
NIOSH	National Institute of Occupational Safety and Health
NDIR	Non-dispersive infrared
OC	Organic Carbon
OM	Organic Mass= OC*1.6
PAHs	Polycylic Aromatic Hydrocarbon
POC	Pyrolyzed Organic Carbon
PM	Particulate Matter
PM_{10}	Particulate Matter with aerodynamic diameter of 10 μm or less
$PM_{2.5}$	Particulate Matter with aerodynamic diameter of 2.5 μm or less
QA/QC	Quality Assurance/Quality Control
QBQ	Quartz behind quartz adsorption detection method
QBT	Quartz behind Teflon adsorption detection method
R^2	Squared Correlation Coefficient
RDL	Reliable Detection Limit
RH	Relative Humidity
RSD	Relative Standard Deviation
TC	Total Carbon (sum of OC and EC)
TC'	Total carbon mass (sum of OC*1.6 and EC)
SJV	San Joaquin Valley

SJVUAPCD	San Joaquin Valley Unified Air Pollution Control District
SVOCs	Semi-volatile Organic Compounds
VOCs	Volatile Organic Compounds
WSOC	Water Soluble Organic Carbon

CHAPTER 1 INTRODUCTION

1.1 Air Pollution Levels in California's Central Valley

The state of California has long been recognized for its air pollution problems. Observations of Los Angeles air quality initiated some of the first work studying photochemical smog and ozone formation and L.A. is one of the first cities in the United States to have recorded health effects due to photochemical smog (Cadle and Magill, 1951; McKee, 1968; Tiao, Box, and Hamming, 1975). The Central Valley of California, while not initially as polluted as L.A., also has high levels of air pollution. Measured concentrations of both ozone, a gaseous pollutant, and particulate matter in California's Central Valley have routinely surpassed National Ambient Air Quality Standards (NAAQS) (San Joaquin Valley Unified Air Pollution Control District, 2003). Particulate matter (PM) is commonly measured to quantify aerosols, which are a mixture of suspended solid and liquid particles. Where much effort has successfully focused on investigating ozone formation pathways (Calvert, 1976; Seinfeld and Pandis, 1998), the complexity of aerosols' chemical composition, physical properties, and formation processes has led to increasingly detailed research.

The continued examination of aerosols is important for understanding their role in climate change, visibility, and health effects. According to the Intergovernmental Panel on Climate Change (IPCC), the magnitude and direction of climate forcing by aerosols have the largest level of uncertainty (IPCC, 2001). It is known that aerosols both scatter and absorb incoming solar radiation which leads to an overall cooling effect; however, the extent to which aerosols indirectly influence climate by altering clouds' formation, optical properties and lifetime is still not well understood (Seinfeld and Pandis, 1998; IPCC, 2001). The optical properties of

aerosols (i.e. scattering and/or absorption of visible radiation) is a function of their chemical composition and size, parameters that change in both space and time. The size distribution and number density of aerosols are of particular importance to visibility degradation in national parks and other scenic areas (Malm, 1999). In addition to regional haze issues, conclusive studies have linked elevated levels of particulate matter with aerodynamic diameter of 10 μm or less (PM_{10}) to increased human morbidity rates and studies regarding a similar effect on asthmatics are ongoing (Wilson et al., 1998; Samet et al., 2000; Smith et al., 2003). Despite the progress that has been made in the area of aerosol research, much remains unknown and what is known relies heavily on aerosol chemical characteristics.

An important step in quantifying the impacts of aerosols is thus determining the chemical composition and dominant sources. A leading, yet relatively low-profile, contributor to measured PM on both local and global scales is biomass combustion. It is estimated that biomass combustion is the second largest anthropogenic source of aerosols globally, and within a particular region wood smoke can be the largest contributor (Andreae et al., 1996; bin Abas, Oros, and Simoneit, 2004). Until recently, much of the public scrutiny regarding aerosols has focused on both large-scale industrial operations that mostly produce sulfur emissions or on reduction of emissions from modern sources such as vehicle exhaust. However, in light of recent studies, emissions from biomass burning are quickly becoming more of a central concern. Combustion of biomass produces greenhouse gases such as carbon monoxide, ozone precursors like nitrogen oxides and organic gases, as well as organic particles and soot (Gao et al., 2003). Although tracers of biomass combustion have been detected in remote regions (Swap et al., 1996), the impact of biomass is of particular concern to local regions where it can be a significant fraction of total PM.

One area that experiences a significant wood smoke influence is the California Central Valley (Schauer and Cass, 2000). The region's continued non-attainment status for both PM_{10} and ozone prompted the initiation of several intensive, valley-wide studies: IMS95, CCOS, and

CRPAQS studies were all focused on improving knowledge of the emissions patterns, source contributions, chemical precursors and meteorological influences of pollution events in the valley basin. Results suggest a seasonal variation in pollutants and meteorologically driven episodic events (Chow et al., 1999; Poore, 2002; Watson and Chow, 2002b; Chu, Paisie, and Jang, 2004). Not all locations in the San Joaquin Valley (SJV), the southern branch of the Central Valley, demonstrated a large wood smoke influence, but several urban areas did (Chow et al., 1999; Schauer and Cass, 2000). It is estimated that approximately 50% of the particulate matter with aerodynamic diameter less than 2.5 μm ($PM_{2.5}$) could be attributed to wood combustion during a pollution event in Fresno, CA over a three-day period following Christmas (Schauer and Cass, 2000). During this event wood smoke was the emissions source with the largest contribution to $PM_{2.5}$. In a developed nation, such as the U.S., it is most likely that wintertime combustion of biomass occurs periodically, with large daily fluctuations. If the other dominant emissions sources maintain a constant emissions level under the federal PM NAAQS, wood smoke emissions could potentially be the impetus for episodic PM events that surpass federal health standards.

1.2 Study Motivation and Objectives

Several issues occurring in tandem drew the attention of the San Joaquin Valley Unified Air Pollution Control District (SJVUAPCD) to the importance of revising the regulations on wood burning in stoves and fireplaces. Due to the continued exceedance of the PM_{10} NAAQS, the CRPAQS results, and the limited disproval by the U. S. EPA of the district's current regulations on wood burning, Rule 4901, the SJVUAPCD chose to revise the regulations on wood burning stoves and fireplaces. Amendments to Rule 4901 regulating wood burning fireplaces and wood burning heaters took place on October 1, 2003. The amendments introduce a limit on the number of new wood burning devices installed in newly constructed housing on a per acre bases, require removal/replacement of wood burning devices that are not EPA certified when

property is sold or transferred, and change voluntary wood burning restrictions to mandatory restrictions when an Air Quality Index (AQI) greater than 150 is monitored (SJVUAPCD Final Draft Staff Report: Amendments to Rule 4901 (Wood Burning Fireplaces and Wood burning heaters), 2003). An AQI of 150 for $PM_{2.5}$ corresponds to a mass concentration of 65.5 $\mu g/m^3$: at this level $PM_{2.5}$ concentrations exceed the 24-hour NAAQS (Air Quality Index: A guide to Air Quality and Your Health, 2003). The first two amendments to Rule 4901 will limit the increase of wood smoke over the long-term, while the last amendment will help reduce the occurrence of episodic events when the level of $PM_{2.5}$ becomes unhealthy as defined by the U.S. EPA (Air Quality Criteria for Particulate Matter (October 2004), 2004). In addition to these amendments, the SJVUAPCD seeks voluntary reductions of wood burning when an AQI of 100 (equivalent to a $PM_{2.5}$ concentration of 40 $\mu g/m^3$) is reached, at which point concentrations have been determined to be unhealthy for sensitive groups.

In order to gauge the impact of these revisions to Rule 4901 and to learn more about wood smoke concentrations, the SJVAPSA commissioned a study to determine the spatial variability of a common wood smoke marker, levoglucosan, and estimate the contribution of wood smoke to total aerosol loading throughout the city of Fresno after the implementation of the amendments. Since the PM episodes exceeding the federal NAAQS have historically occurred over the winter holiday period between Christmas and New Year's (Schauer and Cass, 2000), this period provides the most opportune time to conduct a field study. In line with the objective of monitoring wood smoke contribution, the study period was chosen to commence on Christmas Eve, 2003 and last through the first portion of January, 2004. One common concern is the representativeness of one monitoring location for a much larger area (e.g. an entire city or air basin). This can be especially important for exposure studies aimed at interpreting health effects (Wu et al., 2005). From a regulatory perspective, one monitoring location, which may over- or underestimate total concentrations or source contributions relative to other locations, might mislead regulatory action. To better understand the spatial distribution of wood smoke

throughout the city of Fresno, five different locations within the city were chosen for monitoring. In the past, the quantification of daily wood smoke contribution to $PM_{2.5}$ at five locations would have been expensive; however, a new measurement technique makes this approach more economical.

Traditionally levoglucosan, as well as many other aerosol chemical tracers, have been quantified by extracting and derivatizing collected samples followed by injection into a Gas Chromatograph coupled with a Mass Spectrometer (GC/MS). This technique is time and labor intensive making it expensive to quantify tracers in each unique sample; often samples are combined by time of day or a grouping of days (Schauer and Cass, 2000; Brown et al., 2002; Fraser et al., 2002) to minimize costs. However, by combining samples unique information may be lost. Through the application of a new technique designed to quantify levoglucosan and other anhydrosugars associated with wood combustion, daily samples at all sites can be analyzed to provide higher resolution and capture site-specific, daily variation of wood smoke. This study provides an excellent opportunity to apply this new analytical technique to ambient samples in order to improve the working knowledge of this technique and capitalize on the information contained in individual samples.

1.3 Overview of Study Design

The collection and analysis of aerosol samples was broken into two phases: Phase I sample collection; and Phase II chemical speciation and data analysis of collected samples. The study was carefully designed and implemented in consideration of the objectives of SJVAPSA. In anticipation of a $PM_{2.5}$ non-compliance designation by the federal EPA, this study focuses on PM collection. Although there are a number of anthropogenic sources that contribute to both ozone and PM, biomass combustion is of particular interest due to its large contribution to wintertime PM in the Central Valley of California (SJVUAPCD Final Draft Staff Report: Amendments to Rule 4901 (Wood Burning Fireplaces and Wood burning heaters), 2003). The

dominant season of biomass combustion, for the purpose of home heating, land clearing, and reduction in agricultural waste, is winter and does not typically coincide with peaks in photochemical smog and ozone formation. Due to the seasonal emissions activity and meteorological factors that contribute to wintertime PM events, this study will focus on a winter collection period. Previous studies have shown that in winter $PM_{2.5}$ represents the majority of PM_{10} (Chow et al., 1992; Chow et al., 1993). Therefore, ambient $PM_{2.5}$ concentrations are quantified as well as an estimation of the anthropogenic sources that contribute most to $PM_{2.5}$ in an effort to further understand the role of wood smoke during winter PM events.

1.3.1 Phase I

Ambient aerosol samples were collected at five sites throughout the city from December 24, 2003 until January 15, 2004. Five different sites were chosen for filter based air collection on the basis of parameters such as city location, demographics/expected source influences, and practical restrictions like energy availability, land ownership, etc. The five sites represent urban, suburban and industrial influences. Figure 1 illustrates the location of each site and includes a photograph of each measurement location. A filter based, high-volume collection method was selected primarily for the ease of operation, longevity of samples prior to analysis, and large quantity of sample material collected from which a variety of chemical analyses can be performed. The collection substrate in this study is quartz fiber. Several advantages of quartz include a non-reactive surface and ease of analysis by all laboratory techniques employed in this study, including thermal-optical analysis and solvent or aqueous extractions. One known disadvantage of un-denuded samples collected on quartz is an artifact caused by adsorption of gas-phase compounds — a trade-off for the large amount of sample collected by high-volume instruments.

High-volume collectors were operated at all five sites and collected 20-hour samples. The instruments were operated from 14h00 to 10h00, local time, to accurately capture major

sources and still allow sufficient time for daily filter exchange at all sites. The period of collection might potentially bias the 20-hour average samples higher than a 24-hour average as the diurnal trends in $PM_{2.5}$ concentrations demonstrate that from 10h00 to 14h00 concentrations are typically at a minimum (Chow et al., 1999). The collectors were equipped with a size cut, essentially providing two samples at each site per day by collecting filter samples of two different size ranges. The high-volume collectors sampled larger sized, coarse, particulate matter on a

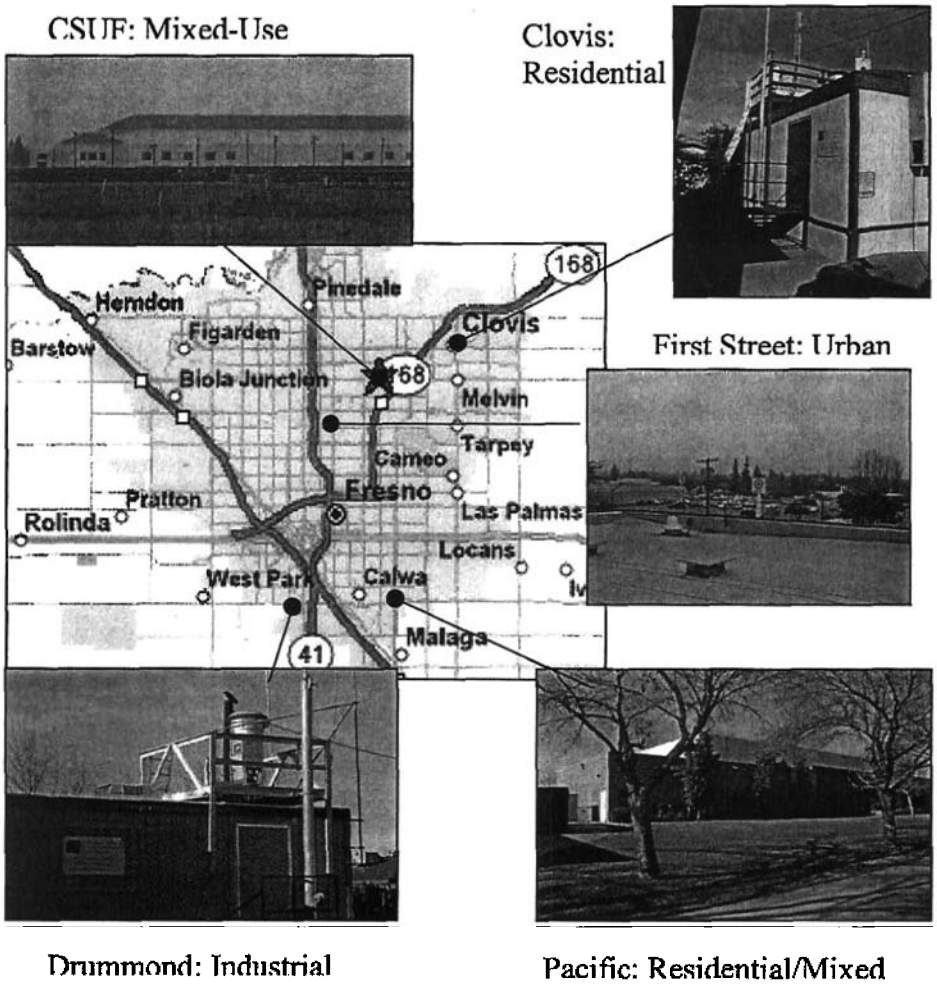

Figure 1. Map of the city of Fresno and the location/classification of the five sampling sites.

slotted pre-filter and a second filter captured smaller sized fine particulate matter less than 2.5 μm aerodynamic diameter ($PM_{2.5}$). The size fraction of the coarse material collected on the slotted pre-filter is dependent on the design of the collector. Two different types of high-volume

collectors were used: at First Street, CSUF and Pacific the coarse fraction is Total Suspended Particles (TSP) greater than $PM_{2.5}$, whereas the collectors at Clovis and Drummond had a size cut on the inlet limiting the coarse fraction to PM_{10} greater than $PM_{2.5}$. The collectors at Clovis and Drummond were owned by the SJVUAPCD and operated by them once every six days. CSU was authorized to use these instruments when they were not operated by SJVUAPCD, thus the data from these sites have regular data gaps appearing for 48-hour intervals once every six days. The collector at First Street is owned by the California Air Resources Board (CARB).

1.3.2 Phase II

The second phase of the study began after the conclusion of Phase I; however, the design of Phase II was considered in conjunction with Phase I. In keeping with the objectives, the mass concentration of $PM_{2.5}$ was determined to provide a fundamental understanding of spatial and temporal variability. All coarse and fine samples were analyzed to determine the carbonaceous component of collected matter and the concentration of the wood smoke marker levoglucosan. The quantity of carbonaceous material that is water soluble was determined for only $PM_{2.5}$ samples. A subset of $PM_{2.5}$ samples and site composite samples were analyzed via GC/MS quantifying specific chemical tracers to provide detailed information for source apportionment.

Results of previous studies show that the mass composition of wintertime $PM_{2.5}$ in Fresno is generally evenly distributed between inorganic and organic components, with ammonium nitrate comprising the majority of the inorganic fraction (Watson and Chow, 2002b). While efforts geared towards further understanding the sources of precursors and conditions favorable to ammonium nitrate formation continue elsewhere (Pun and Seigneur, 1999, 2001; Battye, Aneja, and Roelle, 2003; Fitz et al., 2003), the focus of this study is the chemical speciation of the organic fraction. Chemical species are defined as "organic" if they contain at least one atom of carbon bound to a hydrogen atom. Since carbon is so prevalent in the earth/atmosphere system (Seinfeld and Pandis, 1998), many thousands of compounds found in the atmosphere contain

carbon. Classifying these compounds individually is highly difficult, and typically only a small fraction of all organic compounds are classified (Schauer et al., 1996b; Schauer and Cass, 2000; Brown et al., 2002; Zheng et al., 2002). Although this study will classify a portion of the organic fraction in select samples, the total carbonaceous fraction of all samples collected will be quantified by a Sunset Laboratory, Inc. Semi-Continuous OCEC Analyzer.

Once the carbonaceous fraction of samples is quantified, it is of interest to determine what portion of the carbon is water soluble. The water soluble organics affect the scavenging and uptake of carbonaceous $PM_{2.5}$ into aqueous droplets (Novakov and Corrigan, 1996), which is important in removal processes such as wet deposition and aqueous phase chemical reactions followed by droplet evaporation. Aqueous phase reactions can be of pivotal importance in areas that routinely experience fog formation and evaporation cycles, like those observed in the San Joaquin Valley during winter (Holets and Swanson, 1981; Jacob et al., 1986; Jacob et al., 1987; Pandis and Seinfeld, 1989). The details of processes specifically related to Fresno fog events are evaluated in a tandem study and analyzed elsewhere; however, discussion of variations in $PM_{2.5}$, TC, water soluble carbon, and other pollutants would be misrepresented without inclusion of meteorological influences such as temperature, precipitation, and fog formation.

In keeping with the objectives of this study, the quantification of wood smoke is of critical importance, comprising the major focus of our efforts. Commonly a source's contribution to total $PM_{2.5}$ is estimated by quantifying a source specific chemical tracer (Simoneit, 1999); in other words, a unique chemical compound is used to trace the contribution of emissions from a source at the point of collection. There are several requirements for a compound to be considered an ideal tracer. First of all, the chemical tracer must be source specific, meaning that only one source type produces that compound. Additionally, a tracer should not be readily reactive or otherwise easily removed under atmospheric conditions and typical transport timeframes. The tracer should be emitted at a defined, detectible rate. Most often organic tracers are identified and quantified with Gas Chromatography coupled with Mass Spectrometry (GC-MS). In addition to

this traditional approach, a new technique will be applied here to quantify a common tracer for biomass combustion.

The goals of this study include the application of a newly developed analytical technique designed to quantify levoglucosan, a wood smoke marker, in ambient samples. Past studies have shown a variety of chemical compounds are potential candidates for biomass combustion tracers, including vanillin, acetovanillone, retene, resin acids, and levoglucosan (Simoneit et al., 1993; Standley and Simoneit, 1994; Nolte et al., 2001; Schauer et al., 2001; Hays et al., 2002; Fine, Cass, and Simoneit, 2004a). Relative to the other tracers levoglucosan is emitted in large quantities and is present in the combustion of all types of biomass (Simoneit, 1999; Fine, Cass, and Simoneit, 2004a), while other tracers can be specific to a type of wood or plant part (i.e. leaf, bark, needles). Levoglucosan is present in all biomass burning samples since it is produced by the oxidation (i.e. combustion) of cellulose, a main component of plant cell walls providing structural support for plants. However, different types of biomass emit varying levels of levoglucosan which make source apportionment difficult without knowing the type of biomass combusted and burn conditions (Simoneit, 2002; Engling et al., 2005). Other than this complication, levoglucosan is thought to meet the major requirements for tracer species mentioned above (Fraser and Lakshmanan, 2000). The details regarding the quantification of levoglucosan and other anhydrosugars associated with biomass combustion by liquid chromatography are discussed in detail in Chapter 2.4.

Gas Chromatography coupled with Mass Spectrometery (GC/MS) has been used in the past to quantify and speciate numerous organic compounds in ambient PM samples (Schauer et al., 1996a; Schauer and Cass, 2000; Zheng et al., 2000; Jeon et al., 2001; Zheng et al., 2002; bin Abas, Oros, and Simoneit, 2004). The quantification of specific compounds is especially important for tracers, like levoglucosan. Several dozen tracers are commonly quantified via GC/MS to estimate the contribution of sources recognized to be important in urban regions (Rogge et al., 1993b; Cass, 1998; Schauer and Cass, 2000; Zheng et al., 2002). During winter-

time in Fresno, sources that generally contribute the most to ambient $PM_{2.5}$ levels include motor vehicles, meat cooking operations, and wood smoke (Schauer and Cass, 2000). Thus, efforts in this study are directed towards quantifying markers for these three sources. As discussed already, levoglucosan is a common tracer for biomass combustion. Other tracers include hopanes for motor vehicle emission sources and cholesterol for meat cooking operations. In addition to the quantification of source tracers, condensed phase alkanes and PAHs were examined in samples analyzed by GC/MS.

Once the chemical tracers for major sources are quantified, one needs to determine contributions of emissions generated by each source relative to total aerosol concentrations. Previously published source profiles are used to convert measured source tracer concentrations into relative source contributions. Source profiles are produced by collection of emissions from one source type, such as a car, a diesel truck, charbroiling of meat, etc., in a controlled environment (note that these conditions do not always accurately reproduce real world conditions and as such the source profiles are subject to error) (Schauer et al., 1999b, 1999a, 2001). The process used to estimate the particulate contributions from major sources is discussed in detail in Chapter 3.6.

CHAPTER 2 METHODOLOGY

2.1 Phase I: Sample collection and filter handling

Ambient aerosol samples were collected with high-volume instruments at five sites in Fresno from December 24, 2003 until January 15, 2004. High-volume collectors were deployed at all five sites and collected 20-hour average samples. The instruments were operated from 14h00 to 10h00, local time, to accurately capture major sources and still allow sufficient time for filter exchange at all sites. The high-volume collector used at First Street, CSUF and Pacific is an Andersen type model, equipped with a Tisch Series 231 $PM_{2.5}$ impactor plate. The type of collector and impaction plates used at Clovis and Drummond sites are similar to the other sites, with the exception of a PM_{10} inlet attached to limit coarse filter loading. Photographs in Figure 2 compare Hi-Vol instruments with and without a PM_{10} inlet. The instruments were operated for the specified time interval with the exception of the Pacific site. The instrument at Pacific was not operational until December 28th, 2003. The flow rate at all sites was checked by a Thermo Andersen high-volume calibration kit and maintained at 1.13 m^3/minute ±20%. Over the study period 84% of the samples were within ±10% of 1.13 m^3/minute and all instruments were within ±20% all the time. The operational flow rate was recorded automatically by each instrument on Tisch TE-106 recording charts. From this record the instrument flow rate was known and used in subsequent calculations of ambient concentrations. Samples were collected on pre-fired Whatman quartz fiber filters (QM-A size 20.3 x 25.4 cm (515.6 cm^2)). The area of particle impaction on the filter was somewhat smaller (413 cm^2) as limited by the filter holder. Filters were baked at 600° C for 6 or more hours prior to weighing and sampling. Weighed filters were stored individually in baked aluminum foil jackets and frozen both pre- and post- sampling.

Blank filters were collected several times at each site throughout the study to monitor for sampling artifacts caused by handling, transport, and instrument operation.

Other sampling artifacts may arise that can not be accounted for with a simple blank correction: positive artifacts include filter adsorption of gaseous Semi-Volatile Organic Compounds (SVOCs); negative artifacts include the volatilization of condensed phase SVOCs due to temperature increases or pressure drop. Loss of sample is also possible from rough handling. The positive artifact caused by VOC adsorption is difficult to quantify, although an estimation method is performed as described further in Chapter 3.3.2. No known method is available to estimate SVOC sampling loss post collection, but sampling loss has been reported to range from zero to 80% (Turpin, et al., 2000). After sample collection, care was taken to minimize additional losses by keeping samples frozen until measurement. Additionally, no SVOCs were used as tracers in this study to minimize any error in source apportionment resulting from sampling artifacts.

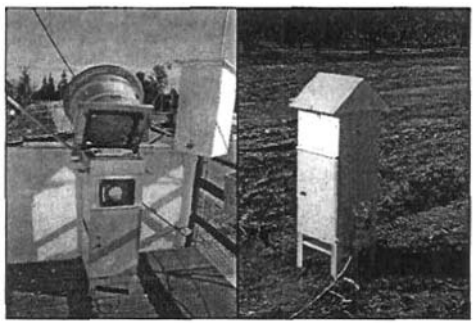

Figure 2. Hi-Vol instruments with a PM_{10} inlet (left side) and without a PM_{10} inlet (right side).

2.2 Mass Determination of $PM_{2.5}$

Measurements of $PM_{2.5}$ mass were made to calculate the variation in ambient fine particle concentrations throughout the duration of the study. The high-volume filters were weighed both pre- and post- sampling on a Mettler Toledo AB104-S scale equipped with a filter weighing chamber. The mass concentration of ambient $PM_{2.5}$ was calculated to be the mass difference between pre- and post exposure measurements (i.e. total mass loading) divided by the total

volume of air (at ambient conditions) that passed through the filter during sampling. The ambient flow measurements recorded for the Hi-Vol multiplied by the recorded length of operation determines the volume of air that passed through the filter. To reduce error while measuring mass accumulation, the filters were allowed to equilibrate in a glove box with stable atmospheric temperature and relative humidity prior to weighing. Humidity control is important to ensure consistent conditions while weighing filters, otherwise the mass can fluctuate because of water vapor adsorption/desorption by collected hygroscopic particles and the quartz itself. The temperature was maintained at 20° ± 5° C and recorded when filters were weighed. The relative humidity was maintained to 35%± 5% R.H. in the glove box by equilibrium with an aqueous solution of saturated calcium chloride. This technique was consistent for both pre- and post-exposure in order to minimize measurement uncertainty when weighing the filters. Method tests were performed prior to filter measurement to test the mass variability and it was found that the masses of the filters stabilize after 48 hours in a stable environment.

Quality Assurance and Quality Control (QA/QC) procedures were implemented to promote and evaluate mass measurement quality. The published accuracy for the balance is 0.2 mg and the precision is 0.1 mg up to the maximum weight of 110 g (Mettler Toledo). The minimum detection level (MDL) is 0.1 mg. Given the published precision and accuracy of this model the total uncertainty is 0.3 mg which is an error of less than 5% for all samples (confidence level not published by Mettler Toledo). All valid data were within the Limit of Quantification (LOQ) for this instrument. The LOQ is defined as values above 10 times the standard deviation of the MDL and below the instrument's limit of linearity. Given a precision of 0.1 mg the lower LOQ is 1.0 mg. All filters, with the exception of some blank checks and a sample where the Hi-Vol did not appear to function, had both raw masses and total mass accumulations above this limit and well below the maximum weight of 110g.

To quality assure the $PM_{2.5}$ mass measurement method, the mass concentration for the First Street site as generated with the method used here was compared with data collected and

published by the California Air Resources Board (CARB) at the same site using a beta attenuation monitor (BAM). Based on hourly average $BAM_{2.5}$ measurements over identical operation periods, the trends in $PM_{2.5}$ are well correlated with a squared correlation coefficient of 0.81 and track each other well (see Figure 3); however, the values measured by CSU lab are greater than those reported by CARB, averaging 14% more than CARB. Care must be taken comparing integrated samples, such as those collected for this study, with continuous sampling as

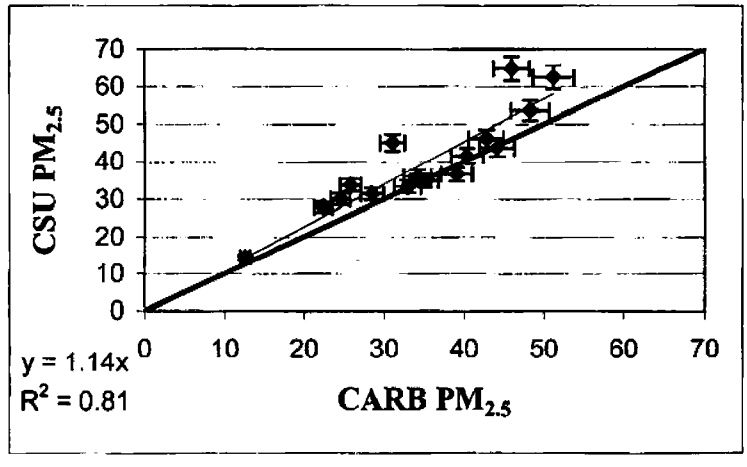

Figure 3. Comparison of CSU lab's 20-hour average $PM_{2.5}$ mass concentration to averaging of CARB's hourly $PM_{2.5}$ mass concentration. The bold line is the 1-to-1 ratio, while the light line is a linear regression between the two measurements. A five percent error is shown for both instruments.

past studies have shown discrepancies are possible (Pang et al., 2001; Watson and Chow, 2002a). The difference between measurements is thought to be due to divergent positive and negative artifacts routinely experienced by both instruments. Although Courtney et al. documented that the BAM instrument corresponds well with gravimetric mass measurements (within 5% at the 90% confidence limit), other studies have shown that BAM instruments can underestimate $PM_{2.5}$ mass (Courtney, Shaw, and Dzubay, 1982; Watson et al., 2002). This is thought to be due to heating of collected samples which could lead to volatilization of SVOCs and other semi-volatiles like ammonium nitrate (i.e. a negative sampling artifact). On the other hand, quartz fiber filters, as used in the high-volume instruments, are documented to have positive SVOC adsorption artifacts (Turpin, Saxena, and Andrews, 2000; Kirchstetter, Corrigan, and Novakov, 2001; Mader

and Pankow, 2001; Subramanian et al., 2004). Considering these opposing sampling artifacts, the correlation between these two different methods is sufficiently high to give confidence in our measured values.

To provide a quality check of the mass determination procedures used at the CSU laboratory, a subset of 5 samples was sent to an independent laboratory, the Colorado Department of Public Health and Environment Laboratory in Denver (CDPHE). The mass determinations at CDPHE were performed at 22 degC and 30% RH for tare and 22 degC and 38% RH for final weights. The results from both laboratories are detailed in Table 1. Both laboratories compare very well for the first 4 samples, with differences of 3% or less. For the last filter there is a surprisingly large difference between both laboratories. No obvious cause has been identified, but it is possible that some material was lost during shipping. The result is surprising, especially considering the agreement between sites and measurement results detailed in Chapter 3.2.

Table 1. Comparison of filter weight differences (g) between CSU and CDPHE.

Filter ID	CSU	CDPHE	% difference
43	0.0572	0.0581	1.6
44	0.0499	0.0514	3.0
45	0.0651	0.0634	-2.6
46	0.0498	0.0510	2.4
48	0.0366	0.0270	-26.2

2.3 Carbonaceous Composition

2.3.1 Measurement Method

The Sunset Laboratory Carbon Aerosol Analysis Field Instrument is a self-contained unit with the exception of external gases and pump shown in Figure 4. The instrument is designed to collect and analyze air samples in real time; however, it was not operated in this manner for the objectives of the study. Instead, discrete filter samples were analyzed post- collection and weighing. The Sunset Analyzer utilizes a thermal-optical technique to quantify total carbon (TC), the sum of organic carbon (OC) and elemental, or "black", carbon (EC). For more details

regarding instrument design and application see previously published articles (Birch and Cary, 1996; Chow et al., 2001). The method of analysis involves optical monitoring of the sample combined with detection of carbon volatilized or combusted in two different gaseous environments with temperatures slowly increased to 870° C. First, with non-reactive helium gas, elevated temperatures are used to volatilize the optically non-absorbing OC in two temperature stages, then the temperature is decreased and the procedure for oxidizing the optically absorbing EC begins with the addition of a mixture of 90% helium/10% oxygen gas. Table 2 shows the temperature ramping routine, the gases used, and the duration of each stage as specified for this study. It is expected that some of the OC pyrolyzes into EC under the high temperatures in an oxygen starved atmosphere. This is corrected for with the optical monitoring of the sample. Much controversy exists regarding the method to detect and quantify pyrolyzed OC (POC) and the issues that pertain directly to this study are discussed below. The carbon species that evolve from the sample are converted to CO_2 by passing through a chamber containing a bed of MnO_2. The produced CO_2 is then measured directly by a non-dispersive infrared detector (NDIR). The final phase of the Sunset's program routine is internal calibration of the NDIR with methane gas and the instrument response is applied to the final calculation of OC, EC, and TC.

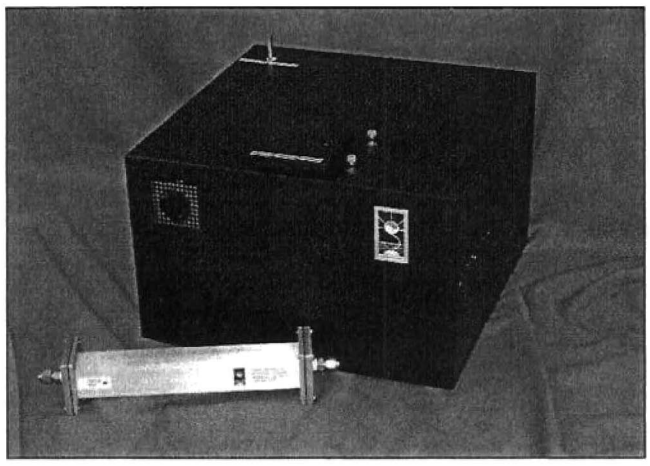

Figure 4. Sunset Laboratory Semi-Continuous Carbon Analyzer [photo from Sunset Laboratory's website, 2004].

Table 2. Sunset OCEC Analyzer environmental controls and routine for sample analysis.

Program Activity	Carrier Gas	Ramp Time (s)	Program Temperature (°C)
Oven Purge	Helium	10	Ambient
1st Ramp	Helium	80	600
2nd Ramp	Helium	90	870
Stabilize Temp	Helium	20	600
He/Ox 1st Ramp	Helium/Ox	40	670
He/Ox 2nd Ramp	Helium/Ox	110	870
Internal Std.Calibration	Cal Gas He/CH4	120	0
Cool down	Helium	various	

The Sunset Carbon Analyzer was used to measure the carbonaceous fraction of all samples collected, both coarse and fine fractions. The total exposed filter area of the fine filters is 413 cm^2, from which a small circular punch of 1.98 cm^2 is taken for analysis. The slitted coarse filters have ten slits where particles greater than 2.5 μm aerodynamic diameter impact. A small circular punch was removed from coarse filters for carbon analysis; however, the coarse material impacted on the filter is a small fraction of the surface area analyzed. The area of coarse particle deposition was measured for each site and the mass of OC and EC on the filter punch were scaled relative to the total deposition area.

To improve the accuracy of results, each $PM_{2.5}$ filter sample was analyzed twice by the Sunset method. A visual examination of the $PM_{2.5}$ filters showed obvious indications of uneven filter deposits, a result of the overlying slitted impactor. Analysis of one filter punch from such uneven deposition could result in under or over estimation of the $PM_{2.5}$ carbonaceous composition. For large filter areas, such as those used for liquid extraction, the noise due to non-homogeneous filter loading is adequately averaged, but for the small area analyzed by the Sunset OC/EC filter inhomogeneities were shown to cause a substantial error. Statistical analysis of results from testing a single $PM_{2.5}$ filter eighteen different times demonstrated that at a 95%

confidence level there would be a 16% and 30% uncertainty in OC and EC values, respectively, if each sample was analyzed only once. On the other hand, by averaging the results of two duplicate tests there would be only a 10% uncertainty in TC at the 95% confidence level. Based on this, two punches from each $PM_{2.5}$ filter are averaged to reduce error associated with non-homogeneous deposits. A scatter plot of duplicate measurements for all $PM_{2.5}$ samples demonstrated that OC was consistent and reproducible with a linear least squares regression correlation coefficient (R^2) of 0.98, but EC values were more variable with an R^2 of 0.86. Coarse filters do not require duplicate carbon measurements since there was no indication of non-uniform deposition.

To convert the mass results detected by the instrument into ambient concentrations of OC, EC, and TC several steps are required. As mentioned above, the mass of $PM_{2.5}$ filter OC and EC in the following calculations are an average of the masses reported for two replicates from the same filter. First, the mass values are scaled by the area of the exposed filter punch relative to the total exposed filter area. Total filter OC as measured by the OC/EC Analyzer is multiplied by a conversion factor of 1.6 to estimate the actual organic mass (OM). This multiplier converts measured carbon mass to an estimate of the actual mass of carbonaceous species which includes hydrogen, oxygen, and other substituents that are not directly measured by the OC/EC Carbon Analyzer. The selection of this particular value for the OC multiplier is two-fold. A common multiplier in winter urban environments is typically 1.4 (Turpin and Lim, 2001) based on mass closure calculations, which is consistent with organic mass-to-organic carbon ratios measured by Fourier Transform Infrared (FTIR) spectroscopy for Asian samples (Russell, 2003). Urban multipliers are generally lower than rural multipliers since emissions are primarily anthropogenic and not significantly oxidized. On the other hand, results from areas heavily impacted by biomass burning typically necessitate higher multipliers: values as high as 2.5 have been reported for Fresno (Turpin and Lim, 2001). For this study, however, multipliers higher than 1.8 result in an estimated carbonaceous mass in excess of total measured $PM_{2.5}$ mass for some samples. Thus,

a conservative value of 1.6 was selected for this study. Most likely the ratio of actual organic mass to carbon mass is not constant throughout the sample collection period, much less through the study period; a fact which further complicates the estimation of OM by the application of a single scaling factor (Russell, 2003). For some sites and days the multiplier 1.6 might be too large or too small. Total carbon mass (TC') is then the sum of EC and OM. To convert mass values into ambient concentrations, the mass is divided by the total volume of air (at ambient conditions) that passed through the filter, similar to the method of calculating $PM_{2.5}$ mass concentration.

2.3.2 Known Interferences

There are several known sources of interference, and there are methods to detect and correct for some of these. Known interferences include the presence of Carbonate Carbon (CC), an inorganic carbon species; problems associated with the determination of pyrolized OC; and filter adsorption of VOCs. Carbonate Carbon is known to volatilize or combust at a wide range of temperatures and can confound results quantifying OC and EC (Chow et al., 2001). There is a test that can be performed to quantify the concentration of CC if the results of the Sunset instrument report values of CC above zero; however, this was not deemed necessary since there was no CC indicated in the samples analyzed.

As discussed briefly above, it is known that in an oxygen starved atmosphere under high temperatures OC can be chemically reduced into EC. The method to accurately quantify and correct for this miscategorization of carbon species is widely disputed (Birch and Cary, 1996; Chow et al., 2001; Bae et al., 2004; Chow et al., 2004). The general premise of quantification revolves around the optical properties of the two compounds: OC is theoretically non-absorbing whereas EC effectively absorbs light in the visible range and is "dark". When the OC is reduced to EC, the sample's optical properties change and the transmission or reflectance of light through the sample decreases. Two primary methods exist to measure this difference between pyrolized

organic carbon (POC) and the original EC: the method used in the Sunset instrument detects the change in light transmission through the sample with a laser, the other method used by Desert Research Institute (DRI) and the IMPROVE program detects the change in the filter surface reflectance. Both methods determine POC to be the quantity of carbon detected from the point of O_2/He atmosphere initiation until the sample returns to the level of original transmission (reflection) intensity and the carbon detected after this point is assumed to be the original EC. An underlying assumption of both methods of POC detection/quantification is that POC has the same light absorbance/reflectance as EC. The main controversy arises because different methods of determining the POC/EC split point demonstrate a systematic variation, while the quantification of TC is generally constant between the two techniques (Chow et al., 2001). Generally, EC from higher temperature protocols is less than for lower temperature protocols, and as such the EC values reported in this study are less than what would be reported from an IMPROVE system. One theory regarding this difference suggests that mineral oxides at high temperatures oxidize EC to OC causing premature volatilization and detection (Chow et al., 2001; Chow et al., 2004). In past studies of Fresno PM a reddish color remained on samples following thermal analysis which might be an indication of mineral deposits (Chow et al., 2004). Similar residual effects were evident on coarse samples collected during this study and laser transmission increased in these samples prior to the initiation of the oxygen stage: an indication of early POC/EC evolution.

An additional source of interference is the adsorption of volatile or gas phase semi-volatile organic compounds onto the quartz filter during sampling, which erroneously increases the measured mass of carbonaceous particulate matter. Quartz fiber filters are recognized as having a large BET surface area relative to other filter materials: BET is a measure of the availability of surface area for gaseous adsorption (Turpin, Huntzicker, and Hering, 1994). Thus, quartz filters are prone to a larger adsorption artifact than other filter surfaces (Turpin, Huntzicker, and Hering, 1994; Turpin, Saxena, and Andrews, 2000; Mader and Pankow, 2001; Subramanian et al., 2004); however, quartz does not thermally decompose in the high temperature

environment of both the DRI/IMPROVE and NIOSH/Sunset carbon analysis instruments. In order to accurately quantify the composition of collected $PM_{2.5}$, this adsorption artifact must be removed from measured OC mass. The best method to accurately measure both positive and negative artifacts involves the use of a split stream inlet with one portion of the flow passing through a denuder prior to the quartz filter followed by a carbon impregnated glass (CIG) filter which captures volatilized PM. The other portion of the flow is used to blank correct for denuder break through and sequentially passes through Teflon, a denuder, quartz filter, and CIG filter. This method is very expensive and complex (Turpin, Saxena, and Andrews, 2000; Subramanian et al., 2004). Instead, the method used to quantify adsorption in this study involves slicing a subset of filters through the plane of the filter producing a top half with the $PM_{2.5}$ deposition and a bottom half, which should not contain any organic material. Theoretically carbon measured on the bottom portion of the filter should be only adsorbed SVOCs because particulate matter will not penetrate far past the filter surface. One can then correct for the gaseous adsorption to the particulate fraction by subtracting the bottom, gaseous component, from the top. This slicing method is theoretically similar to the analysis of two quartz fiber filters placed perpendicular to direction of air flow; however, the depth of the filter which the air flows through is different. Results of testing the adsorption of a quartz filter placed behind a quartz filter (QBQ) have shown that an average of 20% of OC is attributable to adsorption in Fresno filters (Watson and Chow, 2002a), but values from other samples collected elsewhere have been as high as 50% (Turpin, Huntzicker, and Hering, 1994). A comparison between slicing one filter and taking the difference versus the QBQ method show that if the OC from the back half of a filter represents its SVOC adsorption, then the adsorption fraction will be approximately 70% greater than estimated by the QBQ method. Importantly, split stream samplers have demonstrated QBQ values that are approximately half that of quartz filters behind Teflon (QBT) (McDow and Huntzicker, 1990), so perhaps the method of slicing is quantitatively more similar to QBT, while theoretically more similar to QBQ.

2.3.3 Quality Control/Quality Assurance

Quality Control (QC) procedures were implemented to ensure and evaluate data quality, while Quality Assurance (QA) procedures involve independent checks to verify results. Quality control of the system's performance entailed the incorporation of blank measurements, establishment of detection limits, and in-house quantification of instrument precision and accuracy. In addition to quality control procedures, a subset of filters was sent to Sunset Labs for quality assurance purposes.

Evaluation of data quality from the Sunset Laboratory Carbon Analyzer includes several different tests, the results from which are compared with expected instrument performance as published by Sunset Labs. Sunset Laboratories has published the method detection limit (MDL), the limit of quantitation (LOQ), and precision/accuracy estimates for samples analyzed by the NIOSH method and their field instrument is expected to be similar. Sunset Laboratory publishes the Minimum Quantifiable Limit of this instrument as 0.2 μg (Sunset Laboratories). The LOQ as published for the NIOSH method is between 5 and 400 $\mu g/cm^2$ for OC and between 1 and 15 $\mu g/cm^2$ for EC. Independent tests performed in our lab (as explained below) validate the reported values. The measurement of blank filters is an assurance of correct instrument operation and field blanks can be used to establish detection limits. The lower limit of the LOQ is defined as 10 times the standard deviation of field blanks. The MDL estimates for single and paired measurements are calculated as shown in equation 2-1 and 2-2, respectively, where the critical t values are for the 99% confidence level based on a two-tailed t-test (Skoog, West, and Holler, 1996). The degree of freedom is equal to the number of duplicate measurements (1 or 2 depending on single or paired tests) plus the number of method blanks analyzed (N) minus two. The value $s_{\text{method blanks}}$ is the standard deviation of the method blanks.

$$MDL_{single} = t_{critical} * s_{method\ blanks} * \sqrt{((1+N)/1*N)} \quad \text{(Eq. 2-1)}$$

$$MDL_{paired} = t_{critical} * s_{method\ blanks} * \sqrt{((2+N)/2*N)} \quad \text{(Eq. 2-2)}$$

The MDL, Reliable Detection Limit (RDL), and LOQ for the Sunset Carbon Analyzer as calculated from field blanks for single and paired tests are reported in Table 3. The RDL is twice the value of the MDL: minimizing the probability of reporting a false negative. The coarse filters were analyzed once and thus correspond to the limits reported for single tests (Eq. 2-1), whereas the $PM_{2.5}$ filters were analyzed twice to minimize error from non-homogeneous deposits and correspond to limits for paired tests. The MDL for both OC and TC as estimated from field blanks is approximately 10 times the 0.2 $\mu g/cm^2$ published. It is important to note that the evaluation of actual blanks produces an MDL of 0.5 $\mu g/cm^2$ for OC and 0.05 $\mu g/cm^2$ for EC, which corresponds well with the estimates published by Sunset. A comparison of the LOQ estimated here to that published for the NIOSH method shows that the LOQ for OC is similar, but for EC our estimates are about half of the NIOSH values.

Table 3. Independent estimate of method detection limit (MDL), reliable detection limit (RDL), and limit of quantitation (LOQ) for OC, EC and TC based on the standard deviation of 19 method blanks.

	OC ($\mu g/cm^2$)			EC ($\mu g/cm^2$)			TC ($\mu g/cm^2$)		
	MDL	RDL	LOQ	MDL	RDL	LOQ	MDL	RDL	LOQ
Coarse filters	1.84	3.68	6.23	0.15	0.30	0.51	1.81	3.62	6.12
$PM_{2.5}$ filters	1.34	2.67	6.23	0.11	0.22	0.51	1.31	2.63	6.12

The precision and accuracy of the NIOSH method as reported by Sunset Labs are between 4 and 6%. Independent estimates of accuracy and precision tested here result in a 12% error in accuracy and 13% error in precision. The precision of the instrument for the replicate test performed on one non-uniformly deposited filter is ±13%, 14% and 28% for TC, OC, and EC, respectively at a 99% confidence limit, which is larger than published precision because of non-uniform sample deposition. The accuracy of the instrument is tested through the use of spiked samples. Sunset Laboratory estimates the uncertainty of the instrument to be the MDL plus the error in accuracy:

$$\text{Uncertainty} = 0.2\ \mu g + 0.05 * \text{mass} \qquad \text{(Eq. 2-3)}$$

The uncertainty estimated by Sunset labs is less than the uncertainty measured by the accuracy tests described above as both the MDL and accuracy measurements based on field blanks are larger than published values. When reporting the data, uncertainty estimates and the MDL generated by instrument operation in our lab are included.

Quality assurance of the results presented here is performed by comparing 10 samples' OC/EC values with independent measurements from Sunset labs. The overall TC results compared favorably between the two labs with a strong correlation R^2=0.999, but a positive 15% bias by CSU labs. The bias is mostly due to inconsistent EC values for which CSU labs had an average 50% positive bias (based on a linear least squares regression with an R^2=0.95), while the OC bias of 9% (R^2=0.998) was within range of other inter-laboratory comparison studies (Schauer et al., 2003). The inter-comparison study performed by Schauer et al. published that inter-laboratory EC precision ranged from 6-21%, which is approximately half of the bias shown for this study. It is difficult to assess the relative difference between our inter-comparison and Schauer et al.'s inter-comparison because inter-laboratory differences are a function of filter loading and the filter loading of the Fresno filters is larger than in the inter-comparison study.

There are several possibilities to explain this large deviance in EC values between the two labs. Interestingly, Schauer et al. 2003 demonstrated that the OC/EC split for wood smoke emissions is highly sensitive to the temperature ramping routine. As the temperatures in the first stage (OC evolution) decreased, the proportion of EC detected increased. The authors attributed this increase in EC to OC which did not evolve at low temperatures. Alternatively, as Chow et al. suggest, high initial temperatures in a reducing atmosphere could potentially oxidize EC in the presence of minerals causing premature evolution and false detection of EC (Chow et al., 2001). In the operation of the Sunset instrument at CSU, the OC temperature maximum is equal to the maximum in Schauer et al.'s intercomparison study (see Table 2); however, it is possible that the duration of the routine was insufficient for complete OC evolution.

Notably, a manual delay of the automatic split point by 4 seconds reduces the bias in EC results, but increases it for OC. The EC error with this adjustment is 5% while the OC error is 15%: both measures have improved correlations. TC results remained the same. A 15% lab difference is close to the OC precision range of 4-13% published by the inter-comparison study (Schauer et al., 2003). A portion of this inter-laboratory difference may also be due to filter deposit inhomogeneity.

2.3.4 Water Soluble Organic Carbon

To test the carbonaceous water soluble fraction of collected $PM_{2.5}$ samples, aqueous sample extracts are analyzed by a Shimadzu TOC-5000A analyzer. The aqueous extract analyzed by the TOC Analyzer is the remaining extract from the aqueous extraction process outlined in detail in Chapter 2.4.2. The TOC Analyzer analyzes aqueous total carbon content and inorganic carbon content. The difference between these is Total Organic Carbon or TOC, hereafter referred to as Water Soluble Organic Carbon (WSOC) to reduce confusion with total particulate carbon results estimated by the Sunset OC/EC Analyzer. The TOC instrument was calibrated prior to analysis of $PM_{2.5}$ aqueous extracts and the calibration was verified at the beginning of each analysis day.

Interference from dissolved carbon dioxide gas was minimized. When aqueous solutions are exposed to air carbon dioxide (CO_2), which is water soluble, is known to diffuse into the solution. Since the TOC analyzer measures inorganic carbon, carbon dioxide would be detected and quantified as aqueous phase inorganic carbon. High levels of inorganic carbon measured by the TOC might be a positive artifact caused by carbon dioxide absorption. To minimize this artifact, care was taken to reduce the exposure to air during extraction and storage procedures.

The uncertainty of the TOC Analyzer is reported to be less than five percent based on analysis of method blanks (Youngster, 2005). All samples analyzed for total water soluble carbon exceeded the instrument's RLD as determined by Youngster; however, the inorganic

component was typically very low, often below detection. The fact that the inorganic measurements were close to zero is an indication that samples were not contaminated by dissolved carbon dioxide. As a gross check of the instrument operation the water soluble total carbon was compared to total particulate carbon: the WSOC content is always less than TC measured by the Sunset OC/EC analyzer.

2.4 Wood Smoke Tracer Quantification via HPAEC-PAD

2.4.1 Instrument design and application

One of the most important aspects of this study is the quantification of daily, site- specific variability of concentrations in the wood smoke tracer levoglucosan. What enables this approach is the application of an established liquid chromatographic technique called high performance anion exchange chromatography (HPAEC) coupled with pulsed amperometric detection (PAD) newly optimized to quantify anhydrosugars such as levoglucosan. Individual compounds are separated and detected by a Dionex DX-500 series ion chromatograph, which consists of a Dionex LC25 Chromatography Oven, Dionex GP50 Gradient Pump, and Dionex ED50 Electrochemical Detector. The ion chromatograph is operated with a Dionex CarboPac PA 10 Analytical Column (4 x 250 mm) with 18 mM aqueous sodium hydroxide eluent. A more basic eluent of 180 mM aqueous sodium hydroxide is run through the instrument for 25 minutes following each injection to clean and regenerate the column. The eluent is carefully prepared to minimize exposure to carbon dioxide and maintained under a pressurized helium system to prevent carbonate formation and subsequent interference.

The HPAEC-PAD system is optimized to detect anhydrosugars, specifically wood smoke markers levoglucosan, mannosan, and galactosan from ambient samples. Upon exiting the separation column, these compounds are oxidized at the surface of an electrode. The oxidized compounds are then charged by an applied voltage and the change in electrical current is measured. The current generated is directly proportional to the analyte concentration and is thus

a direct method of quantification. As a by-product of the oxidation process the electrode surfaces become contaminated and need to be cleaned. This is accomplished by a sequence of raising and lowering the applied voltage. Figure 5 depicts the waveform of the applied potential as used for this study.

The detection of electrical current generated by analyte oxidation and charging is graphically represented in a chromatogram, shown in Figure 6. A chromatogram is a series of

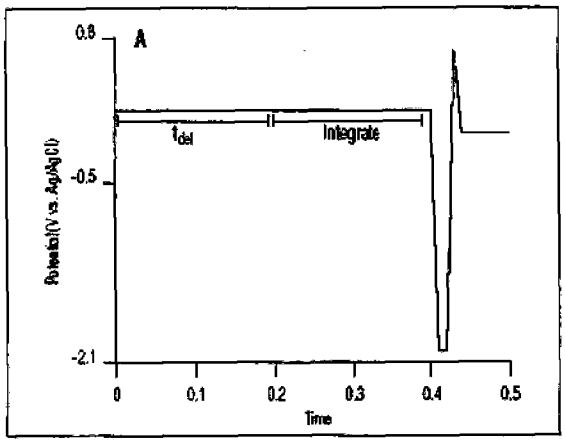

Figure 5. One cycle of the voltage applied across the electrode to charge analyte and clean electrode surface.

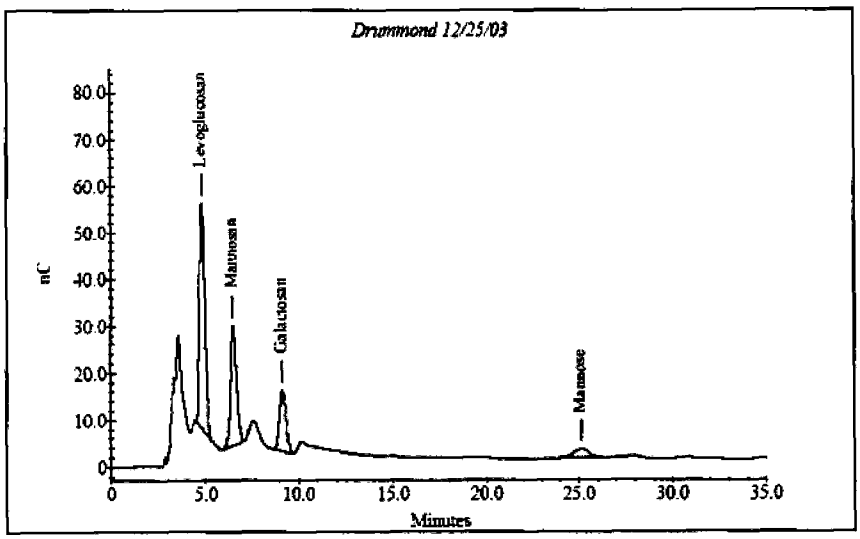

Figure 6. Sample chromatogram produced by HPAEC-PAD showing levoglucosan and other carbohydrates in a sample collected over Christmas Eve.

peaks where the x-axis is in units of time, termed the retention time, which is the length of time required for a species to pass through the column. For the HPAEC-PAD, the y-axis is in units of Coulombs (a measure of charge) and the area of each peak in the chromatogram is proportional to the total compound concentration in the injected sample. The relationship between detected charge and actual analyte concentration is established at the beginning of each day by a calibration of the instrument response to known concentration levels. A least-squares regression between known concentration and detected peak area is performed on a series of 5 or more standards ranging in concentration from 0.02 μg/mL to 5.0 μg/mL. The slope of this regression is the basis for the quantification of individual analytes. Authentic standards are used for calibration and instrument quality control procedures. Instrument checks are performed every 8 to 10 sample injections by injecting a standard of known concentration to control for changes in instrument response. The HPAEC-PAD system as outlined above is used to quantify levoglucosan from an aqueous extract of ambient samples collected in Fresno and map its spatial and temporal variability throughout the city. Although this is not the first study involving an HPAEC-PAD system configured to quantify anhydrosugars from ambient aerosol samples (Gao et al., 2003), very limited information about this technique is available and its use in this study has shed new light on its applications and limitations.

2.4.2 Aqueous Extraction Method

The application of a liquid chromatographic technique to quantify levoglucosan is feasible due to the aqueous solubility of levoglucosan and its suitability for sensitive detection by amperometry. To prepare samples for analysis by HPAEC-PAD, filter fractions must be extracted in an aqueous medium. The aqueous extraction procedure for $PM_{2.5}$ and coarse filters is identical except for different volumes of de-ionized water. Filters were stored frozen prior to aqueous extraction which occurred 5-6 months after collection for fine filters and 10-11 months after collection for coarse filters. Generally, fractions of filter samples are extracted twice using

de-ionized water (using a Barnstead ROpure ST reverse osmosis system and NANOpure ultrapure water system operated with a 0.2 μm filter) and sonicated for 30 minutes each in a Branson 5210 sonic agitator.

Approximately one eighth of the $PM_{2.5}$ filter area is extracted with 15 mL for the first extract and 10mL for the second extract, while one fifth of the coarse filters is extracted with 10 mL for the first extract and 5mL for the second extract. These volumes were selected based on method tests described below and to completely submerge the filter fraction. The amount of coarse filter used for extraction is smaller than the $PM_{2.5}$ filter and in order to minimize sample dilution smaller volumes of water were used for extraction. The first and second extracts are combined with extracted filter piece to allow equilibrium with the water retained in the filter. Insoluble material in the extract is filtered using a microfilter equipped with an injection syringe and Gelman Sciences Pallflex filter (25mm diameter) pre-baked to remove any contaminants. Following extraction and filtration, 100 μL of the aqueous solution extracted from ambient samples is injected into the instrument for analysis and the remaining extract volume is stored in the refrigerator.

The method to extract the collected filters is based on a series of tests analyzing the extraction efficiency and reproducibility for sequential extractions of fine filters. Three different tests were performed with replicate filter extracts to determine the most precise extraction method. Two of the tests compared the extraction efficiency using different volumes of water. Filters were extracted with 15 mL and 10mL of water for 3 extraction/sonication iterations. The precision of replicate extractions improved when comparing 15mL to 10mL extraction volumes: the relative standard deviations (RSD) are 5% and 8%, respectively, for the pooled standard deviation of replicates. This improvement in RSD is thought to be due to complete submersion of the filter with the initial 15 mL volume. The filter absorbs some liquid that is not recoverable and for the second extraction the entire filter is submerged by adding less than 10 mL. It is assumed that the dissolved organic matter is in equilibrium with the water in the filter and the aqueous

solution. Next a test of five sequential extractions using 15 mL was compared to the previous test of three extractions using 15 mL. An increase in variability at lower concentrations was observed, thus the RSD for five extractions was greater than for three extractions: 6% compared to 5%. In order to estimate the relative improvement in extraction efficiency with each extraction iteration, the percent increase in levoglucosan from each extraction is calculated. The percent increase in levoglucosan from an additional extraction demonstrated that 12% of the total levoglucosan is from the second extraction, whereas 0-3% is from the third, fourth, and fifth extracts. Thus, the final extraction method for all filters employs two iterative extractions because the additional sample from the third extract is not deemed significant.

2.4.3 Discovered Interferences

The use of the HPAEC-PAD instrument to quantify the wood smoke marker levoglucosan and other anhydrosugars is widely performed on ambient urban samples for the first time in this study. As with any new analytical technique, laboratory design and quantification of controlled quantities is important; however, application to actual ambient samples can often involve a variety of unanticipated interferences and complications. For this study, the quantification of $PM_{2.5}$ samples by HPAEC-PAD was not hindered by unforeseen difficulties. The quantification of the coarse samples, however, did pose some difficulty. It is known that levoglucosan slowly degrades in aqueous samples, even when refrigerated; however, degradation of levoglucosan from coarse sample extracts appeared to occur much more rapidly than expected. Levoglucosan from various $PM_{2.5}$ samples was tested intermittently over a period spanning several months and the concentration remained stable for longer than one month from extraction. Retesting coarse extracts as soon as 4 days after extraction revealed levoglucosan concentrations that were as low as 10% of the original concentration. The half life of levoglucosan in the coarse filter aqueous extract is on the order of days, while fine filter levoglucosan half life is on the order of weeks or months.

The reduced half-life in coarse sample extracts relative to fine samples is thought to be due to the collection and subsequent activation of coarse microbes. One possible type of microbe is fungal spores which consume levoglucosan and other non-living organic matter as they grow and multiply in the extract solution. These spores are most abundant in the coarse size range as their diameters range in size from one to 10 μm and thrive in moist environments. That their size is generally larger than the $PM_{2.5}$ size cut is potentially why the observed levoglucosan degradation did not occur in the aqueous extract of fine filters. The presence of spores on the stored filters is not likely to decompose levoglucosan prior to aqueous extraction since in a dry/cold environment the spores are not active. There are several possible biocides that could potentially be used to prevent levoglucosan degradation by microbes. Here chloroform was added to coarse samples immediately following extraction. Chloroform was selected due to its availability and low level of human toxicity relative to other biocides. The addition of 100 μL of chloroform to extract solutions (a volume change of less than 1%) unfortunately interfered with the detection of levoglucosan in a non-uniform way. The opportunity to test and resolve the issue of levoglucosan degradation in coarse particle extracts is an area for future work.

2.4.4 Quality Control/Quality Assurance

Quality Control (QC) procedures were implemented to evaluate data quality and establish detection limits, while Quality Assurance (QA) procedures involve verification of results by comparison with a different technique. Quality control of the system's performance entails the incorporation of blank measurements, establishment of detection limits, and in-house quantification of instrument precision. In addition to quality control procedures, a subset of filters was analyzed for levoglucosan by GC/MS for quality assurance purposes. This comparison is included in Chapter 3.4.

As this is a newly developed method for analyzing levoglucosan from ambient samples, there is no available information on detection limits or precision and accuracy. Thus, multiple tests are

performed to estimate the uncertainty associated with this method. A test to establish detection limits from the injection of more than 20 samples of de-ionized water is the basis for the instrument's Limit of Detection (LOD). The result of this test demonstrates the instrument LOD for levoglucosan is 0.01 μg/mL at the 99% confidence level. Note that other significance levels, like the MDL and LOQ, are based on method blanks rather than instrument blanks in a manner similar to the Sunset Carbon Analyzer. Method blanks are those blanks collected during the field study and prepared for analysis in the same manner as all other samples. The MDL, RDL, and LOQ for levoglucosan as analyzed by the HPAEC-PAD at a 99% confidence level are shown in Table 4. The MDL is calculated from analysis of 22 method blanks. The RDL is twice the value of the MDL to minimize the probability of reporting a false negative. LOQ is 10 times the standard deviation of method blanks.

Table 4. Estimate of method detection limit (MDL), reliable detection limit (RDL), and limit of quantitation (LOQ) for levoglucosan analyzed by HPAEC-PAD based on the standard deviation of 22 method blanks.

	MDL (μg/mL)	RDL (μg/mL)	LOQ (μg/mL)
levoglucosan	0.04	0.08	0.13

The precision and accuracy of the HPAEC-PAD should be within 10% at concentrations within the LOQ to have a high confidence in the reported data. Without independent standards the instrument accuracy can not be assessed, thus the following discussion will focus on precision, while a comparison to GC/MS levoglucosan results will provide a qualitative measure of instrument accuracy. The precision of levoglucosan detection with HPAEC-PAD is tested by repeatedly injecting the same standard with a concentration of 3.5 μg/mL. The RSD from this test is 1.3%, which corresponds to an uncertainty of ±4.5% at the 99% confidence level. However, instrument precision is different from the precision calculated from replicate aqueous extraction of samples. The cumulative measurement of precision from both the extraction method and instrument measurement is equivalent to the precision calculated from the aqueous

extraction method tests. The RSD calculated for the extraction method is 3%, which corresponds to an uncertainty of ±9% at a 99% confidence level. Thus, the total uncertainty of the instrument and the extraction procedure combined is ~10% and this is within an acceptable range. When reporting the data uncertainty estimates and the MDL are included.

2.5 GC/MS

Gas Chromatography coupled with Mass Spectrometry (GC/MS) is routinely used to quantify and speciate numerous organic compounds in ambient PM samples (Rogge et al., 1993b; Schauer and Cass, 2000; Brown et al., 2002). The reason that GC/MS is such a powerful analytical tool is that it combines time-resolved quantitative information with compound specific mass fragment information. Thus, this one analytical method can identify, with good certainty, many organic compounds and, if standards of known concentration are available, quantify their concentrations. The instrument used in this study is a HP 6890 Gas Chromatograph coupled to a HP 5973 Mass Selective Detector operating in ion scan mode. A Supelco Equity 5 capillary column (dimensions 30m x 250 um x 0.25um) with a 5% phenyl-methyl-siloxane film to separate individual compounds is operated with an ultra-high purity helium carrier gas. Separation is a function of time as the rate that compounds pass through the column depends on chemical properties that affect solubility such as structure, size and polarity. Some compounds do not elute efficiently as they are too polar; these compounds can be derivatized to improve elution. After the chemical compounds are separated, the carrier gas transports the eluted mixture into the mass spectrometer where compounds are ionized and fragmented by electron impaction. The mass to charge ratios of the ion fragments are measured and produce a distinctive chemical signature depending on the dominant modes of fragmentation and atomic composition. The use of standards of known concentration can be analyzed and the ratio of the instrument peak area to known concentration can be used to quantify individual compound concentrations.

Approximately one μL of sample is injected into the GC/MS; the exact volume is determined with the aid of an internal standard. The GC temperature profile, used to fully separate compounds, initially holds the temperature at 65° C for 10 minutes and then increases the temperature by 10° C/min until reaching 300° C, a temperature that is held constant for another 20 minutes. The entire routine takes 53.5 minutes and data collection begins 6 minutes after injection to allow sufficient time for solvent elution.

As discussed previously, tracers for vehicles, meat cooking, and biomass burning are quantified by GC/MS to perform a rough source apportionment for this study. The specific tracers for these sources are shown in Figure 7. Additional compounds quantified by GC/MS to qualitatively determine primary source influences include condensed phase alkanes, PAHs, and other wood smoke markers. A list of the compounds quantified and associated quantification information are included in Table 5. In areas impacted by biomass burning, levoglucosan is often the most abundant individual organic compound on a mass concentration basis, generally

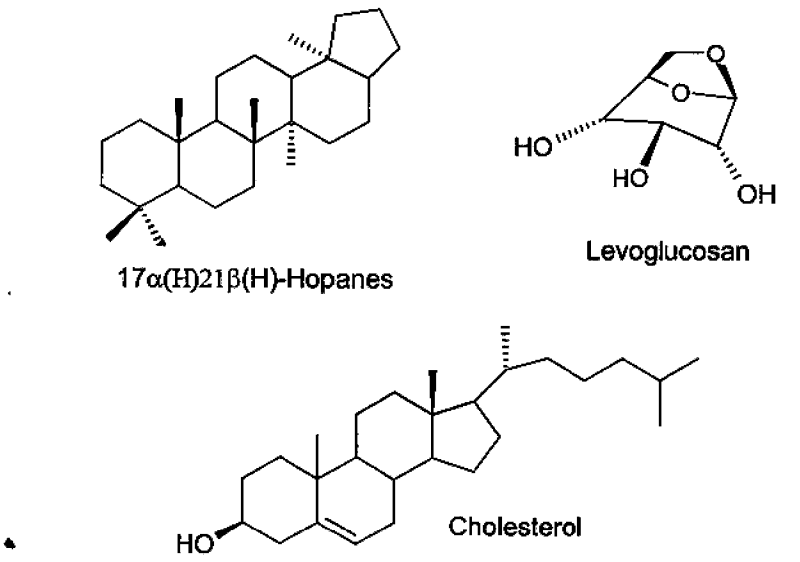

Figure 7. Structures of chemical compounds used as source tracers for the three most significant sources of organic aerosol in Fresno, CA. Cholesterol is a meat cooking tracer, the hopane is a motor vehicle tracer, and levoglucosan is a biomass combustion tracer.

exceeding the next most abundant organic tracer by an order of magnitude or more (Schauer and Cass, 2000; Zheng et al., 2000). Therefore it is not surprising that the concentration of levoglucosan was exceedingly higher than most other tracers. Unfortunately, as a result, samples were extracted for GC/MS twice since levoglucosan in the first extract was heavily concentrated and not quantifiable. This unforeseen problem was costly. The necessity of performing a second extraction highlights an additional, unexpected benefit of the HPAEC-PAD method of levoglucosan quantification, since samples can simply be diluted with de-ionized water if the concentration is outside the calibration range.

Table 5. Compounds quantified by GC/MS and outline of quantification/ calibration method.

Chemical Name	Authentic quantitative standard	Deuterated Internal Standard	Derivatized
N-alkanes			
n-tridecane	Yes	C28D58	No
n-tetradecane	Yes	C28D58	No
n-pentadecane	Yes	C28D58	No
n-hexadecane	Yes	C28D58	No
n-heptadecane	Yes	C28D58	No
n-octadecane	Yes	C28D58	No
n-nonadecane	Yes	C28D58	No
n-icosane	Yes	C28D58	No
n-henicosane	Yes	C28D58	No
n-docosane	Yes	C28D58	No
n-tricosane	Yes	C28D58	No
n-tetracosane	Yes	C28D58	No
n-pentacosane	Yes	C28D58	No
n-hexacosane	Yes	C28D58	No
n-heptacosane	No	C28D58	No
n-octacosane	Yes	C28D58	No
n-nonacosane	No	C28D58	No
n-triacontane	No	C28D58	No
n-hentriacontane	No	C28D58	No
n-dotriacontane	Yes	C28D58	No
n-tritriacontane	No	C28D58	No
n-tetratriacontane	No	C28D58	No
n-pentatriacontane	No	C28D58	No
n-hexatriacontane	Yes	C28D58	No
n-heptatriacontane	No	C28D58	No
n-octatriacontane	No	C28D58	No

Chemical Name	Authentic quantitative standard	Deuterated Internal Standard	Derivatized
n-nonatriacontane	No	C28D58	No
n-tetracontane	No	C28D58	No
Squalene	Yes	C28D58	No
tetramethylpentadecane	Yes	C28D58	No
PAH			
retene	Yes	chrysene-d12	No
naphtalene	Yes	chrysene-d12	No
2-methylnaphtalene	Yes	chrysene-d12	No
1-methylnaphtalene	Yes	chrysene-d12	No
phenanthrene	Yes	chrysene-d12	No
anthracene	Yes	chrysene-d12	No
fluoranthene	Yes	chrysene-d12	No
acephenanthrylene	Yes	chrysene-d12	No
pyrene	Yes	chrysene-d12	No
benzo[*c*]phenanthrene	Yes	chrysene-d12	No
benzo[*ghi*]fluoranthene	Yes	chrysene-d12	No
cyclopentacephenanthrylene	Yes	chrysene-d12	No
cyclopenta[*cd*]pyrene	Yes	chrysene-d12	No
benz[*a*]anthracene	Yes	chrysene-d12	No
chrysene+triphenylene	Yes	chrysene-d12	No
benzo[*k*+*b*]fluoranthene	Yes	chrysene-d12	No
benzo[*j*]fluoranthene	Yes	chrysene-d12	No
benzo[*e*]pyrene	Yes	chrysene-d12	No
benzo[*a*]pyrene	Yes	chrysene-d12	No
perylene	Yes	chrysene-d12	No
indeno[1,2,3-*cd*]pyrene	Yes	chrysene-d12	No
dibenzo[*ah*]anthracene	Yes	chrysene-d12	No
benzo[*ghi*]perylene	Yes	chrysene-d12	No
Guaiacol and Substituted Guaiacols			
acetovanillone	Yes	benzaldehyde-d6	No
vanillin	Yes	benzaldehyde-d6	No
guaiacol	Yes	benzaldehyde-d6	No
Meat Tracers and other Sterols			
nonanal[a]	Yes	chrysene-d12	No
cholesterol	Yes	chrysene-d12	Silylated
ergosterol	Yes	chrysene-d12	Silylated
stigmasterol	Yes	chrysene-d12	Silylated
Hopanes and Steranes			
20R, 5α(H),14β(H),17β(H)-cholestane	No	chrysene-d12	No
20S, 5α(H),14β(H),17β(H)-cholestane	No	chrysene-d12	No
20R, 5α(H),14β(H),17α(H)-cholestane	No	chrysene-d12	No

Chemical Name	Authentic quantitative standard	Deuterated Internal Standard	Derivatized
20S,R-5α(H),14β(H),27β (H)-ergostanes	No	chrysene-d12	No
20S,R-5α(H),14β(H),17β (H)-sitosanes	No	chrysene-d12	No
22,29,30- trisnorneohopane	No	chrysene-d12	No
17α,21β-29-hopane	No	chrysene-d12	No
17α, 21β-hopane	Yes	chrysene-d12	No
22S,R-17α, 21β-30-homohopanes	No	chrysene-d12	No
22S,R-17α, 21β-30-bishomohopanes	No	chrysene-d12	No
Sugars			
levoglucosan	Yes	levoglucosan-d7	Silylated
mannosan	Yes	levoglucosan-d7	Silylated
galactosan	No	levoglucosan-d7	Silylated

[a] particle phase only

2.5.1 Sample Preparation Procedures

It is often the case that these tracers are present in such low concentrations that they are difficult to accurately measure. One method to reduce the cost of GC/MS analysis and to improve the certainty in results is to combine samples from several days or common time periods. This method has been implemented in many studies (Schauer et al., 1996b; Schauer and Cass, 2000; Brown et al., 2002). Likewise, for this study, filter fractions from each day were combined into site composites to assess the average inter-site source variation over the entire study period. Intra-site source variation, the day-to-day variability of source contributions at a site, is not directly measured for all three major sources due to budget and analytical constraints; however, the daily, intra-site variation of wood smoke contribution is quantified and results are presented in Chapter 3.4.

In addition to site composites, a subset of samples was selected for individual analysis by GC/MS (see Table 6). Two different preparation procedures were used on individual samples since the first technique resulted in levoglucosan concentrations that were excessively high. The large concentration of levoglucosan could not be quantified in the first extraction process due to two factors: interference with the internal standard, and concentrations orders of magnitude above

the highest calibration standard (the highest standard concentration is based on the maximum linear response of the GC/MS). Generally, the sample preparation procedure involves the addition of deuterated internal standards prior to three iterations of solvent extraction with Methylene Chloride (DCM) followed by ultrasonic agitation for 15 minutes (totaling 45 minutes of filter sonication). The amount and type of internal standard added prior to solvent extraction is detailed in Table 7. Then, the total extract was reduced in volume by evaporation under pure

Table 6. Sample selection for GC/MS analysis.

Site	Collection Date	Rationale for seletion
Clovis	12/25/2003	High Levoglucosan/OC ratio
CSUF	12/25/2003	High Levoglucosan/OC ratio
Drummond	12/25/2003	High Levoglucosan/OC ratio
First St.	12/25/2003	High Levoglucosan/OC ratio
Clovis	12/27/2003	High OC event following Xmas
CSUF	12/27/2003	High OC event following Xmas
Drummond	12/27/2003	High OC event following Xmas
First St.	12/27/2003	High OC event following Xmas
Clovis	1/6/2004	High PM event (all sites available)
CSUF	1/6/2004	High PM event (all sites available)
Drummond	1/6/2004	High PM event (all sites available)
First St.	1/6/2004	High PM event (all sites available)
Pacific	1/6/2004	High PM event (all sites available)

Table 7. The volume and concentration of deuterated internal standards added to samples prior to extraction.

Deuterated Internal Standard	Concentration (μg/mL)	Volume (μL)
Benzaldehyde-d6	250	50
Phthalic acid-d4	250	50
Decanoic acid-d19	250	50
C28-d58	250	50
Levoglucosan-d7	250	25
Chrysene-d12	25	100

nitrogen and filtered through a pre-fired quartz filter to remove insoluble debris. The objective of evaporation is to increase the concentration of analytes by preferentially evaporating the DCM solvent which has a much higher vapor pressure than the analytes of interest. Information

regarding the exact filter area, amount of internal standard and DCM used in the extraction process is included in Tables 7, 8, and 9.

Table 8. Sample preparation details for chemicals quantified by GCMS for all species quantified in Table 5, except silylated species.

Sample Name	Filter Area Extracted (cm^2)	No. of samples included	IS volume	Total DCM volume (mL)	Final Volume (μL)
Clovis	663	15	Table 7	550	250
CSUF	972	22	Table 7	550	250
Drummond	707	16	Table 7	550	250
First St.	972	22	Table 7	550	250
Pacific	751	17	Table 7	550	250
Clovis Blk	206.5	4	Table 7	150	250
CSUF Blk	206.5	4	Table 7	150	250
Drummond Blk	206.5	4	Table 7	150	250
First St. Blk	206.5	4	Table 7	150	250
Pacific Blk	206.5	4	Table 7	150	250
22	206.5	1	Table 7	150	250
48	206.5	1	Table 7	150	250
49	206.5	1	Table 7	150	250
80	206.5	1	Table 7	150	250
81	206.5	1	Table 7	150	250
82	206.5	1	Table 7	150	250
83	206.5	1	Table 7	150	250
87	206.5	1	Table 7	150	250
89	206.5	1	Table 7	150	250
91	206.5	1	Table 7	150	250
96	206.5	1	Table 7	150	250
100	206.5	1	Table 7	150	250
104	206.5	1	Table 7	150	250

Following extraction, evaporation, and filtration steps, a portion of each sample extract is set aside for further derivatization. Samples were both methylated and silylated to improve quantification of organic species with oxygenated functional groups that generally don't elute efficiently and often stick to the column (Grob, 1995). Addition of diazomethane to sample extract was performed to convert carboxylic acid functional groups into methyl esters. Derivatization of samples with a silylation reagent replaces hydroxyl groups with trimethylsilyl esters- a step that is important for quantifying levoglucosan, cholesterol, and other compounds

Sample	Clovis Composite	CSUF Composite	Drum Composite	First Composite	Pacific Composite	Clovis Blk Composite	CSUF Blk Composite	Drum Blk Composite	First Blk Composite	Pac Blk Composite
n-nonatriacontane	ND	1.29	ND	ND	ND	ND	0.002	0.002	0.002	0.002
n-tetracontane	ND	ND	ND	ND	ND	ND	0.002	0.002	0.002	0.002
Squalene	2.57	2.06	ND	0.79	1.38	ND	ND	ND	ND	ND
tetramethylpentadecane	ND	ND	ND	ND	ND	ND	0.001	0.002	0.001	0.002
CPI[d]	1.31	1.26	1.40	1.42	1.26	—	—	—	—	—
PAHs (ng/m^3)										
retene	0.334	1.070	0.804	1.854	0.225	ND	0.003	0.004	0.003	0.004
naphtalene	0.001	0.001	0.001	ND	0.001	0.001	0.001	0.002	0.001	0.001
2-methylnaphtalene	ND	ND	ND	ND	ND	0.002	0.002	0.003	0.003	0.002
1-methylnaphtalene	ND	ND	ND	ND	ND	0.002	0.002	0.003	0.003	0.002
phenanthrene	0.003	0.002	0.004	0.007	0.003	0.002	0.002	0.003	0.002	0.002
anthracene	ND	0.001	0.001	ND	0.001	0.001	0.001	0.002	0.002	0.001
fluoranthene	0.007	0.007	0.011	0.011	0.008	0.001	0.001	0.002	0.002	0.001
acephenanthrylene	0.001	0.001	0.003	0.003	0.002	0.001	0.001	0.002	0.002	0.001
pyrene	0.011	0.011	0.018	0.021	0.010	0.001	ND	0.002	0.002	ND
benzo[*c*]phenanthrene	ND	ND	ND	ND	ND	0.002	0.002	0.003	0.003	0.002
benzo[*ghi*]fluoranthene	0.026	0.002	0.038	ND	0.024	0.002	0.002	0.003	0.003	0.002
cyclopentacephenanthrylene	ND	ND	ND	ND	ND	0.002	0.002	0.003	0.003	0.002
cyclopenta[*cd*]pyrene	ND	ND	ND	ND	ND	0.002	0.002	0.003	0.003	0.002
benz[*a*]anthracene	0.128	0.035	0.043	ND	0.026	0.002	0.002	0.003	0.003	0.002
chrysene+triphenylene	ND	0.041	0.071	ND	0.045	0.001	0.001	0.002	0.002	0.001
benzo[*k*+*b*]fluoranthene	0.100	0.068	0.111	0.187	0.073	0.001	0.001	0.001	0.001	0.001
benzo[*j*]fluoranthene	0.012	0.009	0.014	0.018	0.011	0.001	0.001	0.001	0.001	0.001
benzo[*e*]pyrene	0.029	0.023	0.039	0.071	0.021	0.001	0.001	0.001	0.001	0.001
benzo[*a*]pyrene	0.042	0.024	0.037	0.087	0.028	0.001	0.001	0.001	0.001	0.001
perylene	0.008	0.003	0.006	0.008	0.005	0.001	0.001	0.001	0.001	0.001
indeno[1,2,3-*cd*]pyrene	0.009	0.008	0.122	0.041	0.006	0.001	0.001	0.001	0.001	0.001
dibenzo[*ah*]anthracene	0.047	0.042	0.069	0.184	0.025	0.004	0.003	0.006	0.005	0.004
benzo[*ghi*]perylene	0.028	0.026	0.043	0.118	0.021	0.001	0.001	0.001	0.001	0.001
Guaiacol and Substituted Guaiacols (ng/m^3)										
acetovanillone	0.15	0.22	0.17	0.08	0.09	ND	0.002	0.002	0.002	0.002
vanillin	0.86	1.72	0.93	2.20	0.45	ND	0.002	0.003	0.002	0.003

Table 16. Mass concentration of chemical compounds identified and quantified by GC/MS for site composites (units as indicated) and total mass of site blank composites (μg)[a].

Sample	Clovis Composite	CSUF Composite	Drum Composite	First Composite	Pacific Composite	Clovis Blk Composite	CSUF Blk Composite	Drum Blk Composite	First Blk Composite	Pac Blk Composite
PM2.5 ($\mu g/m^3$)	26.7	29.1	28.9	35.6	29.7	—	—	—	—	—
OC mass ($\mu g/m^3$)[b]	10.9	11.2	10.6	14.9	10.7	—	—	—	—	—
EC ($\mu g/m^3$)	1.1	1.0	1.2	2.2	1.1	—	—	—	—	—
n-alkanes (ng/m^3)										
n-tridecane	ND[c]	ND	ND	0.34	0.67	ND	0.002	0.002	0.002	0.002
n-tetradecane	ND	ND	ND	0.63	0.35	ND	ND	0.002	0.002	0.002
n-pentadecane	0.52	ND	ND	ND	0.53	ND	0.002	0.002	0.002	0.002
n-hexadecane	1.16	ND	ND	0.76	0.28	ND	ND	ND	ND	ND
n-heptadecane	0.46	ND	0.39	ND	0.34	ND	ND	ND	ND	ND
n-octadecane	0.76	0.74	0.23	ND	ND	ND	ND	ND	ND	ND
n-nonadecane	0.49	0.52	0.49	1.44	ND	ND	ND	ND	ND	ND
n-icosane	0.63	ND	1.74	ND	ND	ND	ND	ND	ND	ND
n-henicosane	1.85	3.28	3.81	5.25	1.40	ND	ND	ND	ND	ND
n-docosane	3.51	4.36	5.72	8.65	2.13	ND	ND	ND	ND	ND
n-tricosane	7.15	8.63	8.38	11.32	3.77	ND	ND	ND	ND	ND
n-tetracosane	10.18	9.25	9.84	12.23	5.38	ND	ND	ND	ND	ND
n-pentacosane	9.84	10.34	9.68	13.12	6.12	ND	ND	ND	ND	ND
n-hexacosane	7.11	6.53	7.81	9.12	5.32	ND	ND	ND	ND	ND
n-heptacosane	7.95	7.75	7.60	10.92	5.40	ND	ND	ND	ND	ND
n-octacosane	5.93	5.47	5.40	7.67	3.94	ND	ND	ND	ND	ND
n-nonacosane	10.44	8.50	9.23	11.45	7.27	ND	ND	ND	ND	ND
n-triacontane	4.51	3.84	4.47	5.80	2.68	ND	ND	ND	ND	ND
n-hentriacontane	6.93	7.14	6.61	9.14	4.04	ND	ND	ND	ND	ND
n-dotriacontane	3.06	4.78	3.17	4.16	1.53	ND	ND	ND	ND	ND
n-tritriacontane	3.33	4.64	3.74	6.07	1.46	ND	0.001	0.002	0.001	0.002
n-tetratriacontane	2.07	3.41	2.73	6.31	0.62	ND	0.001	0.002	0.001	0.002
n-pentatriacontane	1.77	2.99	3.00	6.27	0.85	ND	0.002	0.002	0.002	0.002
n-hexatriacontane	1.03	2.09	1.81	3.19	ND	ND	0.002	0.002	0.002	0.002
n-heptatriacontane	0.53	1.43	1.05	ND	ND	ND	0.002	0.002	0.002	0.002
n-octatriacontane	ND	ND	ND	2.48	ND	ND	0.002	0.002	0.002	0.002

Sample	Clovis Dec 25	CSUF Dec 25	Drum Dec 25	First Dec 25	Clovis Dec 27	CSUF Dec 27	Drum Dec 27	First Dec 27	Clovis Jan 6	CSUF Jan 6	Drum Jan 6	First Jan 6	Pac Jan 6
Total quantified by GC/MS (ng/m^3)	698	576	271	691	1790	2092	1998	1831	1310	1417	719	2392	1379
Percent of OM Quantified (%)[a]	6.7%	6.3%	3.2%	4.9%	7.2%	8.4%	8.4%	5.0%	7.4%	8.0%	4.6%	8.3%	5.8%
Percent of $PM_{2.5}$ Quantified (%)	3.7%	3.2%	1.7%	2.5%	5.2%	5.7%	5.5%	3.4%	3.3%	3.4%	1.8%	3.8%	2.8%

[a] OM is OC multiplied by 1.6
[b] "ND" means not detected
[c] CPI calculated from alkanes C_{17}-C_{40}
[d] Actual standards were not used with the exception of 17α, 21β-hopane and thus are uncertain

Sample	Clovis Dec 25	CSUF Dec 25	Drum Dec 25	First Dec 25	Clovis Dec 27	CSUF Dec 27	Drum Dec 27	First Dec 27	Clovis Jan 6	CSUF Jan 6	Drum Jan 6	First Jan 6	Pac Jan 6
vanillin	1.07	0.06	1.18	2.65	5.56	4.47	3.98	7.20	1.10	2.75	2.09	3.20	3.70
guaiacol	0.02	ND	0.02	0.12	0.25	0.26	0.52	0.62	0.02	0.15	0.07	0.15	0.21
Meat Tracers and Other Sterols (ng/m^3)													
Nonanal	10.5	ND	ND	ND	10.6	12.4	16.1	19.0	ND	12.1	13.3	14.1	13.8
cholesterol	0.7	0.9	ND	1.3	1.5	2.0	0.8	1.7	1.0	1.6	1.2	2.7	1.4
ergosterol	ND	0.7	ND	ND	1.2	ND	2.1	ND	ND	ND	0.8	ND	ND
stigmasterol	1.0	1.0	0.3	0.7	0.9	1.1	1.4	1.3	1.1	0.4	0.3	1.1	0.8
Hopanes and Steranes (ng/m^3)[d]													
20R, 5α(H),14β(H),17β(H)-cholestane	0.0324	ND	0.034	0.040	0.0276	ND	ND	ND	ND	0.026	0.067	0.14	0.03
20S, 5α(H),14β(H),17β(H)-cholestane	0.038	ND	0.039	0.040	ND	ND	ND	ND	ND	0.029	0.052	0.10	0.04
20R, 5α(H),14β(H),17α(H)-cholestane	0.107	0.076	0.098	0.094	ND	ND	ND	ND	0.090	0.069	0.144	0.36	0.13
20S,R-5α(H),14β(H),27β(H)-ergostanes	ND	ND	ND	ND	ND	ND	ND	ND	ND	ND	ND	0.20	ND
20S,R-5α(H),14β(H),17β(H)-sitosanes	0.091	0.106	0.098	0.095	0.088	0.066	0.069	ND	0.090	0.071	0.109	0.26	0.09
22,29,30- trisnorneohopane	0.118	ND	ND	0.129	0.102	0.093	0.122	0.12	0.191	0.094	0.145	0.23	0.14
17α,21β-29-hopane	0.546	0.394	0.327	0.439	0.567	0.336	0.459	0.64	0.696	0.479	0.519	1.03	0.57
17α, 21β-hopane	0.659	0.515	0.488	0.587	0.622	0.480	0.538	0.74	0.780	0.405	0.651	1.46	0.65
22S,R-17α, 21β-30-homohopanes	0.369	0.227	0.307	0.282	0.282	0.240	0.254	0.26	0.399	0.255	0.379	0.71	0.32
22S,R-17α, 21β-30-bishomohopanes	0.227	ND	0.195	0.163	0.169	ND	ND	ND	0.298	0.114	0.207	0.27	0.15
Sugars (ng/m^3)													
levoglucosan	574	484	213	580	1575	1840	1724	1518	1170	1274	584	2139	1213
mannosan	14	9	12	15	34	45	57	45	30	21	17	31	25
galactosan	2	2	2	3	4	5	6	5	4	3	2	5	0

Sample	Clovis Dec 25	CSUF Dec 25	Drum Dec 25	First Dec 25	Clovis Dec 27	CSUF Dec 27	Drum Dec 27	First Dec 27	Clovis Jan 6	CSUF Jan 6	Drum Jan 6	First Jan 6	Pac Jan 6
n-nonatriacontane	1.10	ND	ND	ND	ND	ND	ND	ND	ND	ND	ND	1.87	ND
n-tetracontane	0.81	ND	ND	ND	ND	ND	ND	ND	ND	ND	ND	1.24	ND
Squalene	4.64	9.09	ND	2.72	3.34	8.95	3.06	2.84	2.24	1.86	3.34	3.04	5.26
tetramethylpentadecane	ND	1.809	ND	ND	ND	ND	ND	ND	ND	ND	ND	ND	ND
CPI[c]	1.04	0.54	1.29	1.16	1.14	1.08	1.18	1.15	0.91	1.11	1.19	1.15	1.15
PAHs (ng/m^3)													
retene	0.364	0.170	0.308	0.733	2.425	5.030	4.145	7.89	0.740	2.167	0.914	3.29	2.06
naphtalene	0.004	0.003	0.002	0.013	0.009	0.002	0.002	0.01	0.005	0.002	0.003	0.01	4*E-3
2-methylnaphtalene	ND	ND	ND	ND	ND	ND	ND	ND	0.001	ND	ND	ND	ND
1-methylnaphtalene	ND	ND	ND	ND	ND	ND	ND	ND	ND	ND	ND	ND	ND
phenanthrene	0.005	0.002	0.003	0.033	0.021	0.006	0.005	0.02	0.004	0.001	0.008	0.01	0.02
anthracene	0.001	ND	ND	0.004	0.004	0.002	0.002	0.01	0.029	0.028	0.001	4*E-3	2*E-3
fluoranthene	0.011	0.009	0.013	0.034	0.045	0.033	0.045	0.08	0.028	0.025	0.022	0.03	0.06
acephenanthrylene	0.003	0.002	0.002	0.008	0.010	0.006	0.011	0.02	0.007	0.006	0.005	0.01	0.02
pyrene	0.015	0.012	0.016	0.041	0.060	0.051	0.070	0.13	0.037	0.034	0.032	0.06	0.07
benzo[*c*]phenanthrene	ND	ND	ND	ND	ND	ND	ND	ND	0.002	ND	0.003	ND	ND
benzo[*ghi*]fluoranthene	0.026	0.017	0.021	0.061	0.150	0.132	0.147	0.30	0.092	0.086	0.066	0.19	0.22
cyclopentacephenanthrylene	ND	ND	ND	ND	ND	ND	ND	ND	0.003	ND	0.003	ND	ND
cyclopenta[*cd*]pyrene	ND	ND	ND	ND	ND	ND	ND	ND	ND	ND	ND	ND	ND
benz[*a*]anthracene	0.039	0.016	0.030	0.112	0.236	0.246	0.269	0.37	0.135	0.151	0.120	0.94	0.31
chrysene+triphenylene	0.049	0.039	0.043	0.108	0.279	0.332	0.320	0.53	0.154	0.160	0.122	ND	0.31
benzo[*k*+*b*]fluoranthene	0.127	0.088	0.098	0.173	0.339	0.363	0.387	0.59	0.242	0.254	0.223	0.52	0.38
benzo[*j*]fluoranthene	0.013	0.009	0.008	0.024	0.044	0.049	0.062	0.09	0.042	0.041	0.030	0.09	0.06
benzo[*e*]pyrene	0.047	0.037	0.037	0.061	0.113	0.123	0.150	0.19	0.086	0.084	0.076	0.17	0.19
benzo[*a*]pyrene	0.044	0.017	0.024	0.071	0.133	0.182	0.179	0.28	0.103	0.114	0.081	0.25	0.17
perylene	0.008	0.002	0.005	0.010	0.018	0.025	0.027	0.04	0.018	0.019	0.014	0.03	0.02
indeno[1,2,3-*cd*]pyrene	0.017	0.008	0.014	0.020	0.038	0.042	0.043	0.07	0.073	0.080	0.026	0.16	0.04
dibenzo[*ah*]anthracene	0.089	0.055	0.066	0.104	0.206	0.218	0.240	0.37	0.025	0.027	0.144	0.20	0.20
benzo[*ghi*]perylene	0.060	0.052	0.043	0.064	0.129	0.122	0.141	0.20	0.119	0.096	0.095	0.04	0.13
Guaiacol and Substituted Guaiacols (ng/m^3)													
acetovanillone	0.13	0.01	0.22	0.39	0.90	0.55	0.70	0.84	0.23	0.35	0.32	0.33	0.73

Table 15. Concentration of chemical compounds identified and quantified by GC/MS for individual samples.

Sample	Clovis Dec 25	CSUF Dec 25	Drum Dec 25	First Dec 25	Clovis Dec 27	CSUF Dec 27	Drum Dec 27	First Dec 27	Clovis Jan 6	CSUF Jan 6	Drum Jan 6	First Jan 6	Pac Jan 6
PM2.5 ($\mu g/m^3$)	18.9	17.9	16.2	27.9	34.1	36.6	36.7	53.7	39.4	41.8	39.9	62.5	50.0
OC mass ($\mu g/m^3$)	10.4	9.1	8.6	14.2	24.8	24.9	23.8	36.8	17.7	17.6	15.8	28.9	24.0
EC ($\mu g/m^3$)	1.3	0.9	0.9	3.5	1.3	2.1	2.7	3.5	2.2	2.0	2.3	3.7	3.6
n-alkanes (ng/m^3)													
n-tridecane	ND[b]	0.30	ND	ND	ND	ND	ND	ND	ND	ND	ND	ND	ND
n-tetradecane	ND	0.72	ND	ND	0.94	ND	ND	ND	ND	ND	ND	ND	ND
n-pentadecane	0.39	1.61	ND	ND	0.65	ND	ND	ND	ND	ND	ND	ND	ND
n-hexadecane	0.36	2.17	ND	ND	ND	ND	ND	ND	0.23	ND	ND	ND	ND
n-heptadecane	0.33	1.61	ND	0.35	ND	ND	ND	ND	0.62	0.43	ND	0.25	ND
n-octadecane	1.65	ND	ND	0.27	0.86	0.63	0.49	0.40	0.68	0.49	ND	0.65	0.66
n-nonadecane	1.05	0.59	0.28	0.81	0.80	0.57	0.49	0.50	0.66	0.47	ND	0.78	0.63
n-icosane	1.33	ND	0.30	0.89	1.40	2.29	2.57	2.50	1.15	1.16	1.30	1.60	1.26
n-henicosane	1.06	0.94	0.92	1.76	4.71	7.34	10.15	11.9	1.76	2.72	3.05	4.73	3.27
n-docosane	1.74	1.61	1.33	3.26	8.74	12.45	11.70	17.7	3.76	5.38	5.02	10.3	5.80
n-tricosane	4.38	3.27	2.62	5.80	13.50	15.75	14.93	22.1	7.24	8.42	8.18	16.5	10.6
n-tetracosane	8.41	7.42	4.01	7.46	15.15	16.96	16.97	21.9	9.59	10.68	10.58	19.5	12.3
n-pentacosane	8.83	3.92	4.77	9.11	13.38	14.35	14.73	18.6	10.08	10.12	12.06	19.6	12.0
n-hexacosane	7.36	6.28	3.61	7.75	11.31	12.17	12.36	15.7	9.12	8.47	8.76	15.0	10.6
n-heptacosane	7.90	3.41	4.18	7.72	11.74	12.05	12.63	15.8	7.21	8.33	8.25	15.1	10.0
n-octacosane	7.06	8.32	2.71	6.28	9.57	9.87	10.63	12.4	7.19	6.67	5.53	12.3	7.5
n-nonacosane	6.94	2.76	4.00	6.61	11.46	11.28	13.49	14.4	7.22	7.57	7.13	14.0	8.80
n-triacontane	5.07	2.64	2.18	4.96	7.23	8.06	9.32	10.9	5.17	5.15	4.21	8.86	5.57
n-hentriacontane	5.24	2.01	2.78	4.92	9.63	9.74	12.60	12.6	5.27	5.60	5.11	10.9	6.45
n-dotriacontane	3.67	5.45	1.28	2.60	4.80	6.01	6.97	7.86	4.80	2.90	1.97	5.71	2.85
n-tritriacontane	3.27	1.12	1.34	3.00	5.56	6.44	7.94	8.60	2.71	2.24	2.11	5.98	3.10
n-tetratriacontane	2.36	0.93	1.08	2.28	3.88	4.71	5.22	6.22	2.24	2.09	1.97	5.19	2.27
n-pentatriacontane	2.11	0.88	1.15	1.98	3.48	4.60	4.56	6.96	1.89	2.34	2.56	4.64	1.93
n-hexatriacontane	2.15	6.36	0.63	1.31	2.33	3.12	3.19	4.58	5.95	1.35	1.21	3.42	1.25
n-heptatriacontane	1.24	0.51	ND	0.89	1.94	2.63	2.49	3.55	0.74	1.15	ND	2.42	0.85
n-octatriacontane	ND	ND	ND	ND	1.49	1.95	ND	ND	ND	ND	ND	ND	ND

Similar to other studies, the amount of OM that is speciated by GC/MS is a small fraction of total OM. As shown in Table 15, the identified and quantified OM in individual samples ranges from 3-8.5%, where levoglucosan accounts for 75-90% of quantified OM. Note that the objectives of this study involve the quantification of levoglucosan and wood smoke contribution, not complete speciation of OC. The amount of total $PM_{2.5}$ that is speciated as specific organic compounds in individual samples ranges from 1.7% to 5.8%. In composite samples only 1% or less of OM and 0.5% of $PM_{2.5}$ is chemically speciated directly since levoglucosan could not be quantified in these samples. As discussed in detail in Chapter 2.5, the amount of levoglucosan in composite samples was well beyond the linear response of the GC/MS system and hence could not be accurately quantified in these samples. For composite samples' source apportionment estimates, levoglucosan values as measured by the HPAEC-PAD are averaged by site. Despite the low concentrations of individual compounds, the tracers for wood smoke, meat cooking and motor vehicles combined identify the source contributions of approximately 65-80% of OC.

3.6 Source Apportionment

GC/MS is commonly used to quantify emissions source tracers (Rogge et al., 1993b; Cass, 1998; Schauer and Cass, 2000; Fraser et al., 2002; Zheng et al., 2002). Emissions source tracers are chemical compounds that are characteristic of a single source type, such as automobiles or fireplaces. In order to detail chemical information about common emissions sources, source specific tests are performed and their emissions are collected. The emissions collected are then chemically analyzed to identify a distinctive source profile. If one of the unique chemicals emitted by that source has a lifetime much greater than typical transport timeframes, then this compound is a candidate tracer for that source type. The emitted tracer concentration can be normalized to total emitted OC and/or $PM_{2.5}$, providing a ratio.

several or more compounds from each family are quantified, only cholesterol and 17α, 21β-hopane are used for source contribution estimates. The mass percent of these two tracers relative to OM are shown in Figure 25 for those samples analyzed by GC/MS. While the total contribution to OM and $PM_{2.5}$ by these species is relatively negligible (less than a tenth of a percent by mass), these tracers can apportion a significant amount of OM to meat cooking or motor vehicle emissions sources (Rogge et al., 1993a; Schauer et al., 1996b; Cass, 1998; Kleeman, Schauer, and Cass, 1999; Schauer et al., 1999a, 1999b; Kleeman, Schauer, and Cass, 2000). It is important to note that stigmasterol is also emitted from biomass combustion, and as such would not be an appropriate tracer for meat cooking (Simoneit, 2002; Fine, Cass, and Simoneit, 2004a). Surprisingly, there is not a large motor vehicle tracer signature at the First Street site relative to the other sites. The temporal variation in motor vehicle emissions tracers show that as a percent of OM the amount of vehicle emissions actually decreases on the 27th of December from the 25th, which is opposite of the wood smoke tracers and the PAHs. The temporal variation in meat cooking is highly variable between sites. The only consistency is that the Drummond site average has the largest concentration of meat cooking tracers relative to OM. That Drummond has a large meat cooking signature relative to other sites is not surprising due to the presence of a BBQ near the sampling location.

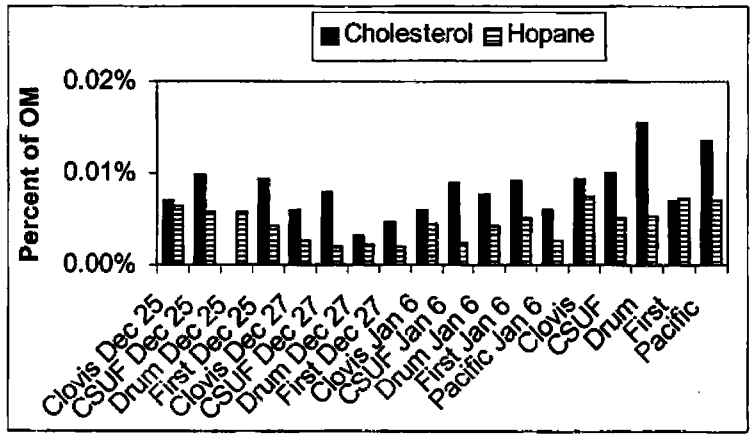

Figure 25. The tracers for meat cooking, cholesterol, and motor vehicles, 17α, 21β-hopane, are shown as a percent of OM based on quantification by GC/MS.

profiles (i.e. from combustion of hardwood/softwood or different types of detritus), transport lifetimes, and other confounding factors. Unlike retene, there does not appear to be a consistent difference in marker concentration between the sites, although First St. and CSUF composite samples have a notably higher concentration of both vanillin and retene than other sites. While the temporal variability of the absolute concentration of tracers is interesting, removing the effects of mixing height variability through calculating the tracer concentration relative to OM is a measure of actual source variability, shown in Figure 24.

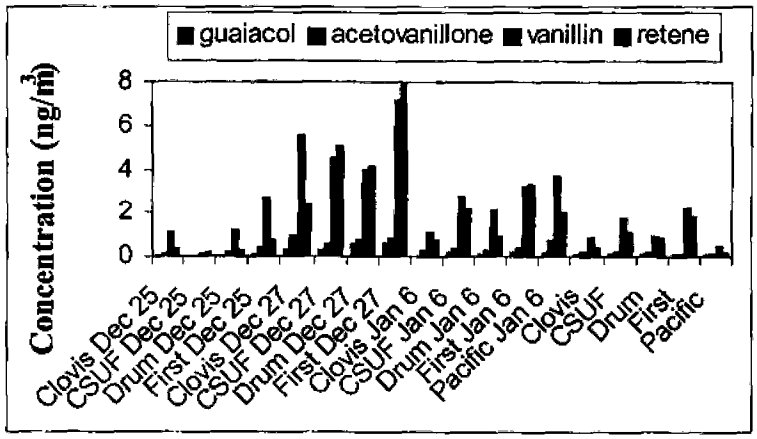

Figure 23. The relative variation of wood smoke markers guaiacol, acetovanillone, vanillin, and retene as identified and quantified by GC/MS, are fairly consistent for each sample.

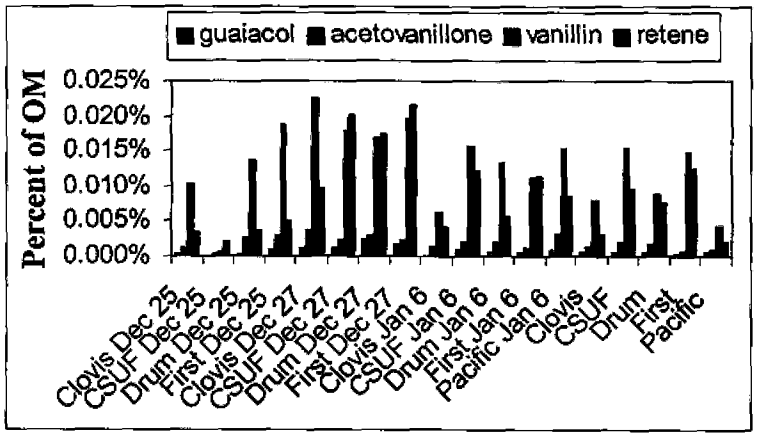

Figure 24. The variation of wood smoke markers guaiacol, acetovanillone, vanillin, and retene as a percent of OM.

Several other emissions source markers are identified and quantified by GC/MS, including sterols from meat cooking and hopane/steranes from motor vehicle exhaust. Although

Overall, the contribution to OC and $PM_{2.5}$ by quantified PAHs is low, less than a tenth of a percent by mass for all samples analyzed. First Street samples have a significantly higher concentration of PAHs relative to other sites; on a particular day concentrations here exceed concentrations at other sites by 40-80% (significantly different at the 90% confidence level with 11 degrees of freedom based on a two-tailed difference of means t-test). In all samples analyzed, the PAH with the largest concentration is retene. The concentration of retene is between 31-77% of the total quantified PAH concentration. The level of retene relative to other PAHs appears larger at CSUF and First St. than at other sites, with retene contributing, on average, 78% and 71% to PAH levels, respectively, while other sites have 40-55% retene contribution. The absolute concentrations of retene and other wood smoke tracers are shown in Figure 23. As retene is a tracer specific to coniferous wood, the fact that First St. and CSUF show higher levels of this tracer than Clovis, which has a large levoglucosan concentration (see Table 14), might indicate a local difference in the type of wood burned. Daily variation of retene levels shows that on December 25th the retene concentration was lowest of the three days analyzed and that the levels are lower than the average over the study period (i.e. lower than the composite samples). This is consistent with the absolute concentrations of levoglucosan for those samples selected for GC/MS analysis (see Table 6). However, the concentrations of retene and levoglucosan normalized to measured OC show that December 25th is one of the days with the highest wood smoke contribution (see Figure 24).

As the focus of this study is the quantification of wood smoke contribution to $PM_{2.5}$, several other wood smoke markers are identified and quantified with GC/MS to provide supplementary, independent measures of wood smoke contribution. In addition to quantifying retene, as mentioned above, guaiacol and substituted guaiacols were also quantified. Shown in Figure 23 is the estimated ambient concentration of these wood smoke markers for samples analyzed by GC/MS. The relative ambient concentrations of these wood smoke tracers track each other fairly well from sample to sample, despite large difference in emissions rates, source

composites are higher than the individual samples. This indicates that biogenic sources may be more important for other samples not examined by GC/MS. There do not seem to be any consistent differences in the CPI between different sites.

The n-alkane with the greatest concentration, the C_{max}, is C_{23}-C_{25} for all but one sample. A C_{max} in this range is an indication of fossil fuel combustion and C_{23} is particular to diesel combustion (Simoneit, 1989). One sample, CSUF on Christmas, had a larger alkane C_{max} than the other samples. The C_{max} for this sample is C_{28} which is associated with plant wax emissions; however, this sample had the lowest CPI and is the only sample with a detectible level of pristane (2,6,10,14-tetramethylpentadecane), a tracer for coal or oil combustion. In general, analysis of the alkane homologues validates the classification of Fresno as an urban environment with predominantly anthropogenic emissions sources.

PAHs are of particular importance due to their known carcinogenic and mutagenic properties (Finlayson-Pitts and Pitts, 2000). Twenty three individual PAH compounds, including retene and benzo[α]pyrene (BaP), were quantified to differentiate between samples dominated by fossil fuel versus biomass combustion sources. Retene is a tracer commonly associated with coniferous biomass combustion (Simoneit, 2002), while benzo[α]pyrene, a compound from coal tar, was one of the first compounds to be identified as carcinogenic in lab rats (Cook, Hewett, and Hieger, 1933). BaP levels were substantially lower than retene and account for approximately 5% of the quantified PAHs. BaP levels are lower than previously quantified in Frenso for both absolute concentrations and relative to $PM_{2.5}$ concentrations (Schauer and Cass, 2000). Other PAHs quantified are indicators of various combustion sources, but can be short lived and suggest the relative age of emissions sources (Finlayson-Pitts and Pitts, 2000; Brown et al., 2002). Since previous studies have demonstrated that most emissions in Fresno are locally generated (Schauer and Cass, 2000; Watson and Chow, 2002b), it is not believed that the degradation of PAHs during transport will significantly affect their measured concentrations.

A least squares regression technique was used for simplicity in Figure 22 despite the presence of variable error in the measurement of both the independent and dependent variables. There is a good, but somewhat non-linear, correlation (R^2=0.95) between the two methods with more variance at higher concentrations.

3.5 Other Compound Measurements

Individual samples as well as site composites were solvent extracted and analyzed by GC/MS to provide detailed chemical speciation for both specific events and for the study as a whole. Table 6 outlines the individual filters selected for GC/MS analysis. Site composites were generated by combining a fraction of each sample for a site and extracting the filters together. The GC/MS sample preparation procedure is detailed in Chapter 2.5.1. The estimated ambient concentrations for the chemical species identified and quantified by GC/MS are listed in Tables 15 and 16 for individual and composite samples, respectively.

The major compounds identified and quantified by GC/MS include n-alkanes, PAH, wood smoke tracers, meat cooking tracers, and hopanes and steranes. A list of actual compounds identified and quantified by GC/MS can be found in Table 5. N-alkanes can be used to help differentiate anthropogenic versus biogenic source contributions. Particle phase alkanes in the size range C_{13}-C_{40} are quantified. Homologous alkanes C_{17}-C_{40} are used to calculate a Carbon Preference Index (CPI). The CPI is a ratio of the summed concentration of odd numbered carbon alkanes to the summed concentration of even numbered alkanes (Finlayson-Pitts and Pitts, 2000). This index is based on the observation that biological material preferentially emits odd length alkane carbon chains, where organic emissions from fossil fuel combustion generally have similar amounts of even/odd length carbon chains and thus a CPI of 1. If an aerosol has a CPI greater than two, it is considered predominantly influenced by biogenic sources rather than anthropogenic sources. The CPI for all samples analyzed by GC/MS is close to one and significantly lower than two, as shown in Tables 15 and 16. Interestingly, the CPIs for the site

sylilated for a larger sample size (N=26) to compare levoglucosan quantified via HPAEC-PAD to traditional GC/MS. These additional samples include filters collected at all sites on December 31st, January 1st, and at three sites the day prior to the PM event, January 5th. In Figure 22, a scatter plot compares ambient levoglucosan concentrations from GC/MS and HPAEC-PAD.

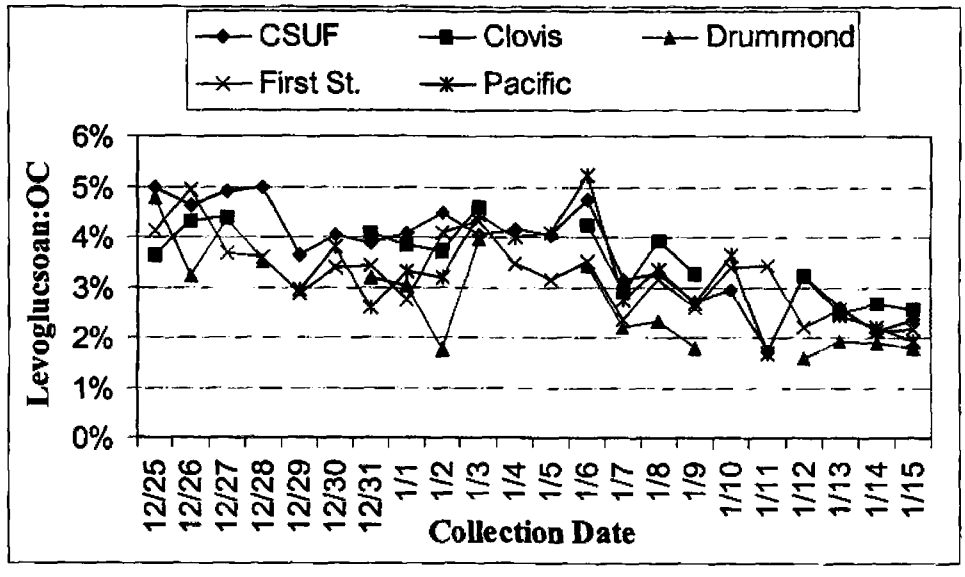

Figure 21. Carbon mass of levoglucosan as a percent of OC over the study period at each site. The cumulative error in levoglucosan and OC measurements results in a 20% uncertainty at the 99% confidence level.

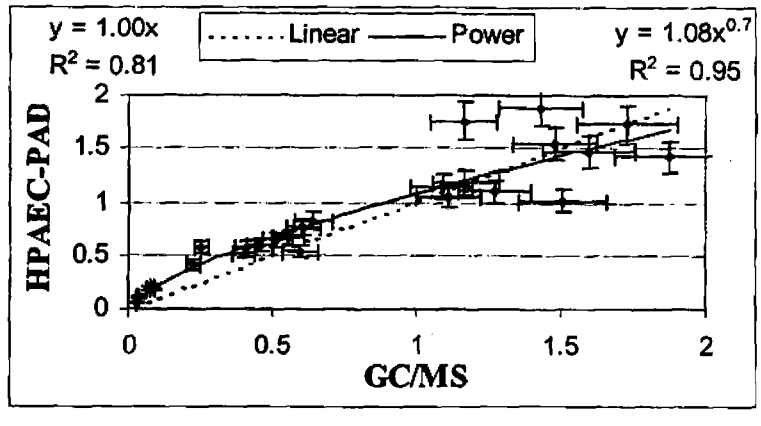

Figure 22. Scatter plot of levoglucosan concentrations ($\mu g/m^3$) estimated from GC/MS and HPAEC-PAD with two different regression forms superimposed. An exponential fit to the data produces a better correlation than a linear fit. Uncertainty is 10% for HPAEC-PAD at the 99% confidence level and GC/MS is assumed to 20%.

levoglucosan levels in Period 2 implies activity differences in residential wood burning or perhaps preferential scavenging and removal of wood smoke particles by fog hydrometeors (Herckes et al., 2005b). Similarly, levoglucosan as a percent of OC also changes over the study period and is significantly higher in the beginning than during Period 2.

Table 14. Site average levoglucosan percent of $PM_{2.5}$ for the first period (12/25/2003-1/9/2004) compared with the second period (1/10/2004-1/15/2004).

Site	Period 1: Levoglucosan to $PM_{2.5}$ (%)	Period 2: Levoglucosan to $PM_{2.5}$ (%)
Clovis	2.65	1.17
CSUF	2.65	0.98
Drummond	2.09	0.63
First St.	2.29	1.20
Pacific	2.06	1.13

The carbon mass of levoglucosan as a percent of OC carbon mass is shown over the study duration in Figure 21. Comparing levoglucosan to OC is useful for several purposes: one is to remove common variations like effects of boundary layer mixing height, another is to gauge when other, non-wood burning sources might contribute more to OC. This first aspect allows for a direct comparison of our levoglucosan:OC ratio to other studies, while this second aspect guided the selection of filters for analysis by GC/MS. From previous samples collected in Fresno it is calculated that the carbon mass of levoglucosan as a percent of OC is 8.5 and 6.5% for two different multi-day episodes (Schauer and Cass, 2000). Comparing these values to a high value in this study of 5.2% might indicate a decrease in wood burning activities relative to other sources of OC. While the difference between these two studies is not large, it may be significant when considering that the largest 3-day average ratio in this study is 4.8%: almost a 30% difference relative to those values reported by Schauer and Cass.

Individual samples chosen for GC/MS analysis are reported in Table 6. Three dates were of particular interest for this study: Christmas eve, a high levoglucosan period; December 27th, a high OC event; and January 6th, a high PM event. Additional samples were extracted and

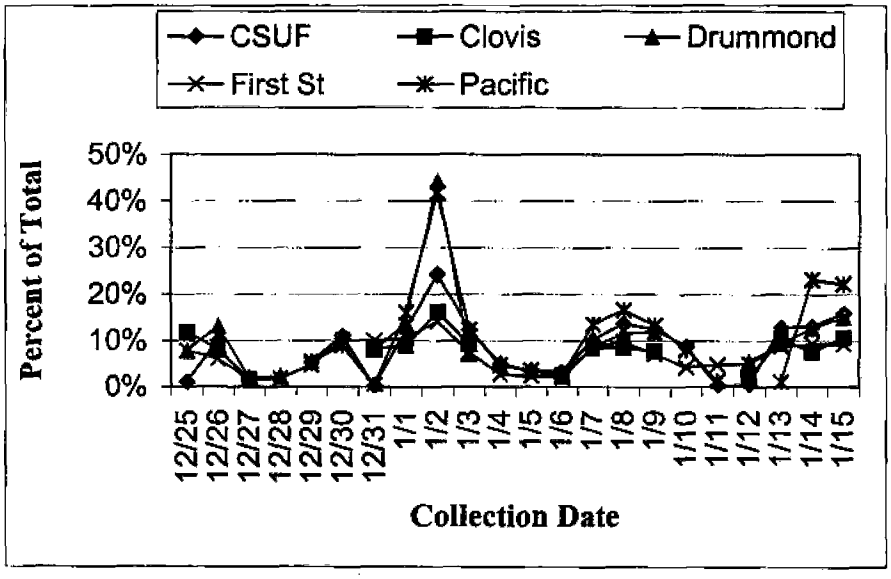

Figure 19. Fraction of total levoglucosan collected by coarse filters. Clovis and Drummond coarse fractions are PM_{10}-$PM_{2.5}$, while other sites' coarse fractions are TSP- $PM_{2.5}$. The cumulative error in coarse and fine samples results in a 20% uncertainty at the 99% confidence level.

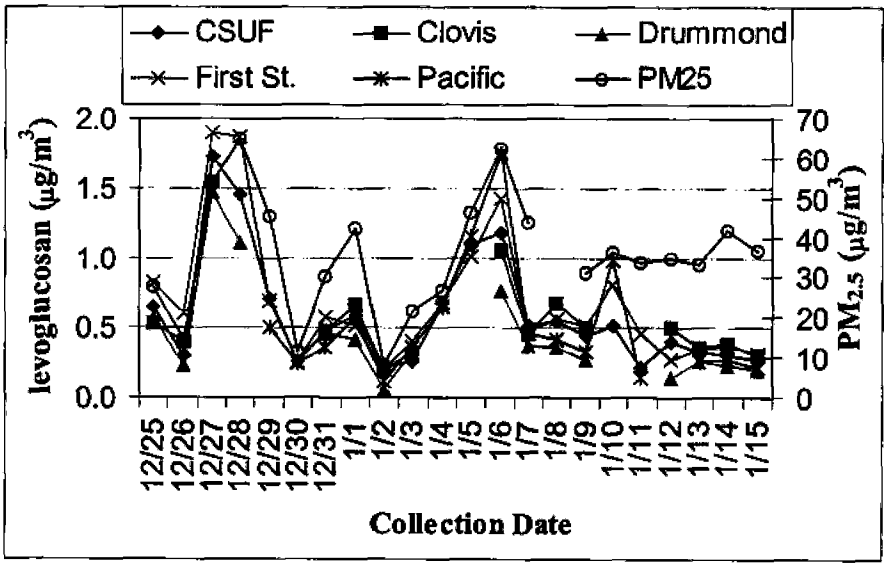

Figure 20. Values of levoglucosan (left axis) at each site and average $PM_{2.5}$ (right axis) concentrations in $\mu g/m^3$ over the study period. Uncertainty is estimated to be 10% at the 99% confidence level.

(the last five days of the study). The strong correlation with $PM_{2.5}$ levels in Period 1 indicates that the concentrations are probably a function of the meteorological conditions, such as stagnation and pressure system oscillations and precipitation. The significant reduction in

The $PM_{2.5}$ filters contain on average 90% of the total levoglucosan (see Figure 19); the remaining levoglucosan is impacted on coarse filters. It is expected that a majority of the levoglucosan is in the fine particulate fraction based on size distribution of levoglucosan from biomass burning samples collected in both a lab and in ambient aerosols (Engling et al., 2005; Herckes et al., 2005a; Schkolnik et al., 2005). Since almost all of the levoglucosan is collected on fine filters, the following discussion of the results will focus exclusively on $PM_{2.5}$ levoglucosan. For actual concentrations of coarse filter levoglucosan see Appendix A.

Similar to OC concentrations, the daily concentrations of levoglucosan from $PM_{2.5}$ filters at the various sites track each other and $PM_{2.5}$ concentrations remarkably well, as shown in Figure 20. The concentration of fine levoglucosan ranges from close to zero to as high as 1.9 $\mu g/m^3$ with site averages ranging between 0.5 and 0.7 $\mu g/m^3$. The maximum values of levoglucosan here are much lower than previously reported Fresno winter values of 7.59 $\mu g/m^3$ in 1995 and 4.05 $\mu g/m^3$ in 2000 (Schauer and Cass, 2000; Poore, 2002). That all sites have such similar levoglucosan concentrations is not expected from known demographic differences; perhaps the sampling period was long enough to allow mixing throughout the city. Although on a daily basis the sites do not have much variation, when comparing site averages a small signal can be detected indicating proximity to residential wood burning sources. The two northern sites, Clovis and CSUF, located in an older residential neighborhood are expected to have more wood heating and when levoglucosan concentrations are normalized by OC levels these sites have a statistically higher fraction of wood burning than other sites (statistically significant at the 95% confidence level based on a difference of means t-test with 75 degrees of freedom).

Interestingly, levoglucosan levels during the first two weeks of the study show a strong relationship to the relative changes in the concentration of $PM_{2.5}$; however, during the last week levoglucosan contributes significantly less to $PM_{2.5}$ than previously (statistically significant at the 99.9% confidence level based on a difference of means t-test with 85 degrees of freedom). Table 14 shows the site average levoglucosan as a percent of $PM_{2.5}$ for Period 1 as compared Period 2

concentrations of levoglucosan were correlated with anomalous results, yet none of these relationships demonstrated a consistent trend. Regardless of the few anomalous results, no correlation could be detected between WSOC concentrations in interstitial particles collected by the Hi-Vol and fog formation. It is interesting that interstitial hydrophilic organic concentrations did not decrease relative to OC levels, yet absolute OC concentrations are significantly lower during fog events.

3.4 Wood smoke Tracer: Levoglucosan

Levoglucosan is commonly used as a chemical marker of biomass combustion. It is emitted in large quantities from source profiles and its measurement is a critical aspect of this study. All valid coarse, fine, and a subset of blank filters were aqueous extracted, as described in detail in Chapter 2.4.2, followed by injection and detection of anhydrous sugars by HPAEC-PAD. The data completeness for levoglucosan analysis via HPAEC-PAD is shown in Table 13. The number of valid coarse and $PM_{2.5}$ filters is more than Table 10 because the mass of select samples could not be determined, but quantification of individual chemical compounds was not compromised. The estimated detection limits of the HPAEC-PAD technique are shown in Table 4 and discussed in Chapter 2.4.4. None of the levoglucosan measurements are invalid and 98% of valid samples are within the estimated LOQ for the HPAEC-PAD. Samples that originally exceeded the LOL of the HPAEC-PAD were diluted with de-ionized water and re-analyzed.

Table 13. Data completeness results for levoglucosan quantification via HPAEC-PAD.

Data Completeness	Number	% of valid filters
Total Samples	186	
valid coarse	92	
valid $PM_{2.5}$	92	
valid OCEC coarse	88	96%
valid OCEC $PM_{2.5}$	92	100%
Below LOQ	4	2%
Blank	22	NA

carbonaceous material was observed on foggy days. It is known that some organic material is effectively scavenged by fog and cloud droplets; however, it is of interest to investigate if water soluble organic matter was preferentially scavenged over non-soluble material. Investigation of the change in the fraction of WSOC to OC in interstitial particles during fog events can provide insight to the lifetimes of hydrophilic species.

The water soluble organic carbon fraction of collected $PM_{2.5}$ samples did not display a pattern of variability similar to $PM_{2.5}$ or TC concentrations. There was no significant change in WSOC to OC concentrations between foggy or non-foggy conditions. The majority of organic carbon (OC) is insoluble. As shown in Figure 18, the water soluble fraction of organic carbon from $PM_{2.5}$ samples was generally between 20 to 40% by carbon mass. A handful of samples had a significantly larger water soluble fraction, up to 68% of OC; however, these data seem anomalous. The WSOC data are provided in Appendix A. Several factors were investigated to attempt to account for these anomalous results. WSOC to IC ratios, OC/EC ratios, and relative concentrations of levoglucosan were correlated with anomalous results, yet none of these relationships demonstrated a consistent trend. Regardless of the few anomalous results, no

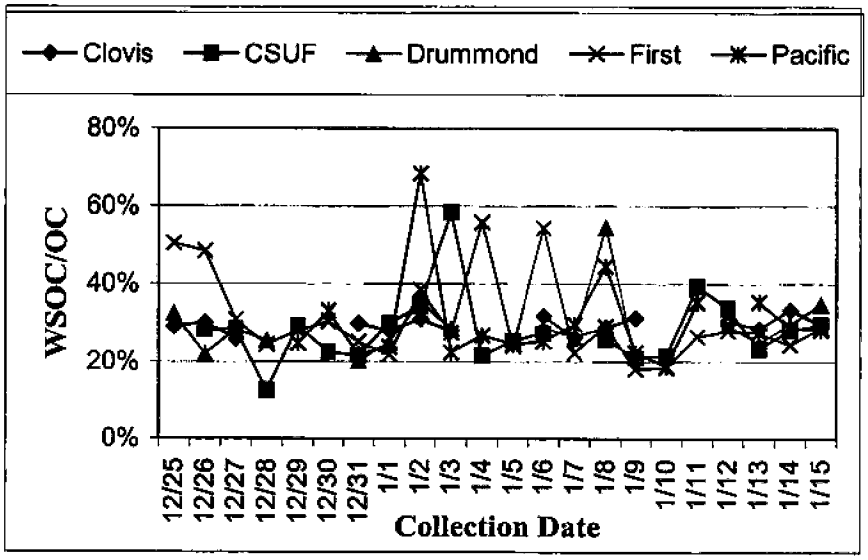

Figure 18. A timeline of the water soluble organic carbon as a percent of OC for $PM_{2.5}$ filters from each site.

hand, a comparison with Subramanian's QBQ adsorption levels as a function of OC concentration is not similar to results shown in Figure 17. The greatest variability in the adsorption as a percent of filter loading appears to be for filters with low levels of OC, while higher concentrations appear to have a smaller adsorption component. The best fit regression of the relationship between OC concentration and the percent adsorption is a logarithmic function. This regression line is the basis for an estimate of all sample's actual particulate OC concentrations. A plot of the residuals relative to values estimated from the regression line produces a Gaussian distribution and the relative error in the particle OC as estimated by this method is ±16% (standard deviation).

The concentrations of TC with removal of the estimated adsorption artifact are, on average, approximately 35% lower than unadjusted values. Given the uncertainty of this approach and lack of acceptance in the field, the adsorption values estimated in this study are purely for informational purposes and will not be included in subsequent calculations involving OC. The main differences resulting from subtraction of the adsorption component are a reduction in the absolute concentrations of OM and TC', as well as a reduction in the estimated organic fraction of $PM_{2.5}$. The average OC concentration decreased by 40% over the study period with removal of estimated adsorption. It is important to note here that this estimate of filter adsorption is approximately double what has previously been estimated for Fresno with the QBQ technique (Watson and Chow, 2002a). The removal of the adsorption artifact also influences the estimated organic fraction of $PM_{2.5}$, decreasing the average organic composition. While the absolute measurement of carbon can be adjusted for adsorption by the slicing method, the relative carbonaceous contribution to $PM_{2.5}$ can not be adjusted by simply removing estimated organic adsorption from OC estimates because the $PM_{2.5}$ mass also includes the mass of adsorbed vapors.

3.3.3 Water Soluble Organic Carbon Content

As shown in Figure 14, the organic fraction of $PM_{2.5}$ fluctuated significantly throughout the study ranging from a high of 85% to a low of 12%. Interestingly, the lowest fraction of

related literature by Turpin, et al. 2000 concluded that QBQ and quartz behind Teflon (QBT) filters did not effectively measure volatility loses, it still may be the case that quartz filters, which are measured to have 5 times the surface area of Teflon filters (Turpin, Huntzicker, and Hering, 1994), collect volatilized SVOCs more efficiently than Teflon. QBT filters are theoretically a better measure of the first quartz filter's adsorption artifact because of Teflon's limited adsorption capacity (McDow and Huntzicker, 1990; Turpin, Huntzicker, and Hering, 1994; Subramanian et al., 2004). Regardless of whether QBQ or QBT is more accurate, split stream samplers have demonstrated QBQ values that are approximately half of QBT (McDow and Huntzicker, 1990). Interestingly, the quantitative difference between QBQ and QBT filters is similar to the difference between QBQ and the slicing technique employed in this study.

Adsorption estimates from a subset of samples as analyzed with the slicing method display a wide range of values. The highest and lowest loaded $PM_{2.5}$ filters from each site were selected for analysis to provide upper and lower bounds on the adsorption artifact. Importantly, the fraction of adsorbed mass as a function of total measured OC concentration closely resembles data published by Subramanian, et al. 2004 for the QBT method; see Figure 17. On the other

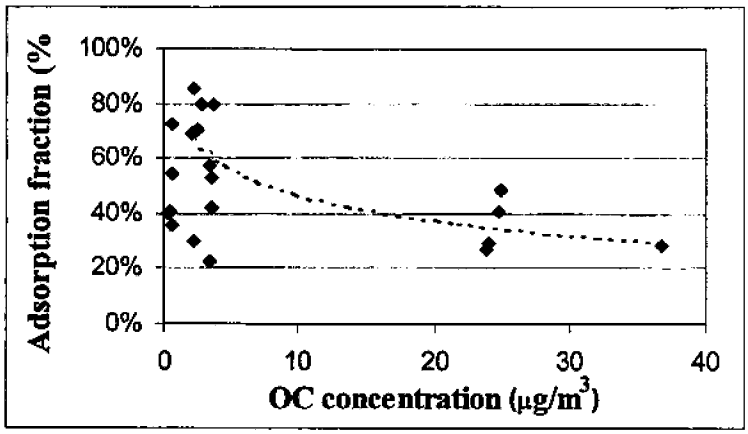

Figure 17. Estimated fraction of OC attributed to gaseous adsorption based on the method of slicing quartz filters plotted against total filter OC concentration. Included is a non-linear regression line for the absorption as a function of OC concentration for fine filters only. Both coarse and fine filter test results are included in the figure.

the bottom, gaseous component, from the top. This slicing method is theoretically similar to the analysis of two quartz fiber filters placed perpendicular to direction of air flow; however, the depth of the filter which the air flows through is different. Results of testing the organic matter captured on a quartz filter placed behind a quartz filter (QBQ) have shown that an average of 20% of OC is attributable to adsorption and/or SVOC volatilization in Fresno filters (Chow et al., 1999; Watson and Chow, 2002a), but values from other samples collected elsewhere have been as high as 50% (Turpin, Huntzicker, and Hering, 1994).

A method test was performed to compare the results obtained from the slicing method to the QBQ method. A Hi-Vol instrument without a PM_{10} impaction plate sampled ambient air in Fort Collins, CO on two quartz fiber filters placed perpendicular to the air flow to replicate the QBQ method of testing the adsorption artifact. The two filters were then analyzed for carbonaceous material in a method identical to the method used for Fresno filters. A portion of the top filter was also sliced in half in a method identical to that described above. Comparing the results from the slicing method versus the QBQ method shows that the adsorption estimates by the slicing method will be approximately 70% greater than the QBQ method. There are several possible explanations for the discrepancy between the QBQ method and filter slicing. It has been hypothesized that the front quartz filter initially depletes the air stream of gas phase compounds and thus the second filter, which is exposed to a smaller concentration of gas phase compounds, would not be an accurate measure of the first filter's absorption artifact (Turpin, Saxena, and Andrews, 2000). In this case the slicing of a single filter would provide a more accurate estimate of organic gas adsorption experienced by the filter. A second hypothesis is that the slicing method measures more than just gaseous adsorption: it also includes particulate-phase SVOCs that volatilized at some point during sampling and re-adsorbed further downstream in the original quartz filter. This scenario would lead to elevated levels of OC measured in the back half of the first filter relative to that measured on the QBQ filter, although the measured OC in this case could not be attributed solely to an adsorption artifact. While a review of available adsorption-

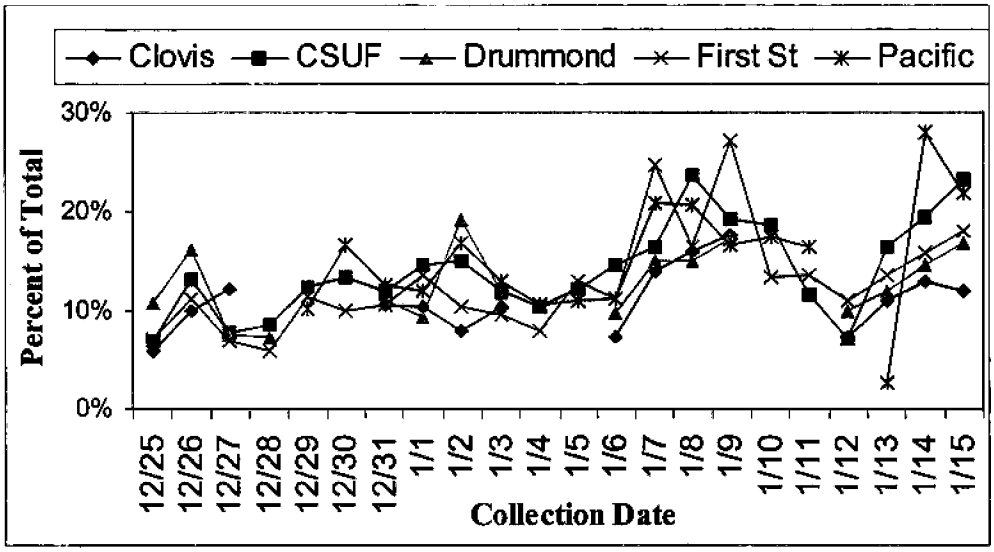

Figure 16. Fraction of total particulate carbon collected by coarse filters. Clovis and Drummond coarse fractions are PM_{10}-$PM_{2.5}$, while other sites' coarse fractions are TSP-$PM_{2.5}$. The cumulative error in coarse and fine samples results in a 20% uncertainty at the 99% confidence level.

3.3.2 Estimation of Organic Adsorption Artifact via Filter Slicing

Since the particulate matter was collected on quartz fiber filters, which are known to adsorb gas-phase organics, the measurement of OC is biased high due to this positive sampling artifact. To quantify and remove the component of OC that is due to gaseous adsorption, is highly complex and not yet well understood (Turpin, Huntzicker, and Hering, 1994; Turpin, Saxena, and Andrews, 2000; Kirchstetter, Corrigan, and Novakov, 2001; Mader and Pankow, 2001; Subramanian et al., 2004). For this study the adsorption artifact is quantified by a novel approach. Given the complications and uncertainties in the scientific community regarding this topic the results are presented here purely for informational purposes and will not be included in subsequent calculations involving OC. The method used to quantify adsorption in this study involves slicing a subset of filters through the plane of the filter producing a top half with the $PM_{2.5}$ deposition and a bottom half. Theoretically carbon measured on the bottom portion of the filter should be only adsorbed SVOCs because particulate matter will not penetrate the filter surface. One can then correct for the gaseous adsorption to the particulate fraction by subtracting

the remaining 15% is EC. This ratio varies by site and date, however. EC as a percent of TC' ranges from almost zero at Pacific on December 29th to a high of 23% at First Street on January 2nd. First Street seems to have the largest EC contribution, but it is not statistically different from other sites. Given that OC influences TC' to such a large degree, the temporal and spatial variability of TC' shown in Figure 15 is essentially the spatial/temporal variability of OC as well.

The carbonaceous component of coarse filters was also analyzed. The fraction of total carbon contained in the coarse filters relative to total particulate carbon (the sum of TC' from both coarse and fine filters) is shown in Figure 16. That the average amount of total carbon contained in the coarse fraction is low (~10-15%) establishes that most TC' is contained in the fine filters, which is similar to $PM_{2.5}/PM_{10}$ ratios of carbonaceous mater found previously (Chow et al., 1999). On a daily basis, however, the TC' partitioning between coarse and fine modes varies and coarse TC' in this study ranges between 28% and 6% of the total particulate carbon.

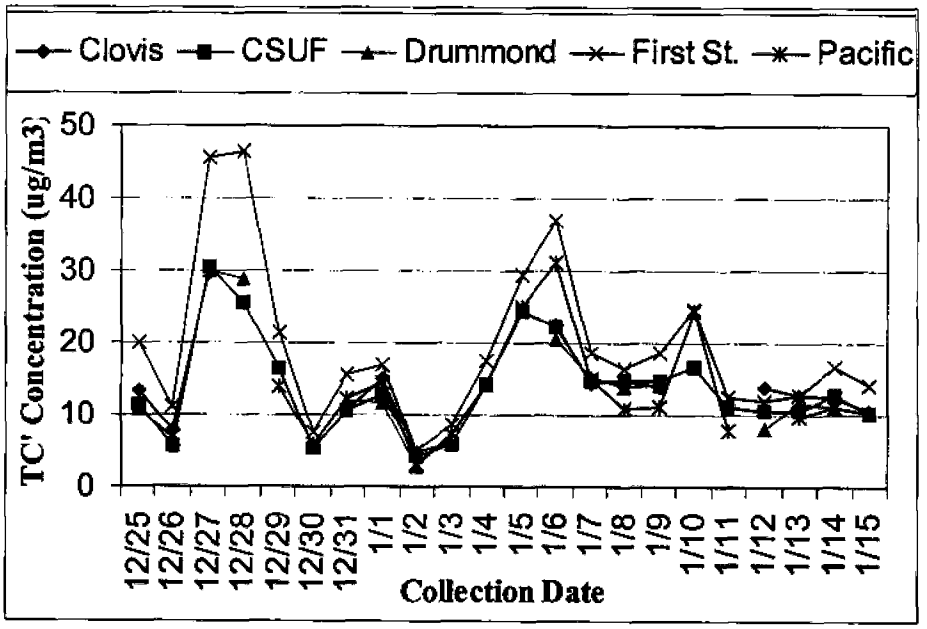

Figure 15. Timeline of fine total carbon mass (TC') concentrations for available sites over the study period. TC' is estimated as the sum of OC*1.6 and EC concentrations. TC' concentrations have a 13% uncertainty based on OC and EC measurement precision at the 99% confidence level. Additional uncertainty in the OC multiplier is not quantified.

by fog hydrometeors. The diurnal profile of TC over the study period shows that the maximum concentrations occur in evening or early morning. During fog events these maximum concentrations are significantly reduced. The difference between the daily maximum TC concentration and the daily average concentration is significantly greater on non-foggy days than on foggy days (statistically significant at the 99% confidence level based on a difference of means t-test with 7 degrees of freedom). Thus, not only is the daily average TC concentration lower during fog events, but maximum values are lower as well. Assuming that the sources of TC remain constant on foggy nights, the lower than normal carbon concentrations observed at night are an indication that organic material is being removed. All else being equal the night-time TC concentration should increase during radiation fogs due to the strong atmospheric stability and reduced mixing height that are typically associated with such fogs. This can be concluded given that carbonaceous PM is locally generated (thus not affected by variations in pollutant transport that might occur with a change in meteorological conditions) and knowing that TC is not simply being diluted by vertical mixing since the boundary layer is generally smaller during strong inversions typical of conditions favorable for radiation fog.

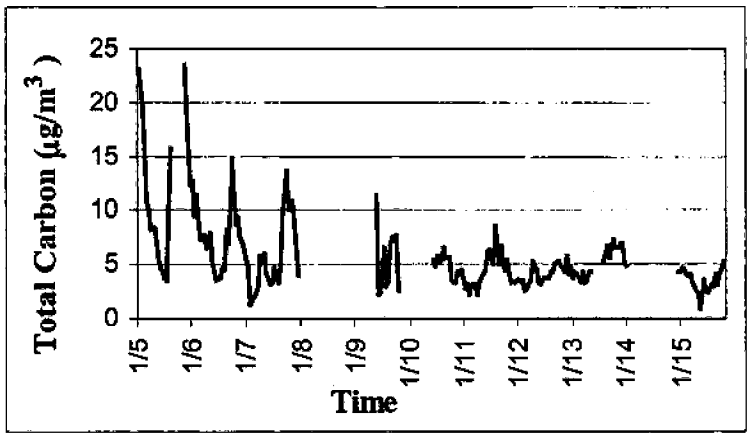

Figure 14. Hourly OC/EC data collected at CSUF.

The temporal and spatial variability of fine total carbon mass (TC'), shown in Figure 15, demonstrates a similarity to $PM_{2.5}$. Generally, OM accounts for approximately 85% of TC' and

the trend in absolute levels of inorganics through out this cycle leads to the speculation that secondary ammonium nitrate formation is favored at the end of these PM events.

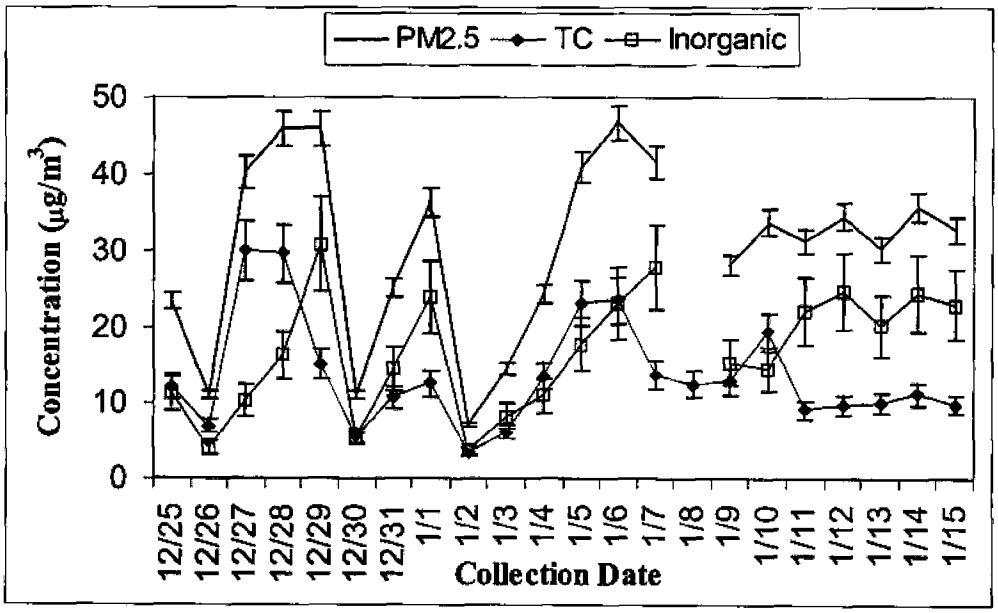

Figure 13. Daily average $PM_{2.5}$, total carbon mass (TC'), and inorganic or unknown (Inorganic) concentrations as averaged over available sites for the study period. Error bars represent the 99% confidence level.

Interestingly, the carbonaceous fraction of $PM_{2.5}$ is lowest during fog events which occur on January 1st and during the second period of the study from January 10th through the 15th. The average concentrations of TC' on foggy days are lower and inorganic fraction higher than on non-foggy, non-rainy days (statistically significant at the 95% and 90% confidence level for organic and inorganic concentrations, respectively, based on a difference of means t-test with 17 degrees of freedom). Although the reduction in the organic fraction of $PM_{2.5}$ during fog events might be due to a shift in equilibrium towards secondary ammonium nitrate formation with the increased RH, this does not explain the decrease in absolute levels of TC' concentrations during Period 2. The overall reduction in TC' may be due to efficient scavenging and deposition of particulate organic compounds by hydrometeors witnessed in a previous fog study (Herckes et al., 2005b). Hourly TC values collected at the CSUF site, shown for the later portion of the study in Figure 14, provide additional support for the conclusion that carbonaceous material is being scavenged

Table 12. Carbon Analysis data completeness for coarse and $PM_{2.5}$ filters.

Data Completeness	Number	% of valid filters
Total Samples	186	
Valid coarse filters	92	
Valid $PM_{2.5}$ filters	92	
Valid OCEC coarse	71	77%
Valid OCEC $PM_{2.5}$	91	99%
Outside LOQ coarse	21	23%
Outside LOQ $PM_{2.5}$	1	1%
Blank	18	NA

In this study the carbonaceous fraction is similar to previous findings where the composition of $PM_{2.5}$ is approximately half organic. Here, the remaining half is assumed to be inorganic. TC', which denotes Total Carbon Mass, is calculated as the sum of OM (OC*1.6)[1] and EC concentrations. On a daily basis the carbon fraction of $PM_{2.5}$ mass can fluctuate dramatically as shown in Figure 13; however, the study average organic fraction ranges from 44 to 55% for individual sites. As with $PM_{2.5}$ concentrations, the carbonaceous fraction of $PM_{2.5}$ demonstrates two distinct periods: first period from December 25th through January 9th shows a cyclical pattern of build-up and cleansing, while the second period from January 10th through the 15th has a relatively constant concentration of carbonaceous material. It is interesting to note a possible pattern of organic/inorganic variation during Period 1. As shown in Figure 13, $PM_{2.5}$ cycles generally begin with an organic fraction greater than or equal to the inorganic fraction and end with a large peak in inorganic levels. The trend in absolute organic concentrations during these cycles is to increase or stay constant and then dramatically decrease right before the end of the cycle, while, on the other hand, the trend in inorganic concentrations is to increase and then spike at the cycle's conclusion. While these cycles are perhaps governed by meteorological conditions,

[1] This value of OC multiplier was selected based on information from Turpin and Lim, 2001 that explain typical winter-time urban carbon multipliers are 1.4 while areas impacted by biomass burning necessitate a higher OC multiplier. See previous discussion of the OM-to-OC multiplier in Section 2.3.1.

Comparing this value to a winter-time three month average of 44.4 $\mu g/m^3$ demonstrates the low levels of PM in this study relative to previous winters (Watson and Chow, 2002b).

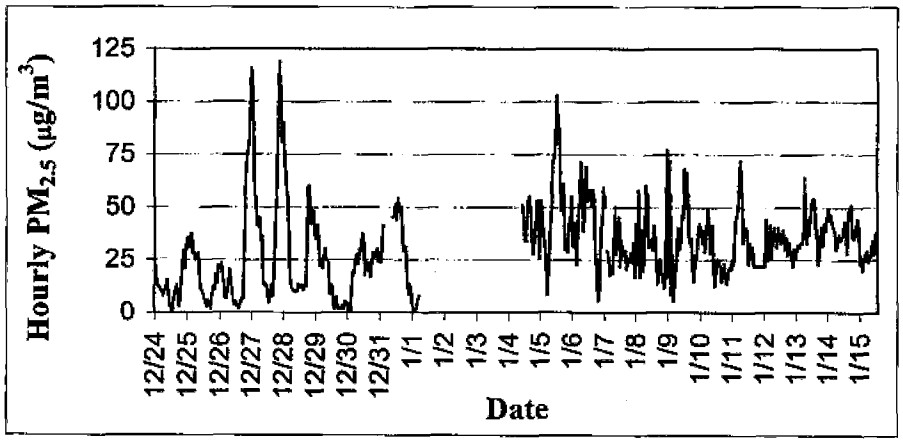

Figure 12. Hourly ARB $PM_{2.5}$ concentration ($\mu g/m^3$) over study period.

3.3 Carbonaceous Component

3.3.1 Total Carbon, Organic Carbon, and Elemental Carbon

The data completeness for carbon analysis is shown in Table 12. The number of valid coarse and $PM_{2.5}$ filters is more than Table 10 because the mass of some samples could not be determined but quantification of individual chemical compounds was not compromised. All ambient samples analyzed exceeded the MDL for the Sunset Carbon Analyzer as estimated by CSU operation and 88% of valid collected samples are within the LOQ (Carbon Analyzer detection limits are reported in Section 2.3.3, see Table 3). Where all but one of the $PM_{2.5}$ filters had TC values within the estimated LOQ for the Sunset instrument, only 77% of the coarse filters were within the LOQ. This is due entirely to carbon content below the estimated LOQ range. The range of EC deposits for all filters analyzed is between zero and 18.2 $\mu g/cm^2$, with 51 filters below the EC LOQ and two above. OC values range between 1.4 and 87.6 $\mu g/cm^2$. Due to the higher OC loading only half of the filters with suspect EC data are also suspect for OC: 26 samples fell below the OC LOQ. Only two samples exceeded the OC LOQ.

1981). The CSU research team was also conducting a fog chemistry study at CSUF during this period, providing some useful additional observations. These two periods will be referred to as Period 1 and Period 2, respectively, and are divided based on meteorological and ambient air pollutant data. A timeline of daily average $PM_{2.5}$ concentrations and measured precipitation and fog are shown in Figure 11. Evident in Figure 11 are the reduced concentrations of $PM_{2.5}$ during periods of rain most likely due to PM scavenging by hydrometeors followed by wet deposition and replacement of the pre-frontal, polluted air mass with cleaner air advected behind the front (Collett et al., 1991).

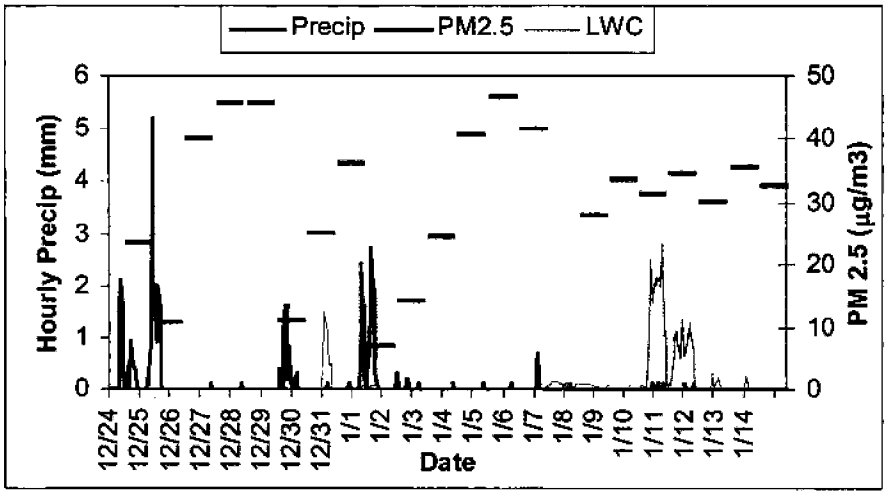

Figure 11. Daily average $PM_{2.5}$ concentration (right axis) shown with continuous precipitation measurements (in dark blue on left axis) and liquid water content (in light grey on left axis: actual values are 100x).

Evaluation of meteorological conditions in conjunction with measured $PM_{2.5}$ in the IMS95 study showed that diurnal variations in $PM_{2.5}$ concentrations were suppressed when rain or fog occurred and scavenging led to reduced $PM_{2.5}$ concentrations (Chow et al., 1999). A brief qualitative review of hourly $PM_{2.5}$ concentrations from the CARB (see Figure 12) show this diurnal suppression to be evident during the period from December 31st to January 1st, and perhaps during the later portion of this study period as well. An additional consequence of the precipitation events, occurring approximately every four or five days, is an overall reduction in study averaged PM levels. The average $PM_{2.5}$ concentration for the study is 30.4 $\mu g/m^3$.

study did not exceed the federal 24-hour average standard, the study average at all sites is approximately double the federal annual standard for $PM_{2.5}$ of 15 $\mu g/m^3$.

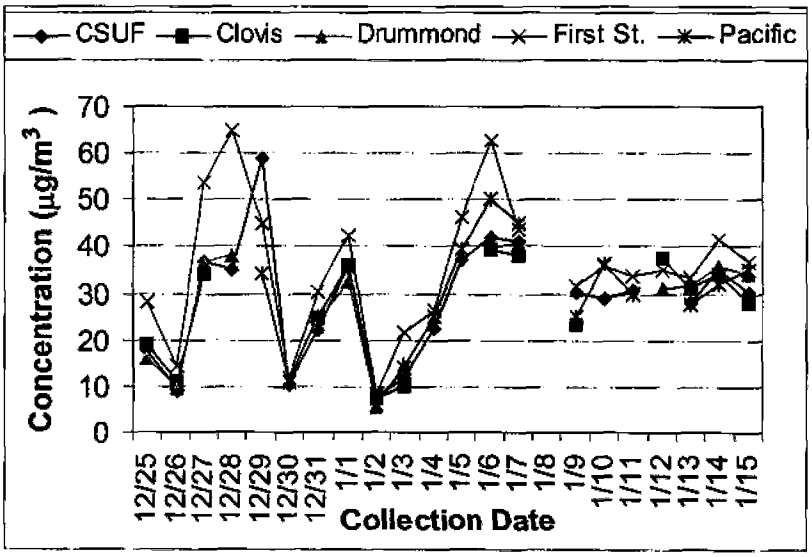

Figure 10. $PM_{2.5}$ concentration ($\mu g/m^3$) at each site with invalid data removed. There is a five percent uncertainty in concentration values.

Table 11. Site average $PM_{2.5}$ concentration for study duration.

Site Name	Average $PM_{2.5}$ ($\mu g/m^3$)
Clovis	26.7
CSUF	29.1
Drummond	28.9
First St.	35.6
Pacific	29.7

Examination of $PM_{2.5}$ concentrations over the study period indicates two distinct periods: the first occurring from December 25th through January 9th displays a very large day-to-day variability with extreme maxima and minima, while the second period from January 10th through the 15th displays consistent concentrations among sites. The cyclical pattern of PM accumulation followed by aerosol scavenging by rain or cleansing by rapid winds is typical of the SJV in winter and has been witnessed previously (Chow et al., 1999; Watson and Chow, 2002b) . This second period, also typical of the SJV, corresponds with a several day fog event (Holets and Swanson,

3.2 $PM_{2.5}$ Mass Concentration

The data completeness of $PM_{2.5}$ measurements is shown in Table 10. Invalid data result from instrument failure, sample weight contamination, and no available tare weight from which to measure accumulated mass. Over 90% of collected samples have valid $PM_{2.5}$ mass measurements.

Table 10. $PM_{2.5}$ gravimetric mass measurements data completeness.

Data Completeness	Number	% of Collected
Expected samples	97	
Actual samples	93	100%
Valid Samples	85	91%
Invalid Samples	8	9%
Blanks	15	NA

A timeline of $PM_{2.5}$ concentration in units of $\mu g/m^3$ at each site over the study period is shown in Figure 10. In general, the filter loadings appear to be rather homogeneous throughout the city, with the First Street site having the highest concentrations. The mass concentrations of $PM_{2.5}$ throughout the study period range from a low of 5.7 $\mu g/m^3$ at Drummond on January 2nd to a high of 64.8 $\mu g/m^3$ at First St. on December 28th. It is important to note that these are 20-hour average samples and given the period of collection and typical diurnal concentration patterns these samples will typically be biased high relative to 24-hour samples. The average concentration at First Street is about 15% greater than the other sites (significant at the 95% confidence limit based on a difference of means test given an *a priori* hypothesis and 80 degrees of freedom), although an episodic study in Fresno indicated that this is not always the case (Chow et al., 1999). The fact that the First Street site has somewhat higher concentrations than other areas of the city is not surprising given its downtown location; however, this has important implications from a regulatory and health effect perspective since the First Street site often is used to represent the whole of Fresno city. Table 11 shows the average $PM_{2.5}$ concentration at each site over the duration of the study. Although the daily concentrations measured during this

quadrant thus generally transporting the emissions from south to north, with the exception of January 3rd, when the wind was from the northwest.

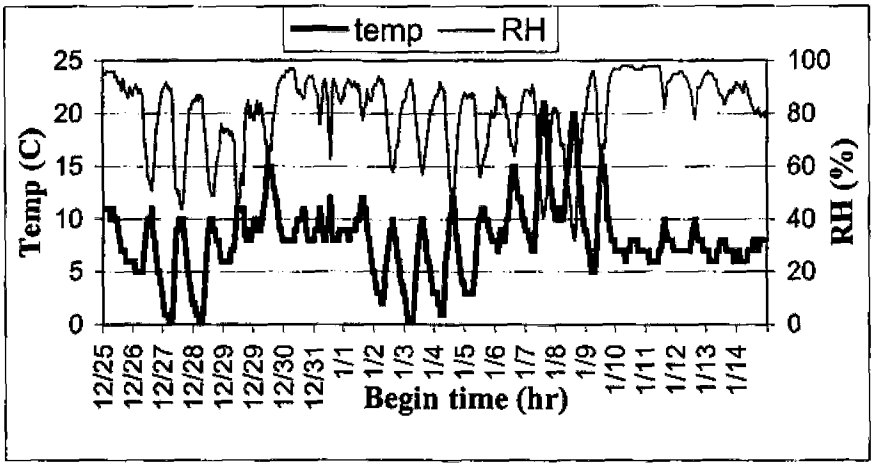

Figure 8. Hourly temperature (left axis) and relative humidity (right axis) over the study period.

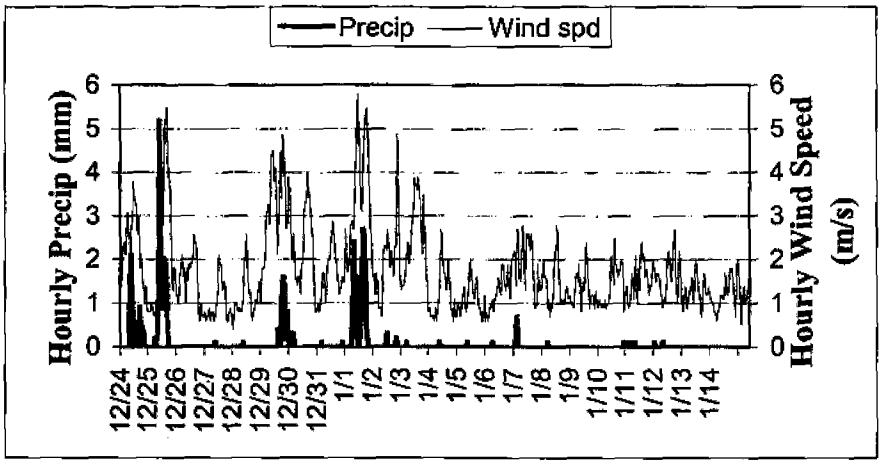

Figure 9. Hourly precipitation (left axis) and wind speed (right axis) over the study period.

Of interest for $PM_{2.5}$ removal processes is the amount and duration of precipitation events shown in Figure 9. Three major precipitation events occurred during the first two weeks of the study. Notably these events correlated with the three minimum values of measured daily $PM_{2.5}$ mass concentrations. The regularity of these precipitation events, occurring approximately every four or five days, moderated the extent of PM build-up.

CHAPTER 3 RESULTS

3.1 Meteorological Conditions and Influence on Results

The meteorological conditions can affect the formation of secondary PM and the gas-to-particle phase partitioning of SVOCs. The meteorological conditions during this study were typical of the area and season. Temperature and relative humidity data are recorded at the First St. site in Fresno and made available by the California Air Resources Board while precipitation and wind speed data are from a meteorological site at the Fresno State University of California. Average daily temperatures varied between 40 and 56° F with the highest temperatures reached during the 8th and 9th of January. Generally the relative humidity (RH) was high, ranging between 60 and 95%, although the RH measurements might not be very accurate for values exceeding 90% as fog was observed over the study period which requires an RH exceeding 100%. Figure 8 shows a timeline of the hourly average temperature and relative humidity for reference throughout the discussion of results and Figure 9 shows a similar timeline for precipitation and wind speed. The diurnal pattern of relative humidity and temperature is fairly distinct in Figures 8 and 9, with rising temperatures and wind speeds midday and corresponding decreases in RH. Notably, there is a smoothing of the diurnal pattern in Figure 8 during two periods: December 30th through January 1st, and January 10th through the 15th. These periods are consistent with observed fog events and occur when measured RH is the greatest over the study period.

General surface wind conditions during the study were light with speeds between one and 3 m/s; daily maxima typically occurred in the early afternoon and minima in the early morning. The wind speed maxima measured over the study duration occurred during periods of measurable precipitation. The predominant daily wind direction was between the southeast and southwest

2.5.2 Sample Analysis

The process required to estimate an ambient concentration from the data produced by the GCMS can be fairly involved. The steps and calculations used in this process are outlined here. Instrument calibration is the first and most critical step. The calibration process is iteratively performed with authentic standards or structurally similar compounds (type of standards are indicated in Table 5). First a calibration series is made to contain a constant concentration of deuterated internal standards (IS) within a range of analyte concentrations. The resulting detection (i.e. peak area) of the analyte relative to the IS is plotted as a function of known analyte concentration. The instrument response, which is the slope of a least squares regression of the calibration data, is then used in conjunction with the actual sample's ratio of IS peak area to analyte peak area to estimate the actual sample concentration of the analyte. Note that not all of the calibration plots demonstrated a linear fit and that the squared correlation coefficient between the best fit line and the data is greater than 0.984 for all the calibration plots, with a few exceptions in the alkane family. The rationale for using a ratio between the analyte and an IS is two-fold: first, the ratio corrects for any variation in the injection volume (due to manual injection); second, the inclusion of an IS of similar structure and chemical composition provides an adjustment for analyte loss during sample extraction and preparation procedures.

After the concentration of the analyte in the extracted solution is calculated, the ambient concentration of the analyte is estimated by adjusting the solution volume by the fraction of filter extracted and dividing by the volume of air that passed through the filter. As is indicated in Table 9 sample blanks are processed in the same manner as samples to quantify any contamination that may have occurred in sampling or extraction procedures.

with hydroxyl groups (see Figure 7). Samples were silylated by addition of an equal volume of sample and bis(trimethylsilyl) trifluoroacetaminde (BSTFA) containing 1% trimethylchlorosilane (TCS), heat sealing the container and placing the vial in a 65°C chamber for 3 to 5 hours for reaction. Care was taken to minimize exposure of the reagent to moisture during the silylation process since moisture has been shown to reduce the effectiveness of the reaction mechanism.

Table 9. Sample preparation details for GC/MS quantification of silylated species.

Sample Name	Filter Area Extracted (cm^2)	No. of samples included	IS volume	Total DCM volume (mL)	Final Volume (μL)
Clovis Blk	206.5	4	Table 7	150	250
CSUF Blk	206.5	4	Table 7	150	250
Drummond Blk	206.5	4	Table 7	150	250
First St. Blk	206.5	4	Table 7	150	250
Pacific Blk	206.5	4	Table 7	150	250
22	20.0	1	2 x Table 7	55	500
43	22.0	1	2 x Table 7	55	500
44	23.7	1	2 x Table 7	55	500
45	18.9	1	2 x Table 7	55	500
48	14.4	1	2 x Table 7	55	500
49	23.0	1	2 x Table 7	55	500
71	20.1	1	2 x Table 7	55	500
72	19.5	1	2 x Table 7	55	500
73	22.4	1	2 x Table 7	55	500
75	21.0	1	2 x Table 7	55	500
76	22.0	1	2 x Table 7	55	500
80	16.4	1	2 x Table 7	55	500
81	18.3	1	2 x Table 7	55	500
82	20.8	1	2 x Table 7	55	500
83	10.8	1	2 x Table 7	55	500
85	23.0	1	2 x Table 7	55	500
86	21.6	1	2 x Table 7	55	500
87	20.8	1	2 x Table 7	55	500
88	23.0	1	2 x Table 7	55	500
89	20.5	1	2 x Table 7	55	500
91	21.4	1	2 x Table 7	55	500
93	21.8	1	2 x Table 7	55	500
94	21.8	1	2 x Table 7	55	500
96	20.8	1	2 x Table 7	55	500
100	22.7	1	2 x Table 7	55	500
104	16.4	1	2 x Table 7	55	500

Sample	Clovis Composite	CSUF Composite	Drum Composite	First Composite	Pacific Composite	Clovis Blk Composite	CSUF Blk Composite	Drum Blk Composite	First Blk Composite	Pac Blk Composite
guaiacol	0.07	0.05	0.06	0.05	0.07	ND	0.003	0.005	0.003	0.004
Meat Tracers (ng/m^3) and Other sterols										
Nonanal	ND	11.7	10.7	ND	6.3	ND	ND	ND	ND	ND
cholesterol	1.0	1.1	1.6	1.0	1.4	ND	ND	ND	ND	ND
ergosterol	1.5	0.4	ND	ND	ND	ND	ND	ND	0.775	ND
stigmasterol	0.4	ND	0.5	0.5	0.1	ND	ND	ND	0.157	ND
Hopanes and Steranes (ng/m^3)[e]										
20R, 5α(H),14β(H),17β(H)-cholestane	0.0413	0.0222	0.0576	0.0276	0.0596	ND	ND	ND	ND	ND
20S, 5α(H),14β(H),17β(H)-cholestane	0.042	0.027	0.065	0.025	0.069	ND	ND	ND	ND	ND
20R, 5α(H),14β(H),17α(H)-cholestane	0.127	0.044	0.099	0.069	0.230	ND	ND	ND	ND	ND
20S,R-5α(H),14β(H),27β(H)-ergostanes	0.148	0.039	0.089	ND	0.142	ND	ND	ND	ND	ND
20S,R-5α(H),14β(H),17β(H)-sitosanes	0.116	0.079	0.098	0.179	0.143	ND	ND	ND	ND	ND
22,29,30- trisnorneohopane	0.167	0.088	0.133	0.139	0.168	ND	ND	ND	ND	ND
17α,21β-29-hopane	0.686	0.492	0.495	0.862	0.452	ND	ND	ND	ND	ND
17α, 21β-hopane	0.801	0.570	0.565	1.062	0.747	ND	ND	ND	ND	ND
22S,R-17α, 21β-30-homohopanes	0.325	0.296	0.340	0.489	0.362	ND	ND	ND	ND	ND
22S,R-17α, 21β-30-bishomohopanes	0.153	0.193	0.226	0.318	0.195	ND	ND	ND	ND	ND
Sugars (ng/m^3)										
Levoglucosan[f]	—	—	—	—	—	ND	2661	ND	ND	ND
mannosan	—	—	—	—	—	ND	ND	ND	ND	ND
galactosan	—	—	—	—	—	ND	ND	ND	ND	ND

Sample	Clovis Composite	CSUF Composite	Drum Composite	First Composite	Pacific Composite	Clovis Blk Composite	CSUF Blk Composite	Drum Blk Composite	First Blk Composite	Pac Blk Composite
Total quantified by GC/MS (ng/m^3)	102	119	116	148	68	—	—	—	—	—
Percent of OM Quantified (%)[b]	0.9%	1.1%	1.1%	1.0%	0.6%	—	—	—	—	—
Percent of $PM_{2.5}$ Quantified (%)	0.4%	0.4%	0.4%	0.4%	0.2%	—	—	—	—	—

[a] Reported mass of species in blanks is in units of μg which is the same order of magnitude of concentrations reported in ng/m^3.

[b] OM is calculated by multiplying OC by 1.6

[c] ND means not detect

[d] CPI calculated from alkanes C_{17}-C_{40}

[e] Actual standards were not used, with the exception of 17α, 21β-hopane, and thus are uncertain

[f] Blank values for levoglucosan, mannosan, and galactosan were all very high; however this is likely a source of contamination or carry over from previous injections. For comparison, levoglucosan from individual blanks measured by HPAEC-PAD were all approximately 2 μg which is about 1/1000 of the mass measured in GC/MS blank composites and less than one percent of ambient samples.

The ambient tracer concentration, if unique to the source, can be divided by this ratio to provide an estimate of the amount of OC and $PM_{2.5}$ in the ambient sample from an individual source type.

During winter-time in Fresno, sources that generally contribute the most to ambient $PM_{2.5}$ levels are motor vehicles, meat cooking operations, and wood smoke (Schauer and Cass, 2000), although source apportionment studies conducted elsewhere indicate that wood smoke is not always a large contributor to urban $PM_{2.5}$ (Fraser, Yue, and Buzcu, 2003). The efforts of this study specific to Fresno will focus on these three sources. As discussed already, levoglucosan is a common tracer for biomass combustion. Other tracers include hopanes and/or steranes for motor vehicle emission sources and cholesterol for meat cooking. In addition to source contribution estimates for samples analyzed by GC/MS, levoglucosan quantified by HPAEC-PAD is used to estimate the contribution of wood smoke to all collected samples. As part of a sensitivity analysis other wood smoke tracers are used to determine the potential error of the wood smoke apportionment method using levoglucosan alone.

Since this project did not include source characterization studies, we use previously published source profiles. In some cases different source profiles have been published for similar sources; when applicable, the profiles are combined. It is important to note that many factors can influence the results of source tests such as operating conditions, test duration, sampling procedures, material differences, water content, burn conditions, etc. Given the high degree of variability, it is beneficial to combine source profiles for a more robust analysis. Tables 17-23 show the selected source profiles, the tracer mass quantity, and the tracer OC and $PM_{2.5}$ normalization factor for all source types. One complication is that while a broad source category may have a unique tracer there are often a variety of different combustion methods for that source category (e.g. fireplaces or wood burning stoves, catalyst or non-catalyst equipped gasoline engines, etc.) which lead to multiple source profiles. In this event, some assumptions may be required in order to estimate the total source contributions to OC/ $PM_{2.5}$.

The general approach followed here to convert tracer concentrations into estimates of source contributions to OC and $PM_{2.5}$ involves the apportionment of tracers to the different combustion methods and then application of published source profiles. The first step of apportioning the tracer to the different combustion methods might require some assumptions necessary for estimation of the total source's contribution. Using vehicles as an example, if 50% of fuel used is diesel and 50% is gasoline, but gasoline only produces 1/3 the tracer that diesel does per unit of fuel, then simply dividing the tracer concentration in half will produce erroneous results. Thus the equation for allocating the total tracer concentration to a specific combustion method (e.g. diesel engines and gasoline engines) is outlined in the following equations. This method of allocating tracers to a combustion method is used in meat cooking, vehicle exhaust and residential wood combustion estimates.

$$Tracer_1=[EF_1]*Fuel_1 \quad \text{(Eq. 3-1)}$$

$$Tracer_{total}= Tracer_1+ Tracer_2 \quad \text{(Eq. 3-2)}$$

$$Tracer_{total}= [EF_1] * Fuel_1+ [EF_2]\ Fuel_2 \quad \text{(Eq. 3-3)}$$

In equations 3-1 through 3-6, different combustion methods are indicated by subscript numbers 1 and 2, emissions factor (EF) is the tracer mass per fuel unit, and Fuel is the amount of fuel used by a combustion method. With some arithmetic, the percent of a tracer attributable to a combustion method can be calculated.

$$Percent_1= Tracer_1 \div Tracer_{total} \quad \text{(Eq. 3-4)}$$

$$Percent_1= ([EF_1] * Fuel_1) \div([EF_1] * Fuel_1+ [EF_2] * Fuel_2) \quad \text{(Eq. 3-5)}$$

$$Percent_2= ([EF_2] * Fuel_2) \div([EF_1] * Fuel_1+ [EF_2] * Fuel_2) \quad \text{(Eq. 3-6)}$$

The percent of $Tracer_1$ and $Tracer_2$ when multiplied by the actual measured total tracer concentrations will sum to 100% of the measured tracer concentrations. Applying these equations to the above example would estimate that 25% of the tracer is from gasoline combustion and 75% is from diesel combustion:

$$Percent_{gasoline}= (1/3 * 0.5) \div(1/3 * 0.5+1*0.5)= 25\% \quad \text{(Eq. 3-7)}$$

$$Percent_{diesel}= 75\% \quad \text{(Eq. 3-8)}$$

The percent of a tracer attributable to a method of combustion is calculated for all three sources (e.g. meat cooking, vehicles, and residential wood combustion). Once the tracer concentration from each combustion method is calculated, the total source contribution to OC and $PM_{2.5}$ can be estimated using the source profiles.

3.6.1 Meat Cooking: source profiles and apportionment results

As outlined in the above example, there are two different combustion methods commonly used in commercial meat cooking operations: frying and charbroiling. For meat cooking there is no tracer specific to frying or charbroiling, rather both cooking techniques have the same tracer, cholesterol, with very different source profiles (i.e. tracer to meat ratios). The source profiles for frying versus charbroiling of meat are shown in Table 17, normalized by weight of meat cooked. Source profiles for meat frying are from Rogge et al. (1991), and the charbroiling source profile is a combination of Rogge et al. (1991) and Schauer et al. (1999a). Note that the source sampling performed in 1991 is based on particulate matter with a aerodynamic diameter less than 2.0 μm. The approach used here is similar to that briefly outlined above. The tracer concentration estimated for each combustion method (e.g. frying versus charbroiling) is multiplied by the source profiles for each method and then summed together to calculate the total contribution of meat cooking. The percentage tracer estimated for each combustion method is shown in Table 18. Two different cases are examined in this study: one uses the ratio of 90% meat fried to 10% charbroiling as published by Rogge et al. in 1991; another considers the effect of increased charbroiling since 1991 to an assumed equal ratio of charbroiling and frying.

Table 17. Meat cooking source profiles and ratio of tracer to OC as used for this study. Mass values are in g/kg of meat cooked.

Source Profiles	OC	cholesterol	OC/cholesterol
charbroiling	20.44	3.44E-02	594.5
frying	0.66	7.10E-03	92.6

Table 18. Percentage of tracer attributable to frying and charbroiling based on the tracer emitted per mass of meat. Two cases are shown: one case with ratios published in 1991, and a second case with a hypothesized increase in charbroiling to an equal ratio of charbroiling and frying.

Cholesterol apportionment	1991 Ratio[a]: 90% frying 10% charbroil	Increase: 50% frying 50% charbroil
charbroiling	35.0%	82.9%
frying	65.0%	17.1%

[a] Ratio of frying to charbroiling is estimated by Rogge et al. 1991 for the Los Angeles basin.

The resulting OC apportionments for both cases are shown in Figure 26. $PM_{2.5}$ estimates are not available for the source profiles published by Rogge et al. (1991) and as such are not included here. For the ratio of frying to charbroiling as published by Rogge et al. (1991), meat cooking in Fresno contributes between 0 and 6% to OC. If the amount of meat charbroiled has increased to 50%, then meat cooking could contribute as much as 12% to OC at some sites. The meat cooking estimates produced by using the 90/10 relative ratio of frying to charbroiling estimated in 1991 are somewhat lower than previous Fresno source apportionment studies, but the apportionment with a 50/50 ratio of frying to charbroiling is remarkably similar. In a CMB analysis of Fresno, meat cooking is estimated to represent approximately 6-14% of OC during two different multi-day episodes (Schauer and Cass, 2000). The estimates performed based on literature values of frying and charbroiling (i.e. 90/10 relative ratio of frying to charbroiling) will be included with the final OC apportionment estimates for this study. The variability of meat cooking in the samples appear to be fairly random with very little coherence between sites or days. Generally, the contribution of meat cooking is highest at Drummond, which is most likely influenced by the BBQ located near an adjacent fire station. It is important to note the recent concern in the atmospheric science community regarding the stability of cholesterol in the ambient environment due to a double carbon bond (see Figure 7) which generally leads to increased reactivity (Finlayson-Pitts and Pitts, 2000). Atmospheric reaction of cholesterol could lead to a possible apportionment bias.

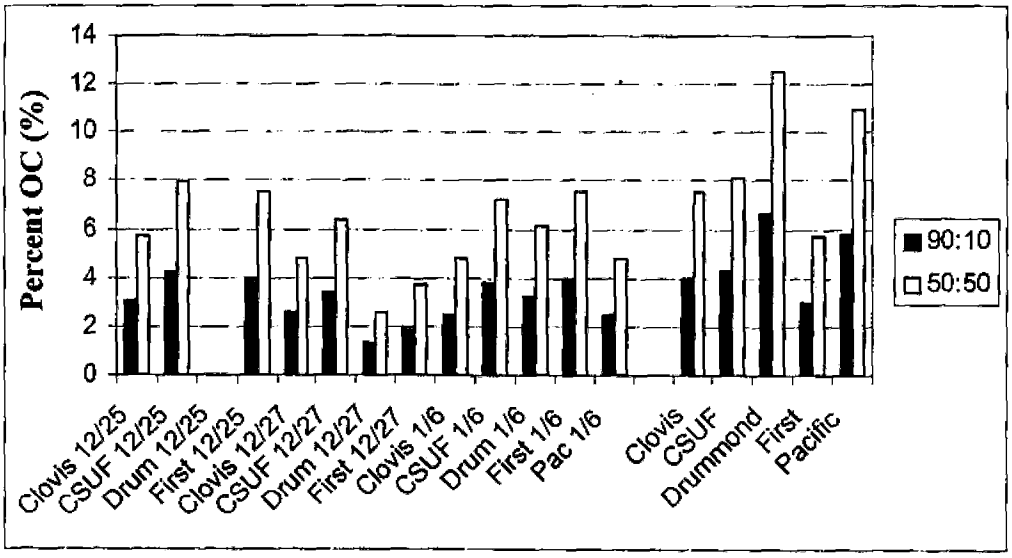

Figure 26. Percent of total OC that is attributable to meat cooking for samples analyzed by GC/MS. Two cases are shown: one with 1991 values, and a second representing a perceived change in meat cooking practice since 1991.

3.6.2 Motor Vehicles: source profiles and apportionment results

Similar to meat cooking, there are several different combustion methods for motor vehicles depending on fuel type and whether the vehicle is equipped with a catalyst. The source profiles for three different vehicle engines are shown in Table 19. The tracer 17α, 21β-hopane is emitted by all three combustion methods. Source profiles for gasoline engines both with a catalyst and without a catalyst are from Rogge et al. (1993a), and the diesel source profile is a combination of heavy-duty diesel from Rogge et al. (1993a) and medium-duty diesel from Schauer et al. (1999b). Unfortunately there is no tracer specific to diesel combustion, rather both gasoline and diesel engines have the same tracer with very different source profiles. Likewise the profiles for catalyst equipped automobiles differ substantially from non-catalyst equipped without an ability to trace the two sources separately. The approach used here is similar to that for meat cooking burning by apportioning the tracer concentration to each combustion method (e.g. diesel engine, gasoline engine with catalyst or gasoline engine without catalyst), then applying source specific emissions profiles.

Table 19. Motor vehicle source profiles and ratio of tracer to OC and $PM_{2.5}$ as used for this study. Mass values are in g/gallon of fuel consumed.

Source Profiles	$PM_{2.5}$	OC	EC	17α, 21β-hopane	OC/hopane	PM/hopane
Gasoline: catalyst	1.50	0.843	0.120	2.28E-04	3705	6600
Gasoline: no catalyst	0.68	0.290	0.153	6.83E-04	425	989
Diesel	4.99	2.803	2.022	1.15E-03	2432	4331

The percentage of tracer estimated to come from each source is shown in Table 20. The base case estimate in units of fuel consumed is 70% catalyst equipped gasoline engines, 10% non-catalyst equipped, and 20% diesel engines. Normalization based on volume of fuel was selected instead of normalizing by distance traveled because one can more easily estimate county-specific fuel sales than vehicle miles traveled per engine type. The California state total ratio of gasoline to diesel fuel sales is available from The California Department of Finance in an annual report, "The California Statistical Abstract" (California, 2005). To generate a ratio of gasoline to diesel fuel consumption specific to Fresno county relative to the state level, county vehicle registration data as provided by the Statistical Abstract were used. Combined these sources provide an estimate of Fresno county fuel sales ratio being 20% diesel and 80% gasoline. Additionally an assumption is made that ~90% of gasoline powered motor vehicles are catalyst equipped.

Table 20. Percentage of tracer attributable to catalyst equipped gasoline engines, non-catalyst equipped gasoline engines and diesel engines based on source profiles normalized by fuel consumed. Three different estimates are shown: a base case, one half diesel fuel, and double the gasoline consumed in non-catalyst equipped engines.

Hopane apportionment	One-half Diesel: 80% catalyst gas 10% non-cat gas 10% diesel	Base Case: 70% catalyst gas 10% non-cat gas 20% diesel	Double non-catalysts: 60% catalyst gas 20% non-cat gas 20% diesel
Gasoline: catalyst	56.47%	42.85%	32.72%
Gasoline: no catalyst	21.18%	18.37%	32.74%
Diesel	22.35%	38.77%	34.54%

The resulting OC and $PM_{2.5}$ apportionment based on these estimates and assumptions are shown in Figures 27 and 28. The error bars on Figures 27 and 28 represent the change in

apportionment for the different cases examined (i.e. an increase in non-catalyst equipped vehicles or a decrease in diesel consumption). The apportionment is not particularly sensitive to the relative ratios of diesel to gasoline, as a reduction in the contribution of diesel engines by half results in a 5% increase in OC emissions; however, by approximately doubling the contribution of non-catalysts equipped automobiles there is a ~15% decrease in OC emissions. The emissions change is in the opposite direction than anticipated because of tracer apportionment technique (i.e. an increase emissions caused by a decrease in diesel fuel consumption occurs because the concentration of the tracer is constant and diesel or non-catalyst equipped autos emit more tracer per OC or PM than catalyst equipped automobiles do). For the base case, motor vehicles contribute between 8 and 30% to OC and 6-17% to $PM_{2.5}$. These estimates are somewhat higher than previous Fresno source apportionment studies, but are remarkably similar given different source profiles, sampling intervals, and apportionment techniques (Schauer and Cass, 2000). A Chemical Mass Balance (CMB) modeling study of Fresno performed by Schauer and Cass estimates vehicle emissions to represent approximately 13-17% of OC and 11-13% of $PM_{2.5}$ during two different multi-day episodes. Given that their estimates are based on three day composite samples, which smooth daily fluctuations, the results presented in this study are within a similar range: an average of December 25th and December 27th samples would result in approximately 17% contribution to OC and 11% contribution to $PM_{2.5}$. The average contribution of motor vehicles over the duration of the study is estimated to be 26% of OC and 11% of $PM_{2.5}$.

Generally, the contribution of motor vehicles to either OC or $PM_{2.5}$ is larger for the site composites than for the individual samples analyzed: an indication that that the samples not identified by GC/MS have a larger motor vehicle influence than those samples that were. The temporal variability in those samples analyzed by GC/MS indicate that the motor vehicle contribution decreases on December 27th relative to Christmas and the high OC event on January 6th. It is important to note that the Clovis sampling site is located near a facility that houses a government vehicle fleet, thus the apportionment of motor vehicle emissions at Clovis might be

biased high. Interestingly, First St. does not appear to have a significantly larger motor vehicle influence than other sites. Although CSUF and Drummond site averages seem to have less motor vehicle influence than the three other sites, the individual samples do not reinforce this difference.

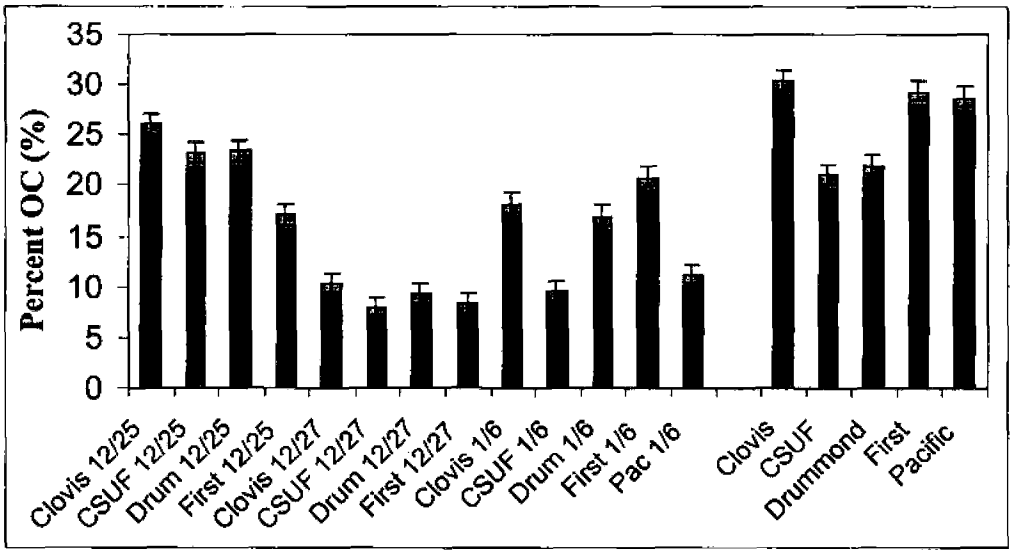

Figure 27. Percent of total OC that is attributable to motor vehicles for samples analyzed by GC/MS. Error bars indicate apportionment changes corresponding to a 50% decrease in diesel fuel or a doubling of gasoline consumed by non-catalyst equipped engines.

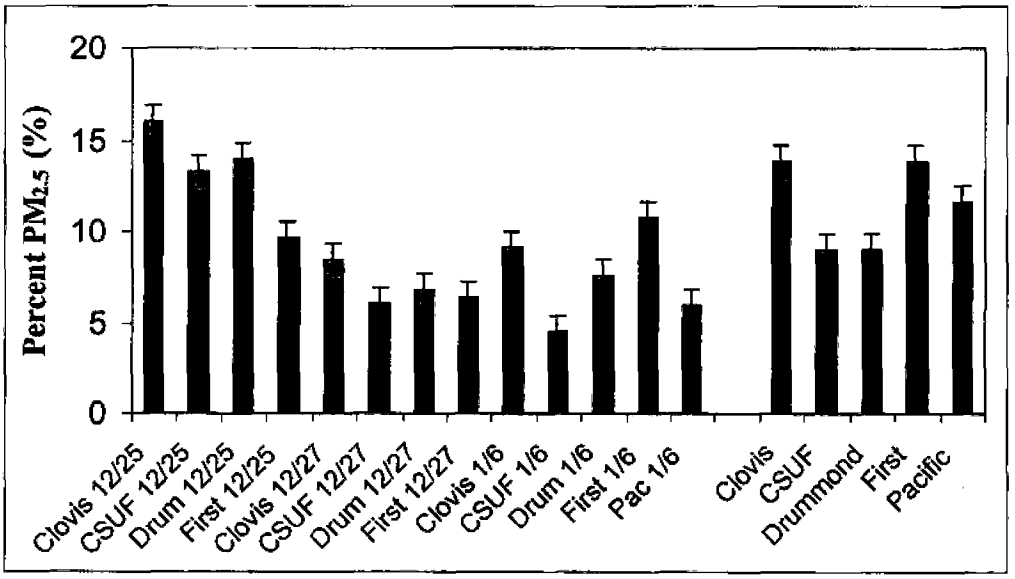

Figure 28. Percent of total PM2.5 that is attributable to motor vehicle primary fine particle emissions for samples analyzed by GC/MS. Error bars indicate apportionment changes corresponding to a 50% decrease in diesel fuel or a doubling of gasoline consumed by non-catalyst equipped engines.

3.6.3 Residential Wood Combustion: source profiles and apportionment results

The approach used here is similar to the method used to estimate the contribution by meat cooking and motor vehicles. Briefly, the tracer concentration estimated for each combustion method (here the different combustion methods are wood stoves or fireplaces) is multiplied by the source profiles for each method and then summed together to calculate the total contribution of residential wood combustion. The percentage tracer estimated for each combustion method is shown in Table 23 and the source profiles for the different combustion methods are shown in Tables 21 and 22. The calculation of residential wood burning is complicated by the wide range of possible fuel types (i.e. different wood). Below is an explanation of the detailed calculations and assumptions used to derive the final tracer apportionment and source profiles.

It is assumed that a large majority of the biomass burning affecting Fresno air quality is residential over the duration of this study. For the purpose of this study the biomass burning source profiles are generated by combining profiles for wood burning stoves and fireplaces with wood types specific to the study area. Fireplace and wood stove source profiles are selected from Schauer et al. 2000, Fine et al., 2004a, and Fine et al., 2004b. Estimates by Fine and co-workers suggest that approximately half the residential wood burned is burned in wood stoves, while the other half is burned in fireplaces (Fine, Cass, and Simoneit, 2004b). Further complicating the apportionment of residential wood burning is the fact that wood stoves sometimes are equipped with a catalyst. For simplicity and lack of current, regional data, it will be assumed that 50% of the wood stoves operated in Fresno have catalysts and 50% do not. This is potentially an overestimate of wood stoves with catalysts (as it was estimated that 11% of wood stoves in use nationally were catalyst equipped in 1998 (Houck et al., 1998)); however, an overestimate of catalyst equipped wood stoves will lead to a conservatively low estimate of contribution to $OM/PM_{2.5}$. This is because wood stoves with catalysts emit less tracer, both on a per mass basis and per measured OC, so by increasing the estimated amount of wood burned by woodstoves with catalysts there is a corresponding decrease in the estimated contribution by wood burning to

Table 21. Fireplace source profiles and ratio of tracer to OC and $PM_{2.5}$ as used for this study. Mass values are in g/kg of wood burned.

Wood Type	$PM_{2.5}$	OC[a]	Levoglucosan	acetovanillone	guaiacol	vanillin	retene[b]
Softwood							
Pine mass[c]	9.5	5.32	1.38	0.0196	0.0004	0.1380	0.0085
		% OC	25.85%	0.37%	0.0067%	2.59%	0.16%
		% PM	14.47%	0.21%	0.0038%	1.45%	0.09%
Douglas fir mass[d]	4	2.76	0.747	0.0251	0.0004	0.0218	NA
		% OC	27.10%	0.91%	0.016%	0.79%	
		% PM	18.68%	0.63%	0.011%	0.54%	
Ponderosa pine mass[d]	6	3.86	0.274	0.0228	0.0008	0.0151	0.0135
		% OC	7.10%	0.59%	0.022%	0.39%	0.35%
		% PM	4.57%	0.38%	0.014%	0.25%	0.23%
Pinyon pine mass[d]	8.1	4.61	0.046	0.0198	0.0007	0.0189	0.0314
		% OC	1.00%	0.43%	0.015%	0.41%	0.68%
		% PM	0.57%	0.24%	0.009%	0.23%	0.39%
EF (g/kg wood)[e]	6.90	4.14	0.61	0.022	0.0006	0.048	0.018
Hardwood							
Oak[c]	5.1	3.01	0.71	0.0011	0.0001	0.0024	0.0011
		% OC	23.46%	0.04%	0.0050%	0.08%	0.04%
		% PM	13.84%	0.02%	0.0029%	0.05%	0.02%
White Oak mass[d]	6.8	3.67	0.360	0.0059	0.0007	0.0059	NA
		% OC	9.80%	0.16%	0.018%	0.16%	
		% PM	5.29%	0.09%	0.010%	0.09%	
Black Oak mass[d]	7.2	3.91	0.915	0.0070	0.0009	0.0082	NA
		% OC	23.40%	0.18%	0.024%	0.21%	
		% PM	12.70%	0.10%	0.013%	0.11%	
EF (g/kg wood)[e]	6.37	3.53	0.66	0.0047	0.00058	0.0055	0.0011

[a] Organic carbon mass values as reported by Fine et al. 2004a were calculated as OC*1.4 and this multiplier was removed to provide a consistent OC value among multiple studies.
[b] Retene is from combustion of coniferous species
[c] Source profiles published by Schauer et al., 2001
[d] Source profiles published by Fine et al., 2004a. A subset of all source tests published are included here, to restrict calculations to wood types available in the study area.
[e] This is the emission factor used to estimate the total mass of tracer attributed to fireplace emissions for softwood or hardwood. Without more detailed information regarding the quantity of wood burned by wood type, available source profiles have to be combined. The calculated tracer quantity as a percent OC or $PM_{2.5}$ is the average of profiles for softwood types or hardwood types.

OC. Since the published emission profiles for wood stove combustion only incorporate two of the wood types found in Fresno that were also profiled in fireplace tests, the emission factors and tracer ratios as calculated in Table 21 will be scaled relative to the observed change in emissions if the same wood types were to be combusted in a wood stove (i.e. on a per wood basis wood

stoves emit approximately about one third of the $PM_{2.5}$ and OC and close to half the levoglucosan as fireplaces). The emission factors for wood smoke tracers and tracer ratios to OC and $PM_{2.5}$ for wood burning stoves as applied in this study are included in Table 22.

Table 22. Wood stove source profiles and ratio of tracer to OC and $PM_{2.5}$ as used for this study. Actual source profile is shown as well as the calculated percent of emissions of the same wood type combusted in a fireplace.

Wood Type	$PM_{2.5}$ (%)	OC (%)	Levog-lucosan (%)	Aceto-vanillone (%)	Guaiacol (%)	Vanillin (%)	Retene (g/ kgwood)[a]
Softwood							
Douglas fir: no catalyst (g/kg wood)	1.1	0.86	0.350	0.0034	0.0003	0.0065	0.0017
Douglas fir: no cat (% of fireplace)	27.5%	31.0%	46.8%	13.4%	77.8%	29.8%	NA
Softwood EF without catalyst (g/kg wood)[b]	**1.90**	**1.28**	**0.29**	**0.0029**	**0.0005**	**0.0144**	**0.0017**
Douglas fir: with catalyst (g/kg wood)	1.20	0.78	0.31	0.00155	0.00018	0.00373	0.00201
Douglas fir: with catalyst (% of fireplace)	30.0%	28.2%	41.1%	6.2%	40.7%	17.1%	NA
Softwood EF with catalyst (g/kg wood)[b]	**2.07**	**1.17**	**0.251**	**0.001**	**0.00024**	**0.008**	**0.002**
Hardwood							
White Oak: no catalyst (g/kg wood)	3.40	1.88	0.24	0.0121	0.0010	0.0135	3.39E-05
White Oak: no cat (% of fireplace)	50.0%	51.3%	65.5%	205.6%	148.2%	230.3%	NA
Hardwood EF without catalyst (g/kg wood)[b]	**3.18**	**1.81**	**0.43**	**0.0096**	**0.0009**	**0.0127**	**3.39E-05**
White Oak: with catalyst (g/kg wood)	2.20	1.21	0.13	0.0053	0.0008	0.0073	1.33E-05
White Oak: with catalyst (% of fireplace)	32.4%	33.0%	36.2%	90.3%	123.8%	124.0%	NA
Softwood EF with catalyst (g/kg wood)[b]	**2.06**	**1.17**	**0.24**	**0.0042**	**0.0007**	**0.0068**	**1.33E-05**

[a] No retene was quantified for these wood types combusted in a fireplace so the values indicated for retene are actual wood stove emissions.

[b] These values reflect the emission factor used to estimate the mass of tracer attributed to woodstove emissions. It is calculated by multiplying wood stove emissions as a percent of fireplace emissions to the fireplace emission factor reported in Table 21 for either softwood or hardwood.

Although the ratio of tracer to OC and $PM_{2.5}$ are similar between wood burning stoves and fireplaces, the total amount of emissions from wood stoves is approximately one half to one third of fireplaces on a per mass basis of wood burned. Given that each combustion process burns approximately the same amount of wood (Fine, Cass, and Simoneit, 2004b), wood stoves

will contribute less to ambient tracer concentrations than do fireplaces. To calculate the percent of the wood smoke tracer attributable to each combustion method (here there are three different methods considered: fireplaces, catalyst equipped wood stoves, and non-catalyst equipped woodstoves) is similar to the method for motor vehicles except here there is the additional concern of two fuel types: hardwood and softwood. Thus the calculation involves six different source profiles: one for each combustion method for each fuel type. It is assumed that equal parts hardwood and softwood are combusted. Additionally a conservative assumption leads to the estimate that half of the fuel is combusted in a fireplace, while the other half is equally divided between catalyst and non-catalyst equipped wood stoves. For simplicity, the percent of tracer attributable to different fuel types is combined for each combustion method and reported in Table 23.

Table 23. Percentage of tracer attributable to wood stoves versus fireplaces based on source profiles calculated as outlined in the text.

Combustion Type	Levoglucosan	acetovanillone	guaiacol	vanillin	retene
Wood stoves: non-catalyst	19.15%	17.62%	28.58%	18.04%	4.17%
Wood stoves: with catalyst	13.08%	7.84%	20.79%	10.07%	4.87%
Fireplaces	67.77%	74.54%	50.63%	71.89%	90.96%

The amounts of OC and $PM_{2.5}$ estimated to come from residential wood burning, calculated as outlined above, do not display the same temporal variability as $PM_{2.5}$, OC, and levoglucosan concentrations. Rather the contribution of wood smoke to OC is identical to the ratio of levoglucosan to OC as shown in Figure 21 with a different scale, of course. Generally, the temporal trend shown in Figure 29 of residential wood burning relative to other OC emissions sources is highest on Christmas in the beginning of the study, peaks again after New Year's, and slowly declines until the conclusion of the study. The maximum contribution by wood smoke to OC is 64% at Pacific on January 6th, while the lowest contributions from wood smoke are during the last 5 days of the study when wood smoke contributes only ~30% to total OC. As discussed

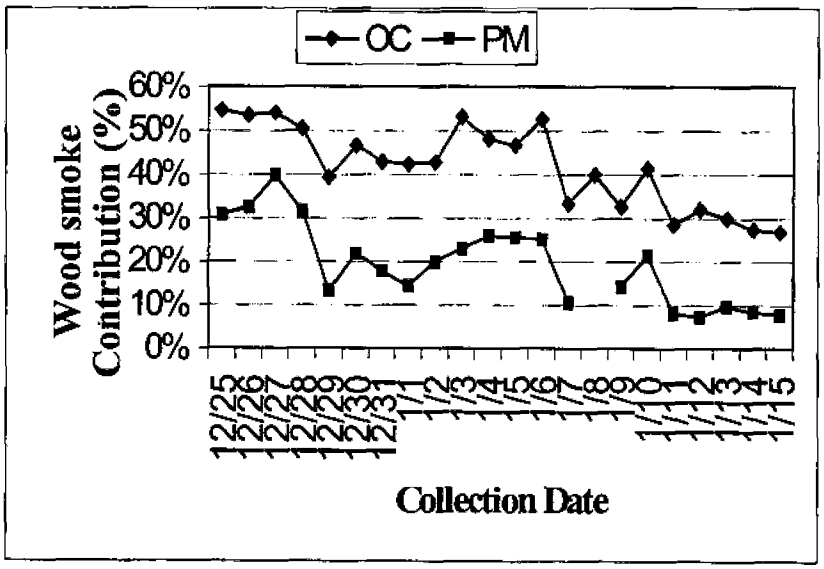

Figure 29. The contribution of wood smoke to total OC and total $PM_{2.5}$ as a daily average of all sites.

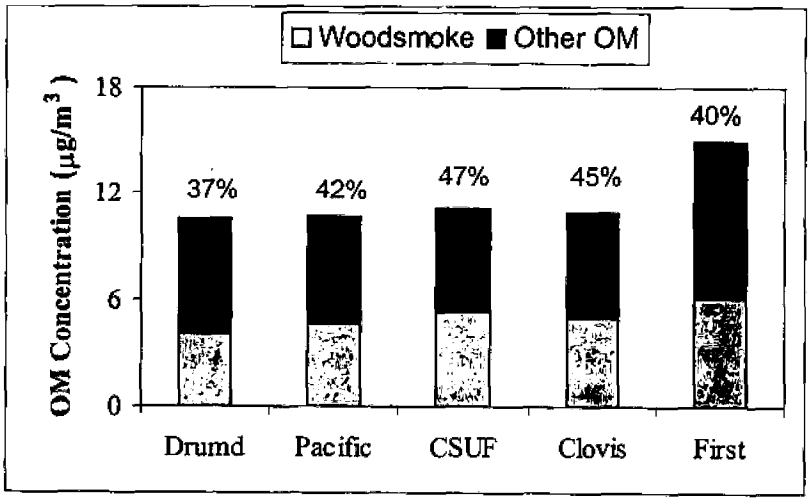

Figure 30. Site average contribution of residential wood burning to OM for the study duration. The percent of OM attributable to wood smoke on average is indicated above each site.

when comparing levoglucosan to $PM_{2.5}$, the wood smoke contribution is less significant in the later portion of the study than it is over the holidays. As shown in Figure 30, CSUF and Clovis have significantly higher contributions of wood smoke to OC relative to the other three sites (significant at the 99% level with 90 degrees of freedom based on a one-tailed difference of means t-test). This inter-city variability is expected based on the site classifications (i.e.

residential) and location within older neighborhoods. As part of a sensitivity test the amount of OM from wood smoke estimated by tracers other than levoglucosan is compared to wood smoke OM estimated with levoglucosan in Figure 31. There is a large variability in the emission rates of tracer compounds for different source profiles (shown in Tables 21 and 22): it is important to note that some of the tracers are specific to hardwood or softwood types (like retene). The application of the combined source profiles, indicated in Table 23, to tracers other than levoglucosan indicate that the amount of OM from wood smoke ranges from less than one percent to 50% of that estimated based on levoglucosan. Some of this discrepancy could be due to guaiacol and substituted guaiacols solid-to-vapor partitioning: collection of both solid and vapor phase guaiacols have shown substantial amounts in the gas phase (close to 100% gas phase concentration in some cases) (Rinehart, 2005). Since gas phase compounds were not evaluated in this study, their loss could lead to an underestimate of wood smoke contribution. Additionally, guiacol and substituted guiacols are thought to be fairly reactive. Both of these issues are of concern regarding the use of these chemicals as source tracers and could potentially explain the apportionment discrepancies shown in Figure 31 for different tracers.

Together the contribution of residential wood burning, motor vehicle emissions and meat cooking represent a considerable fraction of OC and $PM_{2.5}$, as shown in Figure 32. Typically those three sources represent between 65-80% of OC during the study period. Their cumulative contribution to OC can vary substantially from day to day, from a low of 55% to a high of 90%. Previously, these three sources have accounted for ~80-90% of OC in a CMB analysis of multi-day episodes (Schauer and Cass, 2000). For every sample analyzed by GC/MS, wood smoke represents a substantial portion of OC; however, composite samples indicate that the study whole has a lower OC contribution by wood smoke. On average, wood smoke and motor vehicle emissions account for a majority of measured OC contributing approximately 45% and 25% of OC, respectively. Not shown is the contribution of these sources to $PM_{2.5}$, which is

approximately 20 and 10%, respectively. Meat cooking emissions are a substantially lower portion of OC, between 5-9% depending on how they are estimated.

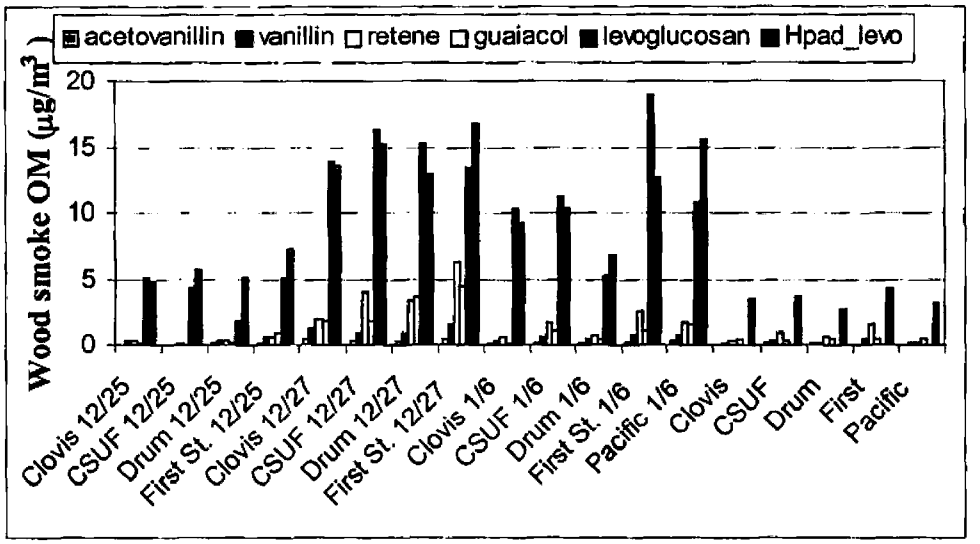

Figure 31. OM concentration from wood smoke (µg/m³) estimated using different wood smoke markers.

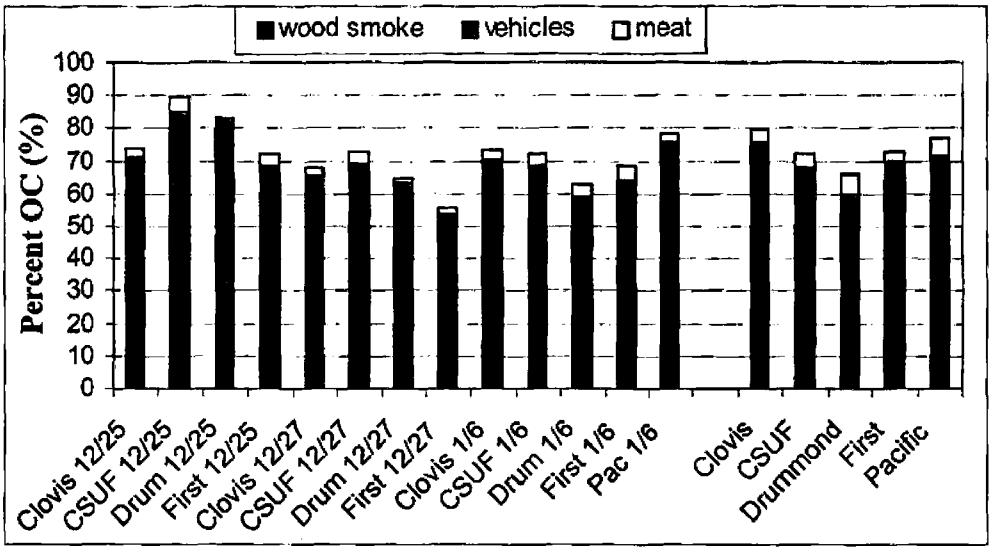

Figure 32. Cumulative contribution to OC as estimated for the three major sources: residential wood burning, motor vehicles, and meat cooking.

CHAPTER 4 CONCLUSIONS

The objectives of this study were three-fold: to examine the spatial variability in wood smoke concentrations in the city of Fresno, CA; to estimate the contribution of residential wood combustion to $PM_{2.5}$; and to meet these goals by using a novel technique to quantify a common wood smoke tracer, levoglucosan. All three of these goals were met. All samples, except for a handful of coarse particle samples below the detection limit, were successfully analyzed for levoglucosan by a HPAEC-PAD system designed specifically to quantify anhydrous sugars. Comparing the results to a subset of the samples analyzed by GC/MS for levoglucosan demonstrates reasonable agreement. Based on levoglucosan concentrations the contribution of residential wood combustion to OC and $PM_{2.5}$ can be estimated; this involves several steps. The total mass and mass concentration of both $PM_{2.5}$ and OC are estimated. A subset of samples are solvent extracted and injected into a GC/MS for quantification of additional source tracers. The assimilation and integration of available source profiles is performed for sources known to be of highest importance for organic $PM_{2.5}$ formation in this region: residential wood burning, motor vehicles, and meat cooking. Once the $PM_{2.5}$ mass, its organic fraction, and several key tracer concentrations are known these pieces can be combined with normalized source profiles to estimate each source's contribution to select samples and to cumulative site samples. Additionally, the contribution of wood smoke to each sample can be estimated since, with the aid of the HPAEC-PAD instrument, levoglucosan concentrations are known for every sample.

All of the results outlined below have been quality controlled/quality assured in some way by comparing with other laboratory results for a subset of samples, comparing duplicate measurements, and blank evaluation.

The daily mass concentrations of $PM_{2.5}$, total carbon (TC), and levoglucosan seem to show a significant relationship to meteorological conditions such as precipitation, wind, and fog events. Two distinct periods are defined based on meteorological conditions and measured ambient air pollution data: Period 1 is the first two weeks of the study when a cyclical pattern of precipitation and pollution accumulation occurs; Period 2 is the last five days of the study from 1/10/2004 to 1/15/2004 when a several day fog event occurs. A high frequency of frontal passage (interpreted from measurement of high wind speeds and precipitation) may have contributed to lower than average $PM_{2.5}$ concentrations. The mass concentration of $PM_{2.5}$ for 20-hour average samples ranges from a low of 5.7 $\mu g/m^3$ at Drummond on January 2nd to a high of 64.8 $\mu g/m^3$ at First St. on December 28th. Although the daily concentrations measured during this study did not exceed the federal 24-hour average standard, the study average at all sites is approximately double the federal annual standard for $PM_{2.5}$ of 15 $\mu g/m^3$ and is still ~2/3 lower than a previous winter average (Watson and Chow, 2002b). Inter-site variability is minimal, however, the average $PM_{2.5}$ concentration at First Street is about 15% greater than other sites.

In this study the carbonaceous fraction is similar to previous findings where the composition of $PM_{2.5}$ is approximately half organic; here the remaining half is assumed to be inorganic. The average amount of total carbon contained in the coarse fraction is approximately 10-15% of the combined total carbon from coarse and fine filters. On a daily basis the carbon fraction of $PM_{2.5}$ mass can fluctuate dramatically with a minimum value of 12% to a maximum of 85%; however, the study average organic fraction ranges from 44 to 55% for individual sites. Of the total carbon mass, generally OM accounts for approximately 85% and the remaining 15% is EC. The temporal and spatial variability of TC demonstrates a similarity to $PM_{2.5}$. Interestingly, the carbonaceous fraction of $PM_{2.5}$ is lowest during fog events which occur on January 1st and in Period 2, the last five days of the study. There also appears to be a relationship in Period 1 between organic and inorganic levels. During Period 1, $PM_{2.5}$ build-up and cleansing cycles generally begin with an organic fraction greater than or equal to the inorganic fraction and end

with a large peak in inorganic levels and a dip in organic levels. While these cycles are perhaps initiated by meteorological conditions, the trend in absolute levels of inorganics throughout this cycle suggests that secondary ammonium nitrate formation is favored at the end of these PM events.

The levoglucosan concentrations and relationships to other pollutants are based on results from a novel analytical liquid chromatography technique configured to quantify anhydrous sugars like levoglucosan. This liquid chromatograph instrument is a high performance anion exchange chromatograph (HPAEC) coupled with pulsed amperometric detection (PAD). The use of this system for quantification of levoglucosan has many advantages. Liquid chromatography is less complex than GC/MS. The extraction process is straightforward, non-toxic, and does not require evaporation/concentration steps. Additionally, this technique is economical which enables the analysis of more samples. Most importantly results compare well with other methods. To verify results from the HPAEC-PAD instrument, a subset of 26 samples was solvent extracted and sylilated for analysis by a better-known analytical technique, GC/MS. A comparison of ambient levoglucosan concentrations as estimated by GC/MS and HPAEC-PAD shows a reasonable agreement between the two methods. Thus there is a strong level of confidence in the levoglucosan results from the HPAEC-PAD instrument and the derived wood smoke contributions to OC and $PM_{2.5}$.

The concentration of levoglucosan in Fresno $PM_{2.5}$ ranges from close to zero to as high as 1.8 $\mu g/m^3$ with site averages ranging between 0.5 and 0.7 $\mu g/m^3$. Levoglucosan concentrations follow a temporal trend that is very similar to $PM_{2.5}$. The variability in coarse particle levoglucosan is markedly different in comparison to the fine filters: levoglucosan concentrations in coarse filters have very little coherence between sites or over time. However, this is not a large concern since the coarse filters contain only 10% of the total levoglucosan. Interestingly, levoglucosan levels during Period 1 show a strong relationship to the relative changes in the concentration of $PM_{2.5}$; however, during Period 2 levoglucosan contributes significantly less to

$PM_{2.5}$ and OC than previously. The strong correlation with $PM_{2.5}$ levels in Period 1 indicate that concentrations are probably a function of the meteorological conditions, such as stagnation and pressure system cleansing, whereas the significant reduction in levoglucosan levels in Period 2 implies activity differences in residential wood burning or differences in removal processes. The carbon mass of levoglucosan as a percent of OC carbon mass ranges from 1.8 to 5.2%. Comparing this to previous studies where the carbon mass of levoglucosan as a percent of OC is 8.5 and 6.5% for two different multi-day episodes (Schauer and Cass, 2000), suggests a decrease in wood smoke emissions relative to other sources. This might reflect the new revisions on wood burning regulations. While the difference between these studies is not large, it may be significant when considering that the largest 3-day average in this study is 4.8%, almost 30% less than previous studies.

A subset of samples was selected for GC/MS analysis based on ratios between key pollutants: OC:$PM_{2.5}$, and levoglucosan:OC. These pollutant ratios might indicate interesting differences between major source contributions. The compounds identified and quantified by GC/MS include n-alkanes, PAHs, wood smoke tracers, meat cooking tracers, and hopanes and steranes. Particle phase n-alkanes in the size range C_{13}-C_{40} are quantified. The Carbon Preference Index (CPI), a ratio of the concentration of odd carbon numbered n-alkanes to the concentration of even numbered n-alkanes (Finlayson-Pitts and Pitts, 2000), is close to one and significantly lower than two for all samples analyzed by GC/MS. This indicates that the samples collected at Fresno were dominated by anthropogenic rather than biogenic sources. Interestingly, the CPIs for the site composites are higher than the selected individual samples, an indication that biogenic sources are generally larger for those samples not examined specifically by GC/MS. There do not seem to be any consistent differences in the CPI between sites.

PAHs are of particular importance due to their known carcinogenic and mutagenic properties (Finlayson-Pitts and Pitts, 2000). Twenty three individual PAH compounds, including retene and benzo[α]pyrene (BaP), were quantified to differentiate between samples dominated by

fossil fuel versus biomass combustion sources. First Street samples have a significantly higher concentration of PAHs relative to other sites, exceeding concentrations at other sites by 40-80%. In all samples analyzed, the PAH with the largest concentration is retene, a wood smoke marker. The concentration of retene is between 31-77% of the total quantified PAH concentration. The level of retene relative to other PAHs appears larger at CSUF and First St. than at other sites, with retene contributing, on average, 78% and 71% to PAH levels, respectively, while other sites have a 40-55% retene contribution. Overall, the contribution to OC and $PM_{2.5}$ by quantified PAHs is low, less than a tenth of a percent by mass for all samples analyzed, with retene, a wood smoke marker, dominating over fossil fuel markers.

As the focus of this study is the quantification of wood smoke contribution to $PM_{2.5}$, several other wood smoke markers are identified and quantified with GC/MS to provide supplementary, independent measures of wood smoke contribution. In addition to quantifying retene, as mentioned above, guaiacol and substituted guaiacols were also quantified. The relative ambient concentrations of these wood smoke tracers track each other fairly well from sample to sample, despite large difference in emissions rates, source profiles (i.e. from combustion of hardwood/softwood or different types of detritus), transport lifetimes, and other confounding factors. These tracers also track levoglucosan concentrations as estimated by GC/MS and HPAEC-PAD techniques.

Several other emissions source markers are identified and quantified by GC/MS, including sterols, from meat cooking, and hopane/steranes from motor vehicle exhaust. Although several or more compounds from each family are quantified, only cholesterol and 17α, 21β-hopane are used for source contribution estimates. The tracers for wood smoke, meat cooking and motor vehicles combined identify the source contributions of approximately 70-80% of OM. Published source profiles for these three sources were selectively combined to derive source profiles that are current and most applicable to the geographic area of this study. Their cumulative contribution to OM can vary substantially from day to day, with a low of 58% to a

high of 93%. On average, wood smoke and motor vehicle emissions account for a majority of measured OM, contributing approximately 45% and 25% of OM, respectively. The average contribution of these sources to $PM_{2.5}$ is approximately 20 and 10%, respectively. Meat cooking emissions are a substantially lower portion of OM, between 5-9% depending on how they are estimated.

The maximum contribution by wood smoke to OC is 65% at Pacific on January 6th while the lowest contributions from wood smoke to OC are during the last 5 days of the study when wood smoke contributes only ~30% to total OC. Generally, the temporal trend of residential wood burning relative to other OC emissions sources is highest on Christmas in the beginning of the study, peaks again a few days after New Year's, and slowly declines until the conclusion of the study. CSUF and Clovis have significantly higher contributions of wood smoke to OC relative to the other three sites, as expected based on the residential nature of the sites and location within older neighborhoods.

For the samples analyzed by GC/MS, motor vehicles contribute between 8 and 30% to OC and 6-17% to $PM_{2.5}$. The sensitivity of these estimates to diesel engines is small (less than 5%), while a doubling in the estimated amount of non-catalyst equipped engines could potentially decrease the contribution to OC and $PM_{2.5}$ by 15% of the estimated vehicle contribution. Depending on the method of estimating meat cooking source contribution, meat cooking could contribute between 0 and 6% to OC, or from 0 to 12% to OC. Generally, the contribution of meat cooking is highest at Drummond, which may be influenced by a BBQ located near an adjacent fire station.

While the results of this study have not conclusively shown a decrease in residential wood burning relative to past years, there were some substantial differences in the amount of OC attributable to wood smoke. The highest three-day average levoglucosan carbon mass as a percent of OC measured in this study is 30% less than the lowest three-day average measured in a special study in 1995 (Schauer and Cass, 2000). Although the relationship of levoglucosan to OC

is independent of meteorological conditions and source apportionment methodology, measurement error could potentially explain this observed difference. Continued measurements of levoglucosan in future samples could provide better information about changes in airborne wood smoke concentrations.

While the efforts of this study focus on the impact of residential wood burning on winter-time levels of $PM_{2.5}$, it is apparent that other sources, both known and unknown, contribute to $PM_{2.5}$ 24-hour and annual NAAQS exceedances. It is likely that through implementation of Rule 4901 and other restrictions of residential wood burning that the organic contribution to levels of $PM_{2.5}$ will decline, but it is unclear if these measures alone will be sufficient to reduce levels of $PM_{2.5}$ to acceptable levels. If residential wood burning were to be completely banned the average $PM_{2.5}$ concentration over the duration of this study is estimated to decline from 30 to 26 $\mu g/m^3$, a 15% reduction, yet still significantly greater than the annual standard of 15 $\mu g/m^3$. In the future, it will be important to further quantify contributions of other sources to organic and total $PM_{2.5}$ levels in efforts to achieve attainment status in urban Fresno as well as in outlying areas such as the agricultural basin of the San Joaquin Valley. Success in reducing pollution in this area of the world with its meteorologically induced problems compounded by ever increasing population density and agricultural land use will set the standard for areas less prone to air quality problems. Perhaps the quest to understand the composition and formation of particulate matter in this region will lead to understanding of more global problems involving particulate matter and its coupled relationships with visibility, human health, and climate change.

CHAPTER 5 FUTURE WORK

During the analysis of samples collected from the Fresno field study, several questions and concerns arose regarding underlying chemical/physical processes, necessary assumptions, and implications of the results. The accuracy of the source apportionment method applied here is influenced by tracer measurement techniques, assumed tracer lifetimes which in turn relies on known atmospheric removal rates, and the applicability of previously published source profiles. In this chapter these issues are addressed in the context of potential areas for future research.

Many questions remain unresolved as a result of sampling limitations or necessary trade-offs. A limitation of sampling on a quartz fiber substrate is the large positive sampling artifact relative to other substrates and, as a result, a filter "memory" effect biasing results towards conditions prevalent at the end of sampling. As with any current study involving aerosol mass concentration, efforts to quantify sampling artifacts are of great benefit. In particular, improving estimations of organic adsorption artifact are especially critical in studies such as this where source contributions are estimated as a percent of organic aerosol. Quantification of the adsorption artifact was attempted in this study by slicing filters and measuring the carbon mass of both the top and bottom portions; however, differences in the carbon content alone is not an indication of the physical/chemical processes that contribute to sampling artifacts and as such more information is needed to accurately quantify particle-phase organic mass. A study aimed to quantify the sampling artifact and contributing factors (such as temperature, photolytic, or emission-type/-age dependence) should be conducted in California to reduce errors associated with sampling artifacts.

Errors can be further reduced by use of different measurement techniques and improved understanding of current techniques. As was explained in the results section, the actual organic

mass (OM) was not measured in this study, instead a factor was used to convert between measured OC and estimated OM. Although actual measurement of OM is highly challenging, it would be beneficial to have more information regarding actual OC-to-OM conversion relating specifically to the SJV, or wood smoke impacted aerosols.

The application of the HPAEC-PAD as optimized to quantify anhydro-sugars is shown to provide an accurate measurement for ambient $PM_{2.5}$ samples; however, the use of this measurement technique was more problematic for coarse particle samples which appeared to rapidly degrade once extracted. To prevent the degradation hypothesized to be from activated microbes, chloroform was added to the extract as a biocide. Unfortunately, chloroform also interfered with the detection of levoglucosan by HPAEC-PAD. In order for the HPAEC-PAD technique to be fully operational, testing and selection of an appropriate biocide should be performed.

In any source apportionment study the tracer lifetime and thus the removal processes are a critical concern. In this study it was assumed that the tracers levoglucosan, 17α, 21β-hopane, and cholesterol were conserved from the source to the sampling location and had lifetimes longer than the time of transport. These are reasonable assumptions for a winter study in an urban environment; however, in light of the results from this and other recent studies, these assumptions are questioned and should be considered further. The use of cholesterol as a tracer for meat cooking might be problematic in this study or in future studies. A laboratory study by Dreyfus, et al. determined that cholesterol reacts with ozone forming oligomers (Dreyfus et al., 2005). Although the authors concluded that cholesterol is appropriate for a local source tracer, the implications of this for future studies and modeling efforts should be noted.

Another tracer, levoglucosan, may not always be conserved in areas that frequently form fog. Much of the discussion of levoglucosan focused on its relationship with $PM_{2.5}$ and meteorological conditions. Its correlation with daily $PM_{2.5}$ concentration, while large in the beginning of the study, decreased significantly during a several day fog event. This might

indicate preferential scavenging of levoglucosan, in particular, and wood smoke, in general, by fog hydrometeors. A previous study in the SJV demonstrated very high fog scavenging efficiencies of organic matter, and levoglucosan relative to other tracers suggesting reduced atmospheric lifetimes as the wet deposition rates of fog droplets are much higher than the dry deposition of accumulation mode particles (Herckes et al., 2005b). Since fogs frequently occur during winter in the SJV, the removal of tracer species by fog has important implications and should be addressed in the future.

To a large extent estimation of wood smoke contribution to organic aerosol and $PM_{2.5}$ is dependent on the application of previously published emissions source profiles for residential wood burning. Uncertainties due to this can be quite large as available profiles vary widely between wood types, burn conditions, and different equipment. For a more accurate estimate of wood smoke influence, a survey of homes should be performed to identify the use of fireplaces relative to wood burning stoves, the type of stoves used (e.g., catalyst equipped), and type of wood or other materials burned (e.g., Christmas wrapping paper). Although the relative contribution of wood smoke to OC can be estimated independent of OM, the absolute amount of wood smoke is more uncertain due to the use of an OC-to-OM conversion factor in the source profiles themselves. Similar to an earlier comment, measurement of actual OM in source profiles, as opposed to solely measuring carbon mass, would enable a more useful analysis for future studies.

Ultimately the results of this work could be incorporated, in combination with other sources of information, with either a regional or global modeling effort. A regional model using the topography of the Central Valley of California could be useful for understanding the formation and accumulation of both PM and ozone. Integrating information from different source apportionment studies and the regional PM study (CRPAQS) would provide a clear framework for a regional transport and accumulation model. Additionally, a more global model is needed to further understand the impact of wood smoke on climate. A General Circulation Model could

incorporate information previously collected about the size distribution, optical properties, and hygroscopic growth of wood smoke influenced aerosol, such as that collected for the Yosemite Aerosol Characterization Study, to commence estimation of climate forcing magnitude and direction by aerosols. In the future perhaps the HPAEC-PAD method could be used to estimate wood smoke spatial variability on a global level for incorporation with modeling efforts. As wood smoke is globally one of the largest anthropogenic sources of aerosol, identifying the climate forcing of this fraction can supply a large amount of information in a research area that currently is highly uncertain.

REFERENCES

U.S. Environmental Protection Agency (2004). Air Quality Criteria for Particulate Matter (October 2004). USEPA:Washington, DC. 600/P-99/002aF-bF

U.S. Environmental Protection Agency (2003). Air Quality Index: A guide to Air Quality and Your Health. EPA:Washington, DC. EPA-454/K-03-002

Andreae, M.O., E. Atlas, H. Cachier, W.R. Cofer III, G.W. Harris, G. Helas, R. Koppmann, J.P. Lacaux, and D.E. Ward, eds. (1996), *Trace gas and aerosol emissions from savanna fires*. Edited by J. Levine, *Biomass Burning and Global Change*. Cambridge, MA: MIT Press.

Bae, M. S., J. J. Schauer, J. T. DeMinter, J. R. Turner, D. Smith, and R. A. Cary (2004), "Validation of a semi-continuous instrument for elemental carbon and organic carbon using a thermal-optical method", *Atmospheric Environment* **38** (18):2885-2893.

Battye, W., V. P. Aneja, and P. A. Roelle (2003), "Evaluation and improvement of ammonia emissions inventories", *Atmospheric Environment* **37** (27):3873-3883.

bin Abas, M. R., D. R. Oros, and B. R. T. Simoneit (2004), "Biomass burning as the main source of organic aerosol particulate matter in Malaysia during haze episodes", *Chemosphere* **55** (8):1089-1095.

Birch, M. E., and R. A. Cary (1996), "Elemental carbon-based method for monitoring occupational exposures to particulate diesel exhaust", *Aerosol Science and Technology* **25** (3):221-241.

Brown, S. G., P. Herckes, L. Ashbaugh, M. P. Hannigan, S. M. Kreidenweis, and J. L. Collett (2002), "Characterization of organic aerosol in Big Bend National Park, Texas", *Atmospheric Environment* **36** (38):5807-5818.

Cadle, R. D., and P. L. Magill (1951), "Study Of Eye Irritation Caused By Los Angeles Smog", *Ama Archives Of Industrial Hygiene And Occupational Medicine* **4** (1):74-84.

California, State Department of Finance (2005), *California Statistical Abstract, 2004* [Electronic version] 2005 [cited May 17 2005]. Available from http://www.dof.ca.gov/HTML/FS_DATA/STAT-ABS/Sa_home.htm.

Calvert, J. G. (1976), "Hydrocarbon Involvement In Photochemical Smog Formation In Los-Angeles Atmosphere", *Environmental Science & Technology* **10** (3):256-262.

Cass, G. R. (1998), "Organic molecular tracers for particulate air pollution sources", *Trac-Trends In Analytical Chemistry* **17** (6):356-366.

Chow, J. C., J. G. Watson, L. W. A. Chen, W. P. Arnott, and H. Moosmüller (2004), "Equivalence of elemental carbon by thermal/optical reflectance and transmittance with different temperature protocols", *Environmental Science & Technology* **38** (16):4414-4422.

Chow, J. C., J. G. Watson, D. Crow, D. H. Lowenthal, and T. Merrifield (2001), "Comparison of IMPROVE and NIOSH carbon measurements", *Aerosol Science and Technology* **34** (1):23-34.

Chow, J. C., J. G. Watson, D. H. Lowenthal, R. Hackney, K. Magliano, D. Lehrman, and T. Smith (1999), "Temporal variations of PM2.5, PM10, and gaseous precursors during the 1995 integrated monitoring study in central California", *Journal of The Air & Waste Management Association* **49**:16-24.

Chow, J. C., J. G. Watson, D. H. Lowenthal, P. A. Solomon, K. L. Magliano, S. D. Ziman, and L. W. Richards (1992), "Pm10 Source Apportionment In California San-Joaquin Valley", *Atmospheric Environment Part A-General Topics* **26** (18):3335-3354.

Chow, J. C., J. G. Watson, D. H. Lowenthal, P. A. Solomon, K. Magliano, S. D. Ziman, and L. Willard Richards (1993), "PM_{10} and $PM_{2.5}$ composition in California's San Joaquin Valley", *Aerosol Science and Technology* **18**:105 - 128.

Chu, S. H., J. W. Paisie, and B. W. L. Jang (2004), "PM data analysis - a comparison of two urban areas: Fresno and Atlanta", *Atmospheric Environment* **38** (20):3155-3164.

Collett, J. L., A. S. H. Prevot, J. Staehelin, and A. Waldvogel (1991), "Physical Factors Influencing Winter Precipitation Chemistry", *Environmental Science & Technology* **25** (4):782-788.

Cook, J.W., C.L. Hewett, and I. Hieger (1933), "The Isolation of a Cancer-producing Hydrocarbon from Coal Tar. Parts I, II, and III." *Journal of Chemistry Society*:395-405.

Courtney, W. J., R. W. Shaw, and T. G. Dzubay (1982), "Precision And Accuracy Of A Beta-Gauge For Aerosol Mass Determinations", *Environmental Science & Technology* **16** (4):236-239.

Dreyfus, M. A., M. P. Tolocka, S. M. Dodds, J. Dykins, and M. V. Johnston (2005), "Cholesterol ozonolysis: Kinetics, mechanism, and oligomer products", *Journal of Physical Chemistry A* **109** (28):6242-6248.

Engling, Guenter, Christian M. Carrico, Sonia M. Kreidenweis, Jr. Jeffrey L. Collett, Derek E. Day, William C. Malm, Wei Min Hao, Emily Lincoln, Yoshiteru Iinuma, and Hartmut Herrmann (2005), "Determination of Levoglucosan in Biomass Combustion Aerosol by High Performance Anion Exchange Chromatography with Pulsed Amperometric Detection", *Atmospheric Environment* **Under review.**

Fine, P. M., G. R. Cass, and B. R. T. Simoneit (2004a), "Chemical characterization of fine particle emissions from the fireplace combustion of wood types grown in the Midwestern and Western United States", *Environmental Engineering Science* **21** (3):387-409.

——— (2004b), "Chemical characterization of fine particle emissions from the wood stove combustion of prevalent United States tree species", *Environmental Engineering Science* **21** (6):705-721.

Finlayson-Pitts, B.J., and J.N. Pitts (2000), *Chemistry of the Upper and Lower Atmosphere: Theory, Experiments, and Applications*. 1st ed. San Diego, CA: Academic Press.

Fitz, D. R., J. T. Pisano, I. L. Malkina, D. Goorahoo, and C. F. Krauter (2003), "A passive flux denuder for evaluating emissions of ammonia at a dairy farm", *Journal of The Air & Waste Management Association* **53** (8):937-945.

Fraser, M. P., and K. Lakshmanan (2000), "Using levoglucosan as a molecular marker for the long-range transport of biomass combustion aerosols", *Environmental Science & Technology* **34** (21):4560-4564.

Fraser, M. P., Z. W. Yue, and B. Buzcu (2003), "Source apportionment of fine particulate matter in Houston, TX, using organic molecular markers", *Atmospheric Environment* **37** (15):2117-2123.

Fraser, M. P., Z. W. Yue, R. J. Tropp, S. D. Kohl, and J. C. Chow (2002), "Molecular composition of organic fine particulate matter in Houston, TX", *Atmospheric Environment* **36** (38):5751-5758.

Gao, S., D. A. Hegg, P. V. Hobbs, T. W. Kirchstetter, B. I. Magi, and M. Sadilek (2003), "Water-soluble organic components in aerosols associated with savanna fires in southern Africa: Identification, evolution, and distribution", *Journal of Geophysical Research-Atmospheres* **108** (D13).

Grob, Robert L., ed. (1995), *Modern Practice of Gas Chromatography*. 3rd ed. New York, NY: John Wiley & Sons, Inc.

Hays, M. D., C. D. Geron, K. J. Linna, N. D. Smith, and J. J. Schauer (2002), "Speciation of gas-phase and fine particle emissions from burning of foliar fuels", *Environmental Science & Technology* **36** (11):2281-2295.

Herckes, P., Guenter Engling, S. M. Kreidenweis, and J. L. Collett Jr. (2005a), "Particle size distributions of organic aerosol constituents during the 2002 Yosemite Aerosol Characterization Study", *Environmental Science & Technology* **Under review**.

Herckes, P., S. Youngster, T. Lee, and J.L. Collett (2005b), "Fog processing of atmospheric organic matter", *Atmospheric Environment* **under review**.

Holets, S., and R. N. Swanson (1981), "High-Inversion Fog Episodes In Central California", *Journal Of Applied Meteorology* **20** (8):890-899.

Houck, J.E., P.E. Tiegs, R.C. McCrillis, G.R. Keithley, and J. Crouch (1998), "Air emissions from residential heating: the wood heating option put into environmental perspective", in, *Emission Inventory: Living in a Global Environment*: U.S. Environmental Protection Agency and Air and Waste Management Association.

IPCC (2001), "Climate Change 2001: Summary for Policymakers", in, http://www.ipcc.ch: Intergovernmental Panel on Climate Change, 1 - 83.

Jacob, D. J., F. H. Shair, J. M. Waldman, J. W. Munger, and M. R. Hoffmann (1987), "Transport And Oxidation Of So2 In A Stagnant Foggy Valley", *Atmospheric Environment* **21** (6):1305-1314.

Jacob, Daniel J., J. W. Munger, Jed M. Waldman, and M. R. Hoffmann (1986), "The H_2SO_4-HNO_3-NH_3 system at high humidities and in fogs 1. spatial and temporal patterns in the San Joaquin Valley of California", *Journal of Geophysical Research* **91** (D1):1073 - 1088.

Jeon, S. J., H. L. C. Meuzelaar, S. A. N. Sheya, J. S. Lighty, W. M. Jarman, C. Kasteler, A. F. Sarofim, and B. R. T. Simoneit (2001), "Exploratory studies of PM10 receptor and source profiling by GC/MS and principal component analysis of temporally and spatially resolved ambient samples", *Journal Of The Air & Waste Management Association* **51** (5):766-784.

Kirchstetter, T. W., C. E. Corrigan, and T. Novakov (2001), "Laboratory and field investigation of the adsorption of gaseous organic compounds onto quartz filters", *Atmospheric Environment* **35** (9):1663-1671.

Kleeman, M. J., J. J. Schauer, and G. R. Cass (1999), "Size and composition distribution of fine particulate matter emitted from wood burning, meat charbroiling, and cigarettes", *Environmental Science & Technology* **33** (20):3516-3523.

——— (2000), "Size and composition distribution of fine particulate matter emitted from motor vehicles", *Environmental Science & Technology* **34** (7):1132-1142.

Mader, B. T., and J. F. Pankow (2001), "Gas/solid partitioning of semivolatile organic compounds (SOCs) to air filters. 3. An analysis of gas adsorption artifacts in measurements of atmospheric SOCs and organic carbon (OC) when using Teflon membrane filters and quartz fiber filters", *Environmental Science & Technology* **35** (17):3422-3432.

Malm, W. C. (1999), "Introduction to Visibility", in, Fort Collins, CO: CIRA.

McDow, S. R., and J. J. Huntzicker (1990), "Vapor Adsorption Artifact In The Sampling Of Organic Aerosol - Face Velocity Effects", *Atmospheric Environment Part A-General Topics* **24** (10):2563-2571.

McKee, J. W. (1968), "Trends In Control of Photochemical Smog In Los Angeles Basin", *Journal Of Environmental Sciences* **11** (3):34-40.

Mettler Toledo (2005), *AB104-S: Overview* [cited May 17 2005]. Available from http://www.mt.com/mt/product_detail/product.jsp?m=t&key=Yy_Tc4NjM1MD.

Nolte, C. G., J. J. Schauer, G. R. Cass, and B. R. T. Simoneit (2001), "Highly polar organic compounds present in wood smoke and in the ambient atmosphere", *Environmental Science & Technology* **35** (10):1912-1919.

Novakov, T., and C. E. Corrigan (1996), "Cloud condensation nucleus activity of the organic component of biomass smoke particles", *Geophysical Research Letters* **23** (16):2141-2144.

Pandis, Spyros N., and John H. Seinfeld (1989), "Mathematical modeling of acid deposition due to radiation fog", *Journal of Geophysical Research* **94** (D10):12911-12923.

Pang, Y. B., Y. Ren, F. Obeidi, R. Hastings, D. J. Eatough, and W. E. Wilson (2001), "Semi-volatile species in PM2.5: Comparison of integrated and continuous samplers for PM2.5 research or monitoring", *Journal Of The Air & Waste Management Association* **51** (1):25-36.

Poore, M. W. (2002), "Levoglucosan in PM2.5 at the Fresno supersite", *Journal Of The Air & Waste Management Association* **52** (1):3-4.

Pun, B. K., and C. Seigneur (1999), "Understanding particulate matter formation in the California San Joaquin Valley: conceptual model and data needs", *Atmospheric Environment* **33** (29):4865-4875.

——— (2001), "Sensitivity of particulate matter nitrate formation to precursor emissions in the California San Joaquin Valley", *Environmental Science & Technology* **35** (14):2979-2987.

Rinehart, Lynn (2005), *The Origin of Polar Organic Compounds in Ambient Fine Particulate Matter*. Environmental Sciences and Health, Reno, Nevada: University of Nevada, Reno.

Rogge, W F, L M Hildemann, M A Mazurek, G R Cass, and B R T Simoneit (1993a), "Sources of Fine Organic Aerosol. 2. Noncatalyst and Catalyst-Equipped Automobiles and Heavy-Duty Diesel Trucks", *Environ. Sci. Technol.* **27** (4):636-651.

Rogge, W. F., M. A. Mazurek, L. M. Hildemann, G. R. Cass, and B. R. T. Simoneit (1993b), "Quantification of Urban Organic Aerosols at a Molecular-Level - Identification, Abundance and Seasonal-Variation", *Atmospheric Environment Part A-General Topics* **27** (8):1309-1330.

Russell, L. M. (2003), "Aerosol organic-mass-to-organic-carbon ratio measurements", *Environmental Science & Technology* **37** (13):2982-2987.

Samet, J. M., F. Dominici, F. C. Curriero, I. Coursac, and S. L. Zeger (2000), "Fine particulate air pollution and mortality in 20 US Cities, 1987-1994", *New England Journal Of Medicine* **343** (24):1742-1749.

Schauer, J J, W F Rogge, L M Hildemann, M A Mazurek, and G R Cass (1996a), "Source Apportionment of Airborne Particulate Matter using Organic Compounds as Tracers", *Pergamon* **30** (22):3837-3855.

Schauer, J. J., and G. R. Cass (2000), "Source apportionment of wintertime gas-phase and particle-phase air pollutants using organic compounds as tracers", *Environmental Science & Technology* **34** (9):1821-1832.

Schauer, J. J., M. J. Kleeman, G. R. Cass, and B. R. T. Simoneit (1999a), "Measurement of emissions from air pollution sources. 1. C-1 through C-29 organic compounds from meat charbroiling", *Environmental Science & Technology* **33** (10):1566-1577.

——— (1999b), "Measurement of emissions from air pollution sources. 2. C-1 through C-30 organic compounds from medium duty diesel trucks", *Environmental Science & Technology* **33** (10):1578-1587.

——— (2001), "Measurement of emissions from air pollution sources. 3. C-1-C-29 organic compounds from fireplace combustion of wood", *Environmental Science & Technology* **35** (9):1716-1728.

Schauer, J. J., B. T. Mader, J. T. Deminter, G. Heidemann, M. S. Bae, J. H. Seinfeld, R. C. Flagan, R. A. Cary, D. Smith, B. J. Huebert, T. Bertram, S. Howell, J. T. Kline, P. Quinn, T. Bates, B. Turpin, H. J. Lim, J. Z. Yu, H. Yang, and M. D. Keywood (2003), "ACE-Asia intercomparison of a thermal-optical method for the determination of particle-phase organic and elemental carbon", *Environmental Science & Technology* **37** (5):993-1001.

Schauer, J. J., W. F. Rogge, L. M. Hildemann, M. A. Mazurek, and G. R. Cass (1996b), "Source apportionment of airborne particulate matter using organic compounds as tracers", *Atmospheric Environment* **30** (22):3837-3855.

Schkolnik, G., A.H. Falkovich, Y. Rudich, W. Maenhaut, and P. Artaxo (2005), "New Analytical Method for the Determination of Levoglucosan, Polyhydroxy Compounds, and 2-Methylerythritol and Its Application to Smoke and Rainwater Samples", *Environ. Sci. Technol.*

Seinfeld, J. H., and S. N. Pandis (1998), *Atmospheric Chemistry and Physics: From Air Pollution to Climate Change.* New York, N.Y.: John Wiley & Sons, Inc.

Simoneit, B R T, W F Rogge, M A Mazurek, L J Standley, L M Hildemann, and G R Cass (1993), "Lignin pyrolysis products, lignans, and resin acids as specific

tracers of plant classes in emissions from biomass combustion", *Environ. Sci. Technol.* **27**:2533-2541.

Simoneit, B. R. T. (1989), "Organic-Matter Of The Troposphere.5. Application Of Molecular Marker Analysis To Biogenic Emissions Into The Troposphere For Source Reconciliations", *Journal Of Atmospheric Chemistry* **8** (3):251-275.

——— (1999), "A review of biomarker compounds as source indicators and tracers for air pollution", *Environmental Science And Pollution Research* **6** (3):159-169.

——— (2002), "Biomass burning - A review of organic tracers for smoke from incomplete combustion", *Applied Geochemistry* **17** (3):129-162.

San Joaquin Valley Unified Air Pollution Control District (2003). SJVUAPCD Final Draft Staff Report: Amendments to Rule 4901 (Wood Burning Fireplaces and Wood burning heaters). California State:California.

Skoog, D.A., D.M. West, and F. J. Holler (1996), *Fundamentals of Analytical Chemistry.* Edited by John Vondeling. 7th ed: Thomson Learning, Inc.

Smith, K. R., S. Kim, J. J. Recendez, S. V. Teague, M. G. Menache, D. E. Grubbs, C. Sioutas, and K. E. Pinkerton (2003), "Airborne particles of the California central valley alter the lungs of healthy adult rats", *Environmental Health Perspectives* **111** (7):902-908.

Standley, L. J., and B. R. T. Simoneit (1994), "Resin Diterpenoids As Tracers For Biomass Combustion Aerosols", *Journal Of Atmospheric Chemistry* **18** (1):1-15.

Subramanian, R., A. Y. Khlystov, J. C. Cabada, and A. L. Robinson (2004), "Positive and negative artifacts in particulate organic carbon measurements with denuded and undenuded sampler configurations", *Aerosol Science And Technology* **38**:27-48.

Sunset Laboratories, Inc. (2005), *Sample Analysis Method* [Electronic] [cited May 22 2005]. Available from http://www.sunlab.com/.

Swap, R., M. Garstang, S. A. Macko, P. D. Tyson, W. Maenhaut, P. Artaxo, P. Kallberg, and R. Talbot (1996), "The long-range transport of southern African aerosols the tropical South Atlantic", *Journal Of Geophysical Research-Atmospheres* **101** (D19):23777-23791.

Tiao, G. C., G. E. P. Box, and W. J. Hamming (1975), "Analysis Of Los-Angeles Photochemical Smog Data - Statistical Overview", *Journal Of The Air Pollution Control Association* **25** (3):260-268.

Turpin, B. J., J. J. Huntzicker, and S. V. Hering (1994), "Investigation of Organic Aerosol Sampling Artifacts in the Los-Angeles Basin", *Atmospheric Environment* **28** (19):3061-3071.

Turpin, B. J., and H. J. Lim (2001), "Species contributions to PM2.5 mass concentrations: Revisiting common assumptions for estimating organic mass", *Aerosol Science And Technology* **35** (1):602-610.

Turpin, B. J., P. Saxena, and E. Andrews (2000), "Measuring and simulating particulate organics in the atmosphere: problems and prospects", *Atmospheric Environment* **34** (18):2983-3013.

Watson, J. G., and J. C. Chow (2002a), "Comparison and evaluation of in situ and filter carbon measurements at the Fresno Supersite", *Journal Of Geophysical Research-Atmospheres* **107** (D21).

——— (2002b), "A wintertime PM2.5 episode at the fresno, CA, supersite", *Atmospheric Environment* **36** (3):465-475.

Watson, J. G., J. C. Chow, D. H. Lowenthal, M. R. Stolzenburg, N. M. Kreisberg, and S. V. Hering (2002), "Particle size relationships at the Fresno supersite", *Journal Of The Air & Waste Management Association* **52** (7):822-827.

Wilson, S. R., P. Scamagas, J. Grado, L. Norgaard, N. J. Starr, S. Eaton, and K. Pomaville (1998), "The Fresno Asthma Project: A model intervention to control asthma in multiethnic, low-income, inner-city communities", *Health Education & Behavior* **25** (1):79-98.

Wu, J., F. Lurmann, A. Winer, R. Lu, R. Turco, and T. Funk (2005), "Development of an individual exposure model for application to the Southern California children's health study", *Atmospheric Environment* **39** (2):259-273.

Youngster, Sarah (2005), *The Processing of Aerosol Particles And Soluble Trace Gases by Radiation Fogs in Fresno, California*. Atmospheric Sciences, Fort Collins, CO: Colorado State University.

Zheng, M., G. R. Cass, J. J. Schauer, and E. S. Edgerton (2002), "Source apportionment of PM2.5 in the southeastern United States using solvent-extractable organic compounds as tracers", *Environmental Science & Technology* **36** (11):2361-2371.

Zheng, M., M. Fang, F. Wang, and K. L. To (2000), "Characterization of the solvent extractable organic compounds in PM2.5 aerosols in Hong Kong", *Atmospheric Environment* **34** (17):2691-2702.

APPENDIX A TABLE OF MEASURED AND CALCULATED COMPONENTS FROM COARSE AND FINE FILTERS

Table A. 1 Daily filter concentrations for $PM_{2.5}$, OC, OM, EC, TC', and levoglucosan (in $\mu g/m^3$), and WSOC (in $\mu gC/m^3$).

Site	Date	Ambient Air Volume (m^3)	$PM_{2.5}$	Fine OC	Fine OM	Fine EC	Fine TC'	Fine Levoglu -cosan	Fine WSOC	Coarse OC	Coarse OM	Coarse EC	Coarse TC'	Coarse Levolglu -cosan
Clovis	25-Dec-03	1336.8	18.93	6.53	10.45	1.26	11.71	0.533	1.91	0.450	0.719	0.000	0.72	0.010
Clovis	26-Dec-03	1232.0	10.71	4.11	6.58	0.39	6.96	0.400	1.24	0.442	0.707	0.059	0.77	0.005
Clovis	27-Dec-03	1336.8	34.11	15.51	24.82	1.34	26.16	1.541	4.00	2.201	3.522	0.099	3.62	0.011
Clovis	31-Dec-03	1344.5	24.69	5.21	8.34	1.03	9.37	0.480	1.56	0.685	1.096	0.005	1.10	0.008
Clovis	01-Jan-04	1344.3	35.93	7.64	12.22	1.01	13.23	0.660	2.15	0.934	1.495	0.015	1.51	0.013
Clovis	02-Jan-04	1344.4	7.51	2.32	3.72	0.47	4.19	0.194	0.72	0.212	0.340	0.024	0.36	0.001
Clovis	03-Jan-04	1344.0	10.12	3.01	4.81	0.66	5.47	0.310	0.84	0.385	0.617	0.015	0.63	0.000
Clovis	06-Jan-04	1346.4	39.36	11.07	17.71	2.22	19.93	1.052	3.53	0.967	1.546	0.000	1.55	0.004
Clovis	07-Jan-04	1344.6	37.93	7.08	11.33	1.42	12.75	0.465	1.86	1.236	1.978	0.085	2.06	0.043
Clovis	08-Jan-04	1344.6		7.68	12.29	0.80	13.09	0.680	2.23	1.519	2.430	0.085	2.51	0.003
Clovis	09-Jan-04	1344.6	23.20	6.80	10.89	1.39	12.28	0.500	2.13	1.573	2.516	0.122	2.64	0.010
Clovis	12-Jan-04	679.8	37.81	6.99	11.19	1.16	12.35	0.511	2.14	1.573	2.516	0.122	2.64	0.010
Clovis	13-Jan-04	680.1	31.02	6.28	10.05	1.13	11.18	0.353	1.80	0.595	0.953	0.023	0.98	0.016
Clovis	14-Jan-04	1344.7	34.13	6.43	10.29	0.74	11.03	0.386	2.15	0.829	1.326	0.045	1.37	0.036
Clovis	15-Jan-04	1344.7	28.18	5.20	8.32	1.04	9.36	0.300	1.55	0.782	1.251	0.031	1.28	0.028
CSUF	25-Dec-03	1353.3	17.88	5.71	9.13	0.87	10.01	0.642		0.459	0.734	0.000	0.73	0.007
CSUF	26-Dec-03	1376.8	9.15	2.93	4.69	0.31	5.00	0.307	0.83	0.474	0.758	0.000	0.76	0.096
CSUF	27-Dec-03	1264.6	36.61	15.54	24.86	2.10	26.96	1.724	4.44	1.404	2.246	0.000	2.24	0.104
CSUF	28-Dec-03	1341.5	35.11	12.95	20.71	1.90	22.61	1.457	1.63	1.247	1.996	0.095	2.09	0.059
CSUF	29-Dec-03	1270.5	58.88	8.60	13.76	0.56	14.32	0.703	2.52	1.237	1.980	0.035	2.01	0.076
CSUF	30-Dec-03	1322.7	10.43	2.77	4.44	0.32	4.75	0.252	0.62	0.434	0.695	0.035	0.73	0.085
CSUF	31-Dec-03	1299.8	22.16	5.38	8.62	0.59	9.21	0.469	1.17	0.761	1.218	0.041	1.26	ND
CSUF	01-Jan-04	1604.0	35.85	6.42	10.27	1.06	11.33	0.588	1.93	1.204	1.926	0.000	1.93	0.189
CSUF	02-Jan-04	1601.6	7.87	2.12	3.39	0.30	3.69	0.213	0.73	0.399	0.639	0.015	0.65	0.109
CSUF	03-Jan-04	1602.4	11.55	2.91	4.66	0.40	5.06	0.263	1.70	0.428	0.685	0.000	0.68	0.029
CSUF	04-Jan-04	1544.6	22.34	7.23	11.56	0.92	12.48	0.676	1.55	0.904	1.446	0.008	1.45	0.026
CSUF	05-Jan-04	1546.9	36.98	12.15	19.44	2.06	21.50	1.100	3.09	1.834	2.935	0.025	2.96	0.027
CSUF	06-Jan-04	1545.4	41.80	11.01	17.62	2.04	19.66	1.178	3.02	2.036	3.257	0.121	3.38	0.059

Site	Date	Ambient Air Volume (m^3)	$PM_{2.5}$	Fine OC	Fine OM	Fine EC	Fine TC'	Fine Levoglu -cosan	Fine WSOC	Coarse OC	Coarse OM	Coarse EC	Coarse TC'	Coarse Levolglu -cosan
CSUF	07-Jan-04	1545.4	41.15	7.31	11.70	1.24	12.94	0.522	1.93	1.569	2.510	0.036	2.55	0.143
CSUF	08-Jan-04	1545.4		7.46	11.94	1.04	12.98	0.551	1.54	2.526	4.042	0.001	4.04	0.168
CSUF	09-Jan-04	1551.6	30.03	7.34	11.75	1.28	13.03	0.450	1.67	1.918	3.069	0.046	3.11	0.140
CSUF	10-Jan-04	1581.2	28.90	7.78	12.45	2.36	14.80	0.515	2.17	2.112	3.379	0.008	3.39	0.121
CSUF	11-Jan-04	1582.0	30.78	5.50	8.80	1.01	9.81	0.215	1.85	0.760	1.217	0.062	1.28	0.002
CSUF	12-Jan-04	1514.0	89.23	5.44	8.70	0.59	9.30	0.396	1.30	0.414	0.662	0.058	0.72	0.009
CSUF	13-Jan-04	1472.9	28.11	5.56	8.90	0.37	9.27	0.325	1.82	1.129	1.807	0.014	1.82	0.103
CSUF	14-Jan-04	1704.2	35.15	6.46	10.34	0.84	11.18	0.309	1.55	1.666	2.666	0.047	2.71	0.112
CSUF	15-Jan-04	1328.4	30.04	5.22	8.36	0.72	9.07	0.276	1.74	1.716	2.746	0.000	2.75	0.127
Drummond	25-Dec-03	1309.6	16.19	5.36	8.58	0.89	9.48	0.580	0.70	0.698	1.116	0.024	1.14	0.094
Drummond	26-Dec-03	1309.4	9.62	3.16	5.05	0.83	5.88	0.230	4.23	0.709	1.134	0.000	1.13	0.074
Drummond	27-Dec-03	1309.4	36.66	14.90	23.84	2.69	26.54	1.467	3.56	1.318	2.109	0.014	2.12	0.055
Drummond	28-Dec-03	1310.2	38.01	13.98	22.37	3.16	25.53	1.114		1.176	1.881	0.128	2.01	0.064
Drummond	31-Dec-03	1309.9	23.97	6.37	10.19	0.43	10.62	0.462	1.29	0.817	1.307	0.000	1.31	0.105
Drummond	01-Jan-04	1309.9	32.29	5.97	9.56	0.77	10.33	0.411	1.50	0.649	1.039	0.031	1.07	0.158
Drummond	02-Jan-04	1309.5	5.73	1.39	2.22	0.32	2.54	0.055	0.50	0.363	0.581	0.024	0.60	0.092
Drummond	03-Jan-04	1309.4	14.82	3.68	5.90	0.53	6.43	0.329	1.05	0.499	0.798	0.059	0.86	0.070
Drummond	06-Jan-04	1309.6	39.86	9.88	15.81	2.33	18.14	0.761	2.87	1.154	1.847	0.112	1.96	0.053
Drummond	07-Jan-04	1309.5	40.63	7.59	12.15	1.22	13.37	0.372	1.99	1.458	2.333	0.013	2.35	0.101
Drummond	08-Jan-04	1309.3		6.81	10.89	1.35	12.24	0.354	3.72	1.321	2.114	0.056	2.17	0.066
Drummond	09-Jan-04	1309.2	30.78	6.65	10.65	1.76	12.40	0.271	1.42	1.625	2.600	0.000	2.60	0.071
Drummond	12-Jan-04	1309.7	30.92	4.01	6.41	0.62	7.03	0.145	1.18	0.456	0.729	0.045	0.77	0.029
Drummond	13-Jan-04	1309.3	31.47	5.86	9.38	0.97	10.35	0.253	1.45	0.850	1.360	0.055	1.42	0.020
Drummond	14-Jan-04	1309.2	35.90	5.45	8.72	1.02	9.74	0.228	1.62	1.033	1.653	0.018	1.67	0.077
Drummond	15-Jan-04	1309.3	34.14	5.07	8.10	1.05	9.16	0.205	1.77	1.127	1.804	0.054	1.86	0.072
First St.	25-Dec-03	1310.8	27.92	8.86	14.17	3.51	17.68	0.824		0.658	1.052	0.315	1.37	0.141
First St.	26-Dec-03	1400.4	14.42	5.36	8.58	1.19	9.76	0.600	4.47	0.563	0.901	0.316	1.22	0.103
First St.	27-Dec-03	1388.1	53.67	22.97	36.75	3.47	40.23	1.895	2.60	0.563	0.901	0.316	1.22	0.103
First St.	28-Dec-03	1379.4	64.81	22.88	36.62	4.17	40.79	1.864	7.09	1.732	2.772	0.209	2.98	0.082
First St.	29-Dec-03	1358.9	45.11	10.53	16.85	1.91	18.76	0.686	5.60	1.516	2.426	0.138	2.56	0.081
First St.	30-Dec-03	1389.9	11.73	3.34	5.35	1.18	6.53	0.256	2.95	1.430	2.287	0.103	2.39	0.048

Site	Date	Ambient Air Volume (m^3)	$PM_{2.5}$	Fine OC	Fine OM	Fine EC	Fine TC'	Fine Levoglu -cosan	Fine WSOC	Coarse OC	Coarse OM	Coarse EC	Coarse TC'	Coarse Levolglu -cosan
First St.	31-Dec-03	1380.6	30.06	7.50	12.00	1.71	13.71	0.582	1.02	0.406	0.650	0.064	0.71	0.040
First St.	01-Jan-04	1397.1	42.45	8.42	13.47	1.58	15.05	0.520	1.88	0.998	1.597	0.034	1.63	0.138
First St.	02-Jan-04	1397.1	8.30	2.18	3.49	1.02	4.51	0.200	1.84	1.407	2.251	0.107	2.36	0.047
First St.	03-Jan-04	1393.2	21.82	4.19	6.71	0.88	7.59	0.409	0.84	0.291	0.466	0.054	0.52	0.007
First St.	04-Jan-04	1374.6	26.48	8.70	13.92	1.50	15.43	0.680	1.15	0.421	0.673	0.129	0.80	0.036
First St.	05-Jan-04	1408.0	46.24	14.33	22.93	2.90	25.83	1.013	4.86	0.737	1.180	0.128	1.31	0.021
First St.	06-Jan-04	1380.0	62.54	18.05	28.89	3.73	32.62	1.425	3.46	2.294	3.670	0.190	3.86	0.065
First St.	07-Jan-04	1386.5	43.63	9.00	14.40	1.97	16.37	0.474	9.82	2.470	3.952	0.140	4.09	0.080
First St.	08-Jan-04	1384.1		7.90	12.63	1.83	14.46	0.563	2.01	3.277	5.243	0.151	5.39	0.007
First St.	09-Jan-04	1383.6	31.44	8.78	14.04	2.29	16.34	0.512	2.30	1.648	2.637	0.199	2.84	0.103
First St.	10-Jan-04	1383.0	36.08	10.64	17.02	4.79	21.81	0.810	1.59	3.652	5.842	0.279	6.12	0.063
First St.	11-Jan-04	1383.0	33.77	5.86	9.37	1.55	10.92	0.454	1.95	2.057	3.292	0.098	3.39	0.065
First St.	12-Jan-04	1390.8	34.94	5.69	9.10	1.33	10.43	0.280	1.55	1.026	1.642	0.065	1.71	0.042
First St.	13-Jan-04	1367.6	33.34	5.87	9.40	1.81	11.21	0.340	1.59	0.742	1.188	0.104	1.29	0.031
First St.	14-Jan-04	1384.3	41.61	7.92	12.68	1.93	14.61	0.379	1.62	1.036	1.658	0.102	1.76	0.057
First St.	15-Jan-04	1383.0	36.66	6.41	10.26	2.19	12.45	0.314	1.94	1.673	2.677	0.080	2.76	0.071
Pacific	29-Dec-03	1259.9	33.97	7.60	12.16	0.00	12.17	0.507	1.85	1.646	2.634	0.121	2.76	0.060
Pacific	30-Dec-03	1328.5	10.91	2.94	4.71	0.38	5.08	0.251	1.88	0.824	1.319	0.042	1.36	0.070
Pacific	31-Dec-03	1331.9	25.00	6.19	9.90	0.88	10.78	0.362	0.97	0.624	0.999	0.016	1.01	0.069
Pacific	01-Jan-04	1312.9	35.49	7.62	12.20	0.43	12.63	0.571	1.35	0.927	1.483	0.073	1.56	0.002
Pacific	02-Jan-04	1287.8	5.98	1.53	2.44	0.15	2.59	0.110	1.81	1.068	1.709	0.000	1.71	0.133
Pacific	03-Jan-04	1333.3	13.88	3.59	5.75	0.61	6.36	0.359	1.04	0.329	0.526	0.000	0.53	0.093
Pacific	04-Jan-04	1348.2	25.14	7.22	11.55	0.94	12.49	0.649	0.80	0.578	0.926	0.021	0.95	0.062
Pacific	05-Jan-04	1264.0	39.48	12.48	19.97	2.18	22.14	1.148	1.94	0.864	1.383	0.091	1.47	0.027
Pacific	06-Jan-04	1331.9	50.00	14.98	23.96	3.57	27.53	1.761	3.06	1.661	2.658	0.069	2.73	0.045
Pacific	07-Jan-04	1326.5	45.01	7.37	11.80	1.54	13.33	0.459	3.78	2.122	3.395	0.064	3.46	0.053
Pacific	08-Jan-04	1316.3		5.46	8.74	0.86	9.59	0.415	2.19	2.088	3.340	0.157	3.50	0.054
Pacific	09-Jan-04	1287.8	25.24	5.49	8.79	1.11	9.89	0.331	2.43	1.547	2.476	0.015	2.49	0.060
Pacific	10-Jan-04	1336.7	36.36	12.03	19.25	2.33	21.59	0.985	1.23	1.235	1.977	0.000	1.98	0.032
Pacific	11-Jan-04	1356.4	29.64	3.79	6.06	0.80	6.87	0.144	2.25	2.863	4.580	0.006	4.59	0.074
Pacific	13-Jan-04	1358.4	27.68	4.79	7.67	0.86	8.53	0.263	1.34	0.782	1.252	0.092	1.34	0.002

Site	Date	Ambient Air Volume (m^3)	$PM_{2.5}$	Fine OC	Fine OM	Fine EC	Fine TC'	Fine Levoglu -cosan	Fine WSOC	Coarse OC	Coarse OM	Coarse EC	Coarse TC'	Coarse Levolglu -cosan
Pacific	14-Jan-04	1331.9	32.13	5.60	8.96	0.93	9.89	0.279	1.70	0.159	0.255	0.000	0.26	0.006
Pacific	15-Jan-04	1358.4	34.97	5.19	8.30	0.86	9.16	0.222	1.62	2.336	3.737	0.098	3.84	0.084